Available online at www.sciencedirect.com
ScienceDirect
Phytochemistry 69 (2008) 112–146
PHYTOCHEMISTRY
www.elsevier.com/locate/phytochem

Metabolite profiling of mycorrhizal roots of *Medicago truncatula*

Willibald Schliemann *, Christian Ammer, Dieter Strack

Department of Secondary Metabolism, Leibniz Institute of Plant Biochemistry, Weinberg 3, D-06120 Halle (Saale), Germany

Received 23 January 2007; received in revised form 27 April 2007
Available online 15 August 2007

Abstract

Metabolite profiling of soluble primary and secondary metabolites, as well as cell wall-bound phenolic compounds from roots of barrel medic (*Medicago truncatula*) was carried out by GC–MS, HPLC and LC–MS. These analyses revealed a number of metabolic characteristics over 56 days of symbiotic interaction with the arbuscular mycorrhizal (AM) fungus *Glomus intraradices*, when compared to the controls, i.e. nonmycorrhizal roots supplied with low and high amounts of phosphate. During the most active stages of overall root mycorrhization, elevated levels of certain amino acids (Glu, Asp, Asn) were observed accompanied by increases in amounts of some fatty acids (palmitic and oleic acids), indicating a mycorrhiza-specific activation of plastidial metabolism. In addition, some accumulating fungus-specific fatty acids (palmitvaccenic and vaccenic acids) were assigned that may be used as markers of fungal root colonization. Stimulation of the biosynthesis of some constitutive isoflavonoids (daidzein, ononin and malonylononin) occurred, however, only at late stages of root mycorrhization. Increase of the levels of saponins correlated AM-independently with plant growth. Only in AM roots was the accumulation of apocarotenoids (cyclohexenone and mycorradicin derivatives) observed. The structures of the unknown cyclohexenone derivatives were identified by spectroscopic methods as glucosides of blumenol C and 13-hydroxyblumenol C and their corresponding malonyl conjugates. During mycorrhization, the levels of typical cell wall-bound phenolics (e.g. 4-hydroxybenzaldehyde, vanillin, ferulic acid) did not change; however, high amounts of cell wall-bound tyrosol were exclusively detected in AM roots.

Principal component analyses of nonpolar primary and secondary metabolites clearly separated AM roots from those of the controls, which was confirmed by an hierarchical cluster analysis. Circular networks of primary nonpolar metabolites showed stronger and more frequent correlations between metabolites in the mycorrhizal roots. The same trend, but to a lesser extent, was observed in nonmycorrhizal roots supplied with high amounts of phosphate. These results indicate a tighter control of primary metabolism in AM roots compared to control plants. Network correlation analyses revealed distinct clusters of amino acids and sugars/aliphatic acids with strong metabolic correlations among one another in all plants analyzed; however, mycorrhizal symbiosis reduced the cluster separation and enlarged the sugar cluster size. The amino acid clusters represent groups of metabolites with strong correlations among one another (cliques) that are differently composed in mycorrhizal and nonmycorrhizal roots. In conclusion, the present work shows for the first time that there are clear differences in development- and symbiosis-dependent primary and secondary metabolism of *M. truncatula* roots.

Keywords: *Medicago truncatula* Barrel medic; Leguminosae; *Glomus intraradices*; Metabolite profiling; GC–MS; RP-HPLC-DAD; LC–MS; Arbuscular mycorrhiza; Isoflavonoids; Apocarotenoids; Saponins; Primary polar metabolites; Fatty acids and fatty alcohols; Cell wall-bound phenolics; Tyrosol; Principal component analysis; Hierarchical cluster analysis; Network analysis

1. Introduction

Arbuscular mycorrhizas (AMs) are one of the oldest mutualistic symbioses of plants relying on the formation of intimate relationships between fungi of the phylum Glomeromycota (Schüßler, 2001; Schüßler et al., 2001) and roots of the majority of plants. This symbiosis is based

Abbreviations: AM, arbuscular mycorrhiza(l); dai, days after inoculation; M_{20P}, mycorrhizal (20% phosphate supply); NM_{20P}, nonmycorrhizal (20% phosphate supply); NM_{100P}, nonmycorrhizal (100% phosphate supply).

* Corresponding author. Tel.: +49 345 5582 1510; fax: +49 345 5582 1509.
E-mail address: willibald.schliemann@ipb-halle.de (W. Schliemann).

0031-9422/$ - see front matter © 2007 Elsevier Ltd. All rights reserved.
doi:10.1016/j.phytochem.2007.06.032

on the beneficial exchange of reduced carbon from the plant and mineral nutrients, especially phosphate and nitrogen (Toussaint et al., 2004; Jin et al., 2005; Govindarajulu et al., 2005) as well as water from the fungus (Smith and Read, 1997). This intimate association is accompanied with an increased resistance to abiotic stress and to root pathogens (Gianinazzi-Pearson et al., 1996, 2006; Cordier et al., 1998; Liu et al., 2007). Interaction between plants and AM fungi demands marked changes in root metabolism, some of which were recently shown in our study on the organization and metabolism of plastids and mitochondria, these being limited to 40-day-old AM roots of barrel medic (*Medicago truncatula*) (Lohse et al., 2005). Within the last years, this plant became an important model legume (Cook, 1999; Bell et al., 2000) in studies of both rhizobial and mycorrhizal symbiotic interactions of plants.

Earlier attempts to unravel the AM-specific alterations focused mainly on differential gene expression and protein profiles. On the basis of accumulating EST sequence data (see review, Hause and Fester, 2005), Electronic Northern analyses have been performed (Journet et al., 2002) with the sequence information used for constructing microarrays (Küster et al., 2004) for analysis of mycorrhiza-specific gene expression (van Buuren et al., 1999; Franken and Requena, 2001; Liu et al., 2003; Wulf et al., 2003; Brechenmacher et al., 2004; Manthey et al., 2004; Hohnjec et al., 2005; Massoumou et al., 2007). These approaches and suppressive subtractive hybridization experiments resulted, for example, in the identification of AM-induced genes for a phosphate transporter (Harrison et al., 2002), for water and proton transporters (Krajinski et al., 2000, 2002), germins (Doll et al., 2003), lectins (Frenzel et al., 2005), hemoglobins (Vieweg et al., 2004, 2005) as well as for isoprenoid (Walter et al., 2002) and sucrose biosynthesis (Hohnjec et al., 2003) with an annotated function. Detailed analyses of the *M. truncatula* root transcriptome resulted in the identification of 568 genes, differentially regulated in AM roots colonized with AM fungi (*Glomus mosseae*, *Glomus intraradices*, *Gigaspora rosea*) and some seem to be related to arbuscule development (Grunwald, 2004; Grunwald et al., 2004). On the basis of the mapped proteome of *M. truncatula* (Mathesius et al., 2001; Asirvatham et al., 2002; Watson et al., 2003), AM root protein profiles were studied using both peptide mass fingerprinting and tandem mass spectrometry (Bestel-Corre et al., 2002). Protein modifications in relation to the development of the symbiosis included down- and up-regulation, as well as newly synthesized proteins (Bestel-Corre et al., 2002). In a survey of the *M. truncatula* root plasma membrane proteome, clear differences were found upon inoculation with *G. intraradices* (Valot et al., 2005, 2006).

Despite substantial knowledge of the symbiosis-related changes of the transcriptome and proteome (Gianinazzi-Pearson et al., 2006), only sparse clues regarding metabolite alterations are available. Earlier targeted studies on AMs focused mostly on selected groups of metabolites of mycorrhizal roots, e.g. isoflavonoids (Harrison and Dixon, 1993, 1994; Larose et al., 2002), hydroxycinnamoyl amides (Peipp et al., 1997) and apocarotenoids (Strack et al., 2003; Strack and Fester, 2006). It has also been shown in relation to carbohydrate and lipid metabolism that accumulated trehalose in AM roots is of predominant fungal origin (Douds et al., 2000). Furthermore, plants and AM fungi produce different typical sets of fatty acids (Olsson, 1999; Stumpe et al., 2005; Trépanier et al., 2005).

In spite of these results, our understanding is still limited concerning the metabolic changes occurring during development and maintenance of a functional mutualistic AM symbiosis. Additionally, a profound grasp of the molecular dialogue between the two partners (Harrison, 1998, 1999, 2005; Hause and Fester, 2005; Akiyama et al., 2005; Reinhardt, 2007) is only just emerging. This is in contrast to another well-studied legume symbiotic system, the root nodules. Here, flavonoids function as signaling compounds that induce gene expression in the microbiont (Peters et al., 1986; Zhang and Smith, 1996, 2002). Recently, it was shown that nodules displayed a distinct metabolic phenotype, different from other organs of the symbiotic plant, e.g. *Lotus japonicus* (Desbrosses et al., 2005). For these analyses, GC–MS was used to analyze the metabolite levels in the different plant organs. This method proved to be one of the important tools in metabolomics, permitting non-targeted, comprehensive temporal and spatial analysis of metabolites. GC–MS has also turned out to be a key technology in functional genomics and systems biology (Fiehn et al., 2000a,b; Fiehn, 2001, 2002; Roessner et al., 2001; Hall et al., 2002; Duran et al., 2003; Fernie, 2003; Weckwerth and Fiehn, 2002; Fiehn and Weckwerth, 2003; Urbanczyk-Wochniak et al., 2003; Weckwerth, 2003; Bino et al., 2004; Kopka et al., 2004).

In continuation of our previous work (Lohse et al., 2005), results of an extensive non-targeted and unbiased approach to analyze time-dependent metabolic changes (metabolite kinetics) in *M. truncatula* roots during colonization with *G. intraradices* are presented here for the first time.

2. Results and discussion

2.1. Plant development and course of mycorrhization

To characterize colonization of *M. truncatula* roots with *G. intraradices*, plant growth-related and mycorrhiza-specific parameters were analyzed. Alterations of fresh and dry weights of shoots and roots were measured during the course of mycorrhization from each five parallels of three different plant sets. These are M_{20P} (mycorrhizal,, 20% phosphate supply), NM_{20P} (nonmycorrhizal, 20% phosphate supply) and NM_{100P} (nonmycorrhizal, 100% phosphate supply). The latter plant set was supplied with five times the amount of phosphate included in the applied modified Long Ashton nutrient solution (see Section 3). The weights of M_{20P} and NM_{100P} shoots exceeded the

NM_{20P} control by about 30–35% in fresh weight and about 20–25% in dry weight. Thus mycorrhizal plants exhibited nearly the same increase in shoot biomass as plants receiving 100% phosphate. In contrast, for the root fresh weights, no significant differences between the three different plant sets were observed, whereas the dry weights of M_{20P} roots were about 10–20% higher than those of NM_{100P} and NM_{20P} (data not shown). One of the major factors in AM-promoting plant growth is supposed to be an increased uptake of phosphate (Smith and Read, 1997) due to the exploration of a larger soil volume by extraradical hyphae with highly efficient phosphate absorption systems (Ning and Cumming, 2001). The often observed effect of root mycorrhization on plant shoot and root weights depends on the plants and fungi studied, and the culture conditions (nutritional status, temperature, light). In most cases, AM symbiosis causes preferentially higher shoot biomass (Gavito et al., 2000; Valentine et al., 2001; Diop et al., 2003; Ruotsalainen and Kytoviita, 2004; Duponnois et al., 2005; Rabie, 2005; Wu and Xia, 2006). The results obtained in the present study thus correspond to those published by Burleigh et al. (2002) and Bestel-Corre et al. (2004).

To analyze the progress of mycorrhization, expression of the mycorrhiza-specific phosphate transporter MtPT4 and Glomus rRNA (as fungal marker) were determined, besides the conventional staining of fungal material in mycorrhizal roots. Both the MtPT4 and Glomus rRNA expression data, normalized to 100%, show a synchronous behavior during the experimental period (Fig. 1). The curve diagrams are characterized by a slow increase at the beginning of mycorrhization, followed by a steep increase between 21 and 49 days after inoculation (dai). The staining results, however, indicate a saturation curve reaching a steady state level already at 35 dai.

For a functioning mycorrhizal symbiosis, the MtPT4 expression is a reliable parameter (Isayenkov et al., 2004). Its expression increase proceeds in a different way compared to the data obtained from staining of the fungal material (Fig. 1). The latter reflects only root length frequency of mycorrhization, whereas both MtPT4 and Glomus rRNA expressions are measures of its overall (three-dimensional) colonization intensity. In this connection, it has been shown that knockdown of the mycorrhiza-inducible phosphate transporter gene of *Lotus japonicus* (LjPT3), under phosphate-limiting growth, conditions suppresses AM symbiosis as indicated by growth retardation, decreased formation of arbuscules, and reduced phosphate uptake (Maeda et al., 2006).

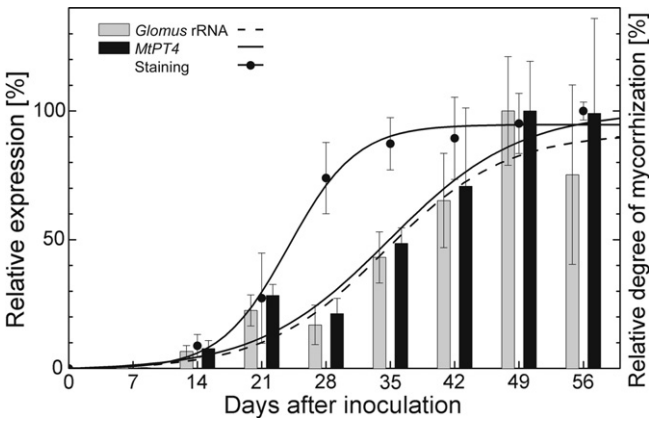

Fig. 1. Time course of AM root formation of *M. truncatula*. Determination of root length frequency of mycorrhization (staining), overall root colonization (expression of *Glomus* rRNA) and functional arbuscules (expression of *MtPT4*).

2.2. Data variance and normalization

Polar and nonpolar metabolites, as well as cell wall-bound components, of lyophilized *M. truncatula* roots were analyzed by GC/TOF-MS, LC–MS and RP-HPLC-DAD, respectively. The majority of compounds showed a biological variance of less than 50%, decreasing from primary to secondary metabolites and cell wall-bound components with less than 20%. The variance of data in the present study is comparable with those published recently on the same plant material (Duran et al., 2002; Sumner et al., 2003). The data obtained were normalized to 30 mg dry weight, the amount used for extraction and recalculated to individual whole roots. The relation of the metabolite levels to roots or to constant dry weight reflects different kinetics, especially at early harvest days. This is demonstrated for phosphate in Fig. 2. Thus, Fig. 2b shows that the phosphate content per root is significantly higher in

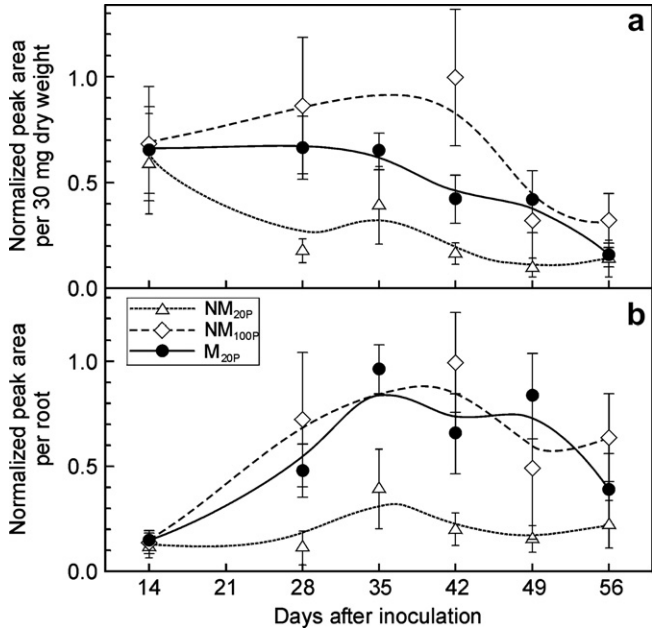

Fig. 2. Phosphate accumulation in mycorrhizal and nonmycorrhizal roots (integration of the characteristic fragment ion *m/z* 299), calculated per dry weight (a) and individual root systems (b). Quantification in mycorrhizal roots gave at 42 dai 25 ± 6 μmol (g dry wt)$^{-1}$ and 0.9 ± 0.3 μmol (root system)$^{-1}$.

M_{20P} samples (AM roots) compared to NM_{20P} ones. Thereby, the enhanced phosphate uptake by the mycorrhizal roots (Cress et al., 1979; Smith and Gianinazzi-Pearson, 1990) was verified. The amount of phosphate reached similar levels to those of the NM_{100P} controls (nonmycorrhizal roots supplied with high amount of phosphate). Therefore, the latter material turned out to be dependable controls to discriminate between phosphate- and mycorrhiza-induced effects.

Metabolites of primary metabolism in the symbiotic roots cannot clearly be assigned to be of plant or fungal origin, especially at high degrees of mycorrhization. However, it is most likely that the mycorrhiza-specific changes in primary metabolism, described in this communication, are mainly due to fungus-induced alterations of plant root metabolism. This assumption is based on correlations found between certain metabolites and corresponding transcripts of plant-specific biosynthetic genes of *M. truncatula* (Lohse et al., 2005).

2.3. Primary polar root metabolites

The polar metabolites of the methanol extracts of roots were analyzed by GC/TOF-MS. Fig. 3a shows a representative chromatogram obtained from extracts of mycorrhizal roots (35 dai). Peak numbers correspond to compound numbers in Table 1, listing 81 compounds including 18 unknowns of which five are unknown disaccharides. Following the metabolite levels during mycorrhization, most of the amino acids reached their highest levels at 42 dai, among which asparagine, aspartic, glutamic and pyroglutamic (derivatization artifact of glutamic acid) acids exhibit marked AM-specific accumulation patterns (Fig. 4, lower panel). The levels of hexoses (glucose, fructose) and sucrose, as well as pentoses and inositol, show a general plant development-dependent increase in all samples (M_{20P}, NM_{20P} and NM_{100P}) (Fig. 5). It is known that mycorrhizal roots take up hexoses mainly through the intraradical hyphae, thereby forming a carbon sink for the plant (Bago et al., 2000). But this is not reflected in the hexose accumulation pattern (Fig. 5). Analyzing the carbon sink strength of AM roots by split-root system, it became apparent that it was both fungus and plant species dependent (Lerat et al., 2003). In strong sink organs, like developing potato tubers, restriction of sucrose supply led to an increase of amino acid levels by transcription regulation of amino acid biosyntheses (Roessner-Tunali et al., 2003). However, the special features of this model system cannot be applied to AM roots. We did not observe an inverse relation between carbohydrates and amino acids in mycorrhizal roots, developing a highly complex metabolic network of a mutualistic system between two partners.

Only in mycorrhizal roots could trehalose be detected due to its fungal origin, reaching maximal levels at 42–49 dai. Some metabolites of the mitochondrial tricarboxylic acid cycle, i.e. aconitic and fumaric acids, showed reduced levels in mycorrhizal roots in comparison to controls. The levels of succinic and citric acids in mycorrhizal roots, however, did not differ significantly from those of controls (Fig. 6). These results may be indicative for an activation of the mitochondrial and the plastidial metabolism during mycorrhization, supported by the proven proliferation of plastids and the changes in transcript levels of biosynthetic genes (Lohse et al., 2005).

In general, metabolite profiling of primary polar compounds of methanolic extracts of *M. truncatula* by GC/TOF-MS turned out to be reliable in the present study proving good selectivity and sensitivity. This was also shown in GC–MS analyses of metabolites of leaves of *Arabidopsis thaliana* (Fiehn et al., 2000a), tuber tissue of *Solanum tuberosum* (Roessner et al., 2001) and different plant parts of *L. japonicus* (Desbrosses et al., 2005). Recently, GC–MS analyses of metabolites of cell suspension cultures derived from *M. truncatula* roots established marked effects of biotic (yeast) and abiotic (methyl jasmonate, UV-light) elicitors (Broeckling et al., 2005). The possible role of jasmonates and some other plant hormones in AM interactions has recently been reviewed (Hause et al., 2007).

2.4. Primary nonpolar root metabolites

A representative separation and detection of nonpolar metabolites by GC/TOF-MS is given in Fig. 3b. In these analyses, most of the fatty acids, fatty alcohols, and alkanes were assigned by a recursive procedure. This method is based on the calculation of a best-fitting curve of the characteristic fragments of some reference compounds versus retention times. The characteristic mass fragment must be typical for the whole compound class, e.g. fatty acids, i.e. by splitting off of a methyl residue from the trimethylsilylated molecule, yielding $m/z = [M-15]^+$. In the case of monoglycerides, the mass fragment after splitting off of the terminal $CH_2 = O^+-TMS$ ($m/z = [M-103]^+$) exhibited higher intensities than the $[M-15]^+$ fragment. Afterwards, the missing peaks of the possible compounds of the same class are scanned in the two-dimensional (R_t, m/z)-space corresponding to the best-fitting curves. Thus, fatty acids and fatty alcohols of even- and odd-numbered C-chains could be detected in a range between C_8 and C_{30} (Table 2). It may be noticed that, in many cases, the C_n:0 fatty acid peak is accompanied by a C_{n+1} fatty alcohol peak having a 36 mDa higher m/z. For instance, the odd-numbered pentadecanoic acid (derivatized fragment ion $[M-15]$ at m/z 299.2406, $C_{17}H_{35}O_2Si$) and the accompanying even-numbered hexadecanol (derivatized fragment ion $[M-15]$ at m/z 299.2770, $C_{18}H_{39}O_2Si$) have the same nominal mass. Nevertheless, they could be assigned both by the described recursive procedure using the characteristic retention time and the high resolution mass spectrometric data provided by the TOF-MS.

Furthermore, a useful method for detecting a group of saturated and unsaturated fatty acids of the same carbon number is via inspection of two-dimensional R_t–m/z-plots

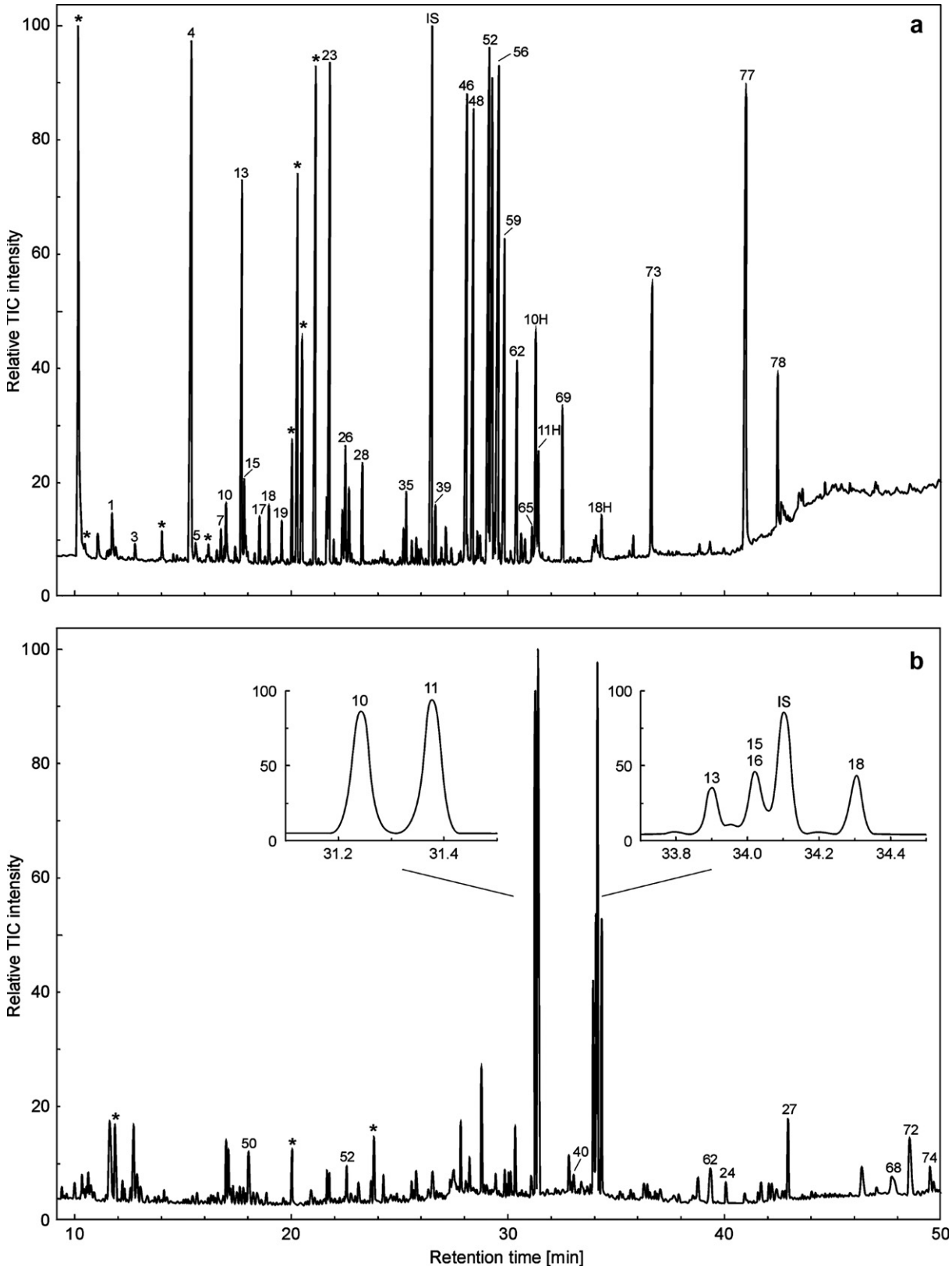

Fig. 3. GC/TOF-MS chromatograms of primary polar root metabolites (M_{20P}, 35 dai) (a) and of primary nonpolar root metabolites (M_{20P}, 56 dai) (b). Peak numbering in a corresponds to metabolite numbering in Table 1 (peak numbers with the extension H refer to co-occurring nonpolar metabolites listed in Table 2); peaks marked by asterisks result from derivatization reagents; IS = internal standard (ribitol). Peak numbering in b corresponds to metabolite numbering in Table 2. Insets show enlarged sections of fatty acid areas; IS = internal standard (methyl nonadecanoate).

Table 1
Primary polar metabolites of mycorrhizal roots of *M. truncatula* (42 dai), GC/TOF-MS characteristics (fragment mass, R_t) and M_{20P}/NM ratios

Peak	R_t (min)	Characteristic fragment *m/z*	Assignment (identification[a])	Ratio	
				M_{20P}/NM_{20P}	M_{20P}/NM_{100P}
1	11.73	191	Lactic acid (a, c)	1.14	0.96
2	12.11	205	Glycolic acid (a, c)	Tr.[b]	Tr.
3	12.78	116	L-Alanine (a, b, c)	0.94	0.84
4	15.32	233	Malonic acid (a, b, c)	0.67	0.74
5	15.58	144	L-Valine (a, b, c)	1.43	1.25
6	16.10	189	Urea (a, b, c)	1.02	1.06
7	16.76	174	Ethanolamine (a, c)	0.51	0.65
8	16.91	158	L-Leucine (a, b, c)	1.95	1.20
9	16.99	205	Glycerol (a, b, c)	1.04	0.66
10	17.02	299	Phosphoric acid (a, b, c)	**3.00**[c]	0.65
11	17.42	158	L-Isoleucine (a, b, c)	1.40	1.51
12	17.50	142	L-Proline (a, b, c)	1.16	0.74
13	17.67	245	Maleic acid (a, b, c)	**0.31**	0.66
14	17.70	174	Glycine (a, b, c)	1.08	1.05
15	17.83	247	Succinic acid (a, b, c)	0.62	1.03
16	18.32	189	Glyceric acid (b, c)	0.74	1.06
17	18.53	245	Fumaric acid (a, b, c)	**0.20**	0.91
18	18.96	204	L-Serine (a, b, c)	1.20	1.11
19	19.32	247	Threonic acid-1,4-lactone (c)	0.68	1.40
20	19.56	218	L-Threonine (a, b, c)	0.86	1.07
21	20.34	248	β-Alanine (c)	1.03	0.95
22	20.87	218	L-Homoserine (b, c)	1.03	1.17
23	21.70	233	Malic acid (a, b, c)	1.29	1.16
24	22.35	232	Aspartic acid (a, b, c)	2.42	2.00
25	22.44	156	Pyroglutamic acid (a, b, c)	1.76	2.58
26	22.47	174	4-Aminobutyric acid (a, b, c)	1.10	0.77
27	22.64	226	UM1[d]	**0.31**	1.31
28	23.26	292	Threonic acid (c)	0.86	1.43
29	23.48	304	2-Ketoglutaric acid (a, c)	Tr.	Tr.
30	24.27	246	L-Glutamic acid (a, b, c)	**2.54**	**6.89**
31	24.44	192	L-Phenylalanine (a, b, c)	1.58	1.36
32	24.70	217	Xylose 1 (a, b, c)	0.78	0.89
33	25.01	217	Arabinose (a, c)	1.11	0.84
34	25.17	217	Xylose 2 (a, b, c)	1.04	0.90
35	25.29	231	L-Asparagine 1 (a, b, c)	1.79	**2.52**
36	25.56	217	Ribose (a, b, c)	1.27	0.40
37	25.90	217	Xylitol (b, c)	1.35	1.59
38	26.06	260	2-Aminoadipic acid (b, c)	2.78	**3.96**
39	26.63	375	*cis*-Aconitic acid (b, c)	0.45	1.90
40	26.93	297	Vanillic acid (a, b, c)	1.04	1.45
41	27.12	217	UM2	1.04	**3.36**
42	27.16	292	Ribonic acid (b, c)	1.12	**1.72**
43	27.43	292	2-Keto-L-gluconic acid (b, c)	0.48	0.77
44	27.83	437	Fructose 1 (a, b, c)	1.13	1.06
45	27.96	437	Fructose 2 (a, b, c)	0.98	0.94
46	28.02	375	Citric acid (a, b, c)	1.08	1.39
47	28.09	437	Fructose 3 (a, b, c)	1.13	0.94
48	28.32	318	Pinitol (c)	1.47	1.09
49	28.50	217	Galactose (a, b)	0.74	1.75
50	28.58	217	UM3	Tr.	Tr.
51	28.82	188	L-Asparagine 2 (a, b, c)	0.77	1.75
52	29.03	307	Fructose 4 (a, b, c)	1.30	1.06
53	29.21	307	Fructose 5 (a, b, c)	1.50	1.17
54	29.27	217	UM4	1.45	0.87
55	29.34	435	Glucose 1 (a, b, c)	0.87	1.20
56	29.48	319	Glucose 2 (a, b, c)	1.20	1.22
57	29.60	317	L-Lysine (a, b, c)	**3.47**	**1.79**
58	29.73	306	UM5	0.78	1.14
59	29.78	319	Glucose 3 (a, b, c)	1.79	1.01
60	29.94	218	L-Tyrosine (a, b, c)	Tr.	Tr.
61	30.10	319	Mannitol (c)	0.93	0.65
62	30.37	217	Inositol 1 (c)	1.16	0.67
63	30.78	435	Glucose 4 (a, b, c)	1.03	1.29
64	31.09	433	Galactonic acid (b, c)	1.14	1.60
65	31.10	305	Ononitol (c)	1.22	1.44
66	31.16	333	Gluconic acid (b, c)	2.55	1.21
67	31.57	319	UM6	1.21	0.85
68	31.86	333	Glucaric acid (b, c)	1.41	1.49
69	32.50	305	Inositol 2 (a, b, c)	0.99	0.84
70	34.33	202	L-Tryptophan (a, b, c)	1.59	2.07
71	35.59	204	UM7	1.15	**2.34**
72	35.77	204	Galactosylglycerol (b, c)	**0.56**	**3.06**
73	36.59	204	UM8	**0.46**	1.54
74	38.83	361	Unknown disaccharide	Tr.	Tr.
75	39.22	361	Unknown disaccharide	Tr.	Tr.
76	39.97	361	Unknown disaccharide	Tr.	Tr.
77	40.90	361	Sucrose (a, b, c)	0.96	2.00
78	42.41	361	Trehalose (a, b, c)	F[e]	F
79	42.60	361	Unknown disaccharide	0.71	1.10
80	42.77	361	Unknown disaccharide	0.98	0.75
81	46.97	204	Digalactosylglyceride	0.74	1.70

[a] (a) MS of reference compounds and/or nonpolar reference extract from hyphae and spores of *Glomus intraradices*; (b) NIST Mass Spectral Library 2002; (c) The Golm Metabolome Database.
[b] Tr., trace.
[c] Significant differences ($p < 0.05$) of the mean values (M_{20P}, NM_{20P}, NM_{100P}) are shown in boldface.
[d] UM – unknown metabolite.
[e] F-Fungal origin.

(Fig. 7). The peaks of mass-selective chromatograms can clearly be resolved. Note that linolenic and vaccenic acids co-elute in a TIC chromatogram as shown by the peaks 15 and 16 in Fig. 3b (inset). Using the recursive procedure, the complete set of fatty acids (C_{12}–C_{24}) observed by Trépanier et al. (2005) were found both in hexane extracts of mycorrhizal roots and the AM fungus *G. intraradices* (spores and hyphae, data not shown). However, the range of chain length of fatty acids was larger, C_8–C_{28} for mycorrhizal roots and C_5–C_{27} for *G. intraradices*. Moreover, additional odd-numbered fatty acids, even- and odd-numbered

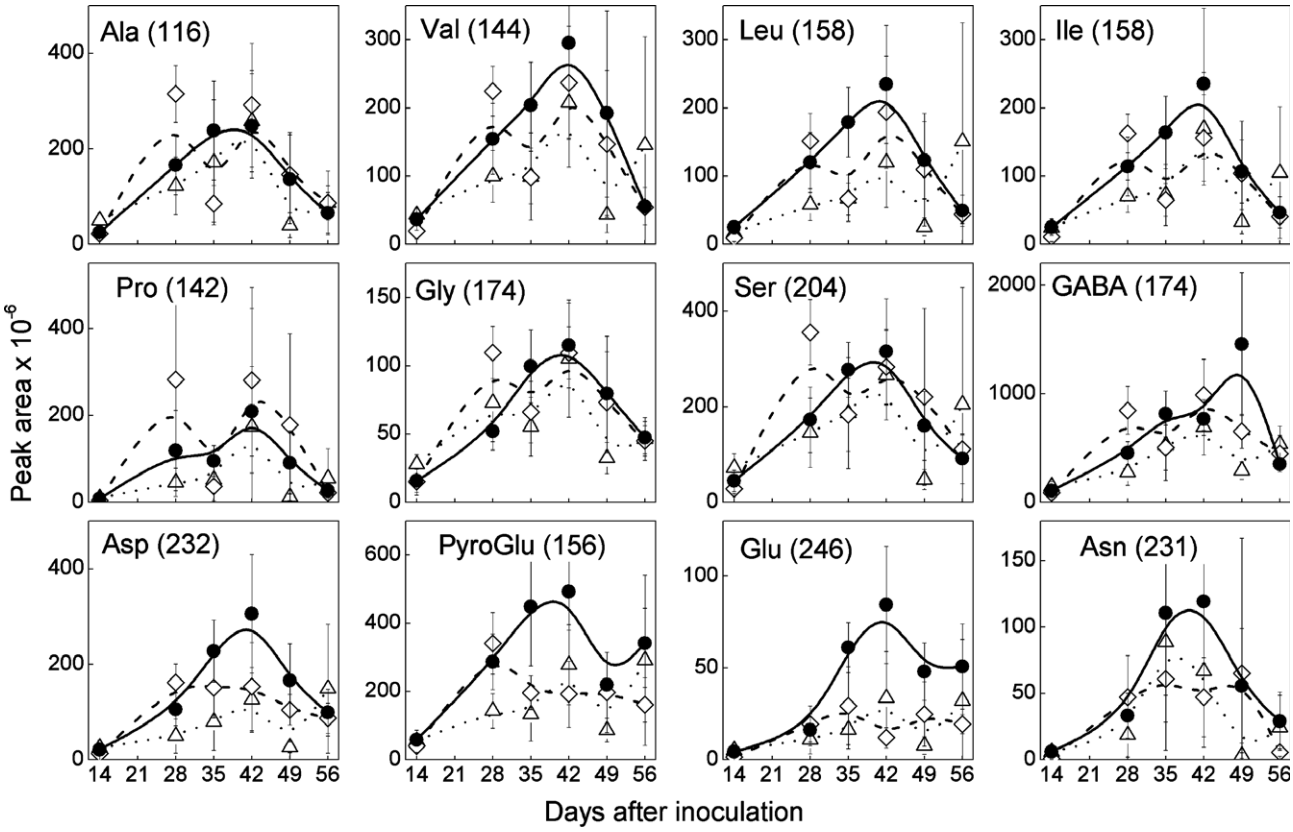

Fig. 4. Accumulation pattern (GC/TOF-MS) of selected amino acids. In brackets are the *m/z* values of characteristic fragment ions used for quantification (symbols as in Fig. 2). The amounts of some amino acids from mycorrhizal roots at 42 dai were calculated as μmol (root system)$^{-1}$ and μmol (g dry wt)$^{-1}$: Ala = 0.2 ± 0.1 and 5 ± 2; Pro = 0.1 ± 0.04 and 2 ± 1; Asn = 1.4 ± 0.6 and 38 ± 15; Asp = 0.3 ± 0.1 and 8 ± 3; Glu = 1.8 ± 0.5 and 51 ± 15; GABA = 3.9 ± 0.8 and 109 ± 17.

fatty alcohols (C_{10}–C_{30} for mycorrhizal roots and C_6–C_{24} for *G. intraradices*), even- and odd-numbered alkanes (C_{11}–C_{23}), different glycerides and sterols were assigned (Table 2).

During the mycorrhization kinetics, an increase of the fungal specific palmitvaccenic and vaccenic acids was observed (Fig. 8). Additionally, increased levels of palmitic and oleic acids in comparison to nonmycorrhizal controls (NM_{20P} and NM_{100P}) was detected. The most abundant fatty alcohols showing a time-dependent increase like the shorter ones are hexadecanol and octadecanol. However, there were no differences between mycorrhizal and nonmycorrhizal roots. Among the detected C_{20}–C_{24} alcohols, the major ones were even-numbered. Palmitic acid (16:0) is the dominant fatty acid that is partitioned between distinct metabolic pathways: (i) elongation stepwise to long chain fatty acids coupled with limited reduction (to yield preferentially even-numbered fatty alcohols) and decarboxylation (to yield preferentially odd-numbered alkanes); (ii) desaturation at different elongation stages to yield unsaturated fatty acids; (iii) esterification with glycerol to yield different glycerides (mono-, di- and triglycerides). The desaturation of 16:0 and 18:0 takes place in plants at C-9, whereas the typical fungal fatty acids are desaturated at C-11 yielding palmitvaccenic ($16{:}1\Delta^{11}$) and vaccenic ($18{:}1\Delta^{11}$) acids (Harwood, 1996; Yang and Bernards, 2006). Formation of odd-numbered fatty acids arises when fatty acid biosynthesis is initiated by propionyl-CoA, instead of acetyl-CoA, or from α-oxidation of even-numbered fatty acids (Hamberg et al., 2002). Odd-numbered fatty acids are precursors of odd-numbered fatty alcohols and even-numbered alkanes, both occurring at trace amounts. The monoglycerides were detected as minor components. Campesterol and 24-methylene cholesterol are markers for either fungal or fungal-induced sterols (Nordby et al., 1981; Schmitz et al., 1991). However, these sterols were detected only in mycorrhizal roots and their levels increased with the degree of mycorrhization (Fig. 8).

The metabolites of roots with nonpolar properties comprise mainly sterols, different classes of lipids (mono-, di- and triglycerides, phospholipids, free fatty acids) and fatty alcohols. It was established for the first time that 11-*Z*-hexadecenoic acid (palmitvaccenic acid, $16{:}1\Delta^{11c}$) occurring in mycorrhizal citrus roots is of fungal origin (Nordby et al., 1981). Also in mycorrhizal leek roots (*Allium porrum*/*G. mosseae*), palmitvaccenic acid was detected in large amounts (Grandmougin-Ferjani et al., 1995). In alfalfa (*Medicago sativa*) roots, colonized with *Glomus versiforme*, an increase of the fungal-specific fatty acid in the lipids was

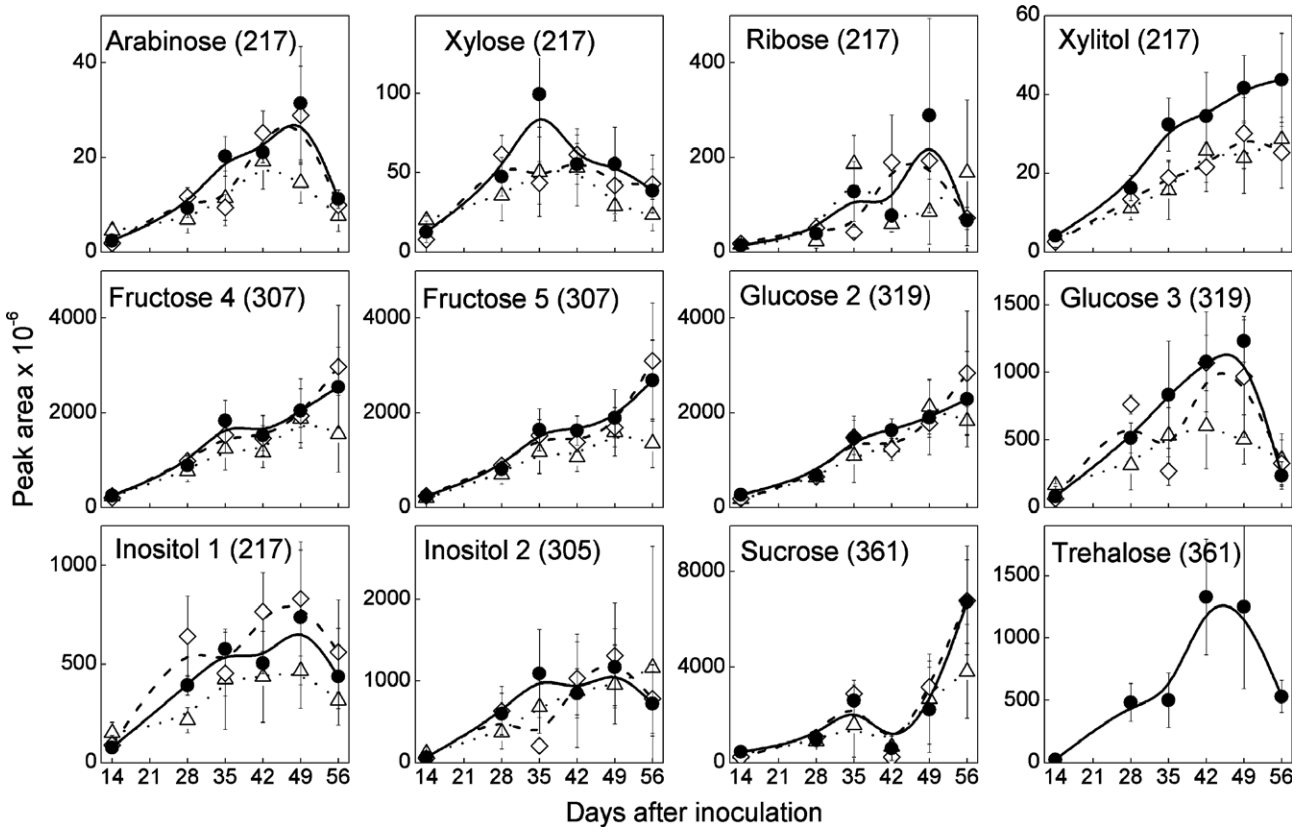

Fig. 5. Accumulation pattern (GC/TOF-MS) of selected sugars/polyols. In brackets are the *m/z* values of characteristic fragment ions used for quantification (symbols as in Fig. 2). The amounts of some sugars and μ-inositol from mycorrhizal roots at 42 dai were calculated as μmol (root system)$^{-1}$ and μmol (g dry wt)$^{-1}$: glucose = 1.1 ± 0.3 and 31 ± 9; fructose = 1.5 ± 0.5 and 42 ± 12; sucrose = 0.1 ± 0.07 and 2 ± 1; trehalose = 0.2 ± 0.07 and 5 ± 2; μ-inositol = 0.3 ± 0.1 and 9 ± 3.

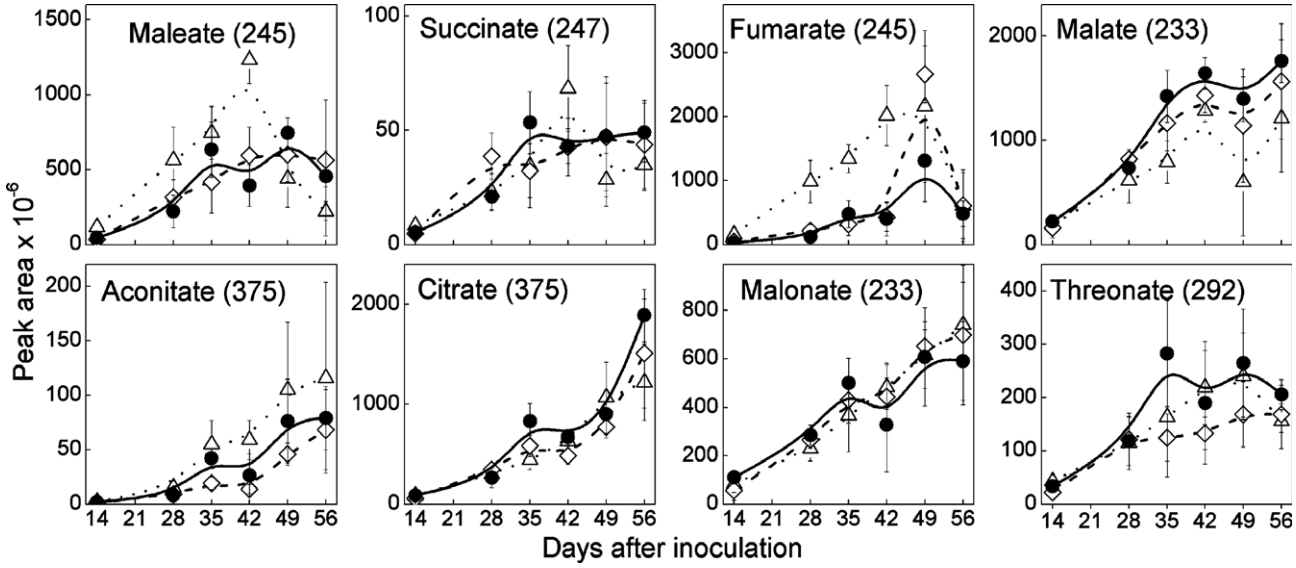

Fig. 6. Accumulation pattern (GC/TOF-MS) of selected aliphatic acids. In brackets are the *m/z* values of characteristic fragment ions used for quantification (symbols as in Fig. 2). The amounts of some aliphatic acids from mycorrhizal roots at 42 dai were calculated as μmol (root system)$^{-1}$ and μmol (g dry wt)$^{-1}$: malonic acid = 2.5 ± 1 and 84 ± 37; malic acid = 7.3 ± 0.7 and 200 ± 30; succinic acid = 0.1 ± 0.02 and 2.1 ± 0.4; citric acid = 1.1 ± 0.02 and 31 ± 5.

observed, correlating with the course of AM fungus interaction (Gaspar et al., 1997). Fatty acid analysis of spore lipids of three *Glomus* species revealed that palmitvaccenic acid is the dominant component like in *G. intraradices*, and

Table 2
Primary nonpolar metabolites and sterols of mycorrhizal roots of *M. truncatula* (56 dai), GC/TOF-MS characteristics (fragment mass, R_t) and M_{20P}/NM ratios

Peak	R_t (min)	Characteristic fragment[a] *m/z*	Assignment (Identification[b])	Ratio	
				M_{20P}/NM_{20P}	M_{20P}/NM_{100P}
Fatty acids					
1	16.64	201	Caprylic acid (8:0) (b, c, d)	0.95	0.94
2	18.80	215	Pelargonic acid (9:0) (b, c, d)	0.79	0.91
3	20.87	229	Capric acid (10:0) (c, d)	0.87	0.88
4	22.82	243	Undecanoic acid (11:0) (d)	0.72	0.90
5	24.70	257	Lauric acid (12:0) (c, d)	0.88	0.79
6	26.48	271	Tridecanoic acid (13:0) (d)	0.99	0.91
7	28.18	285	Myristic acid (14:0) (b, c, d)	0.90	0.70
8	29.81	299	Pentadecanoic acid (15:0) (b, c, d)	0.90	0.83
9	31.09	311	Palmitoleic acid ($16:1\Delta^{9}$) (a, c, d)	1.33	1.25
10	31.24	311	Palmitvaccenic acid ($16:1\Delta^{11}$) (a, d)	**F**[c]	**F**
11	31.38	313	Palmitic acid (16:0) (a, b, c, d)	1.88	1.51
12	32.87	327	Margaric acid (17:0) (b, c, d)	0.81	0.76
13	33.90	337	Linoleic acid ($18:2\Delta^{9,12}$) (a, b, c, d)	1.07	0.76
14	33.96	339	Oleic acid ($18:1\Delta^{9}$) (a, b, c, d)	**2.34**[d]	**1.84**
15	34.02	335	α-Linolenic acid ($18:3\Delta^{9,12,15}$) (a, b, c, d)	1.01	0.90
16	34.05	339	*cis*-Vaccenic acid ($18:1\Delta^{11}$) (a, b, d)	**F**	**F**
17	34.20	339	*trans*-Vaccenic acid ($18:1\Delta^{11}$) (a, b, d)	**F**	**F**
18	34.30	341	Stearic acid (18:0) (a, b, c, d)	1.46	1.20
19	35.68	355	Nonadecanoic acid (19:0) (b, c, d)	0.74	0.92
20	36.26	361	Arachidonic acid ($20:4\Delta^{5,8,11,14}$) (b, d)	Tr.[e]	Tr.
21	36.69	367	Gondoic acid ($20:1\Delta^{11}$) (a, b,d)	**F**	**F**
22	37.00	369	Arachidic acid (20:0) (a, b, c, d)	1.11	1.05
23	38.39	383	Heneicosanoic acid (21:0) (d)	1.12	0.78
24	40.04	397	Behenic acid (22:0) (b, c, d)	1.05	0.87
25	41.62	411	Tricosanoic acid (23:0) (b, c, d)	0.83	0.60
26	42.65	423	Tetracosenoic acid (24:1) (a, d)	Tr.	Tr.
27	42.90	425	Lignoceric acid (24:0) (b, c, d)	1.21	0.90
28	44.00	439	Pentacosanoic acid (25:0) (c, d)	1.17	0.78
29	44.87	451	Hexacosenoic acid (26:1) (d)	Tr.	Tr.
30	45.07	453	Cerotinic acid (26:0) (c, d)	1.20	1.09
31	46.29	467	Heptacosanoic acid (27:0) (d)	Tr.	Tr.
32	47.62	481	Montanic acid (28:0) (d)	Tr.	Tr.
Fatty alcohols					
33	19.07	215	Decanol (d)	0.99	1.02
34	21.18	229	Undecanol (d)	0.74	0.81
35	23.07	243	Dodecanol (d)	0.79	0.81
36	24.92	257	Tridecanol (d)	0.86	0.78
37	26.69	271	Tetradecanol (b, d)	0.76	0.73
38	28.37	285	Pentadecanol (d)	0.93	0.82
39	29.99	299	Hexadecanol (b, c, d)	0.88	1.05
40	33.01	327	Octadecanol (b, c, d)	0.92	0.91
41	35.79	355	Eicosanol (c, d)	0.87	0.75
42	37.10	369	Heneicosanol (d)	0.93	0.78
43	38.51	383	Docosanol (c, d)	1.06	0.81
44	41.69	411	Tetracosanol (d)	1.12	1.04
45	44.05	439	Hexacosanol (b, c, d)	Tr.	Tr.
46	46.32	467	Octacosanol (d)	Tr.	Tr.
47	49.21	495	Triacontanol (c, d)	Tr.	Tr.
Alkanes					
48	12.67	141	Undecane (c)	Tr.	Tr.
49	15.39	155	Dodecane (d)	Tr.	Tr.
50	17.97	169	Tridecane (c)	0.95	0.92
51	20.69	183	Tetradecane (d)	Tr.	Tr.
52	22.50	197	Pentadecane (c)	0.96	0.86
53	24.56	211	Hexadecane (d)	Tr.	Tr.
54	26.50	225	Heptadecane (c)	Tr.	Tr.
55	28.85	239	Octadecane (d)	Tr.	Tr.
56	30.09	253	Nonadecane (c)	Tr.	Tr.
57	32.15	267	Eicosane (d)	Tr.	Tr.

Table 2 (*continued*)

Peak	R_t (min)	Characteristic fragment[a] *m/z*	Assignment (Identification[b])	Ratio	
				M_{20P}/NM_{20P}	M_{20P}/NM_{100P}
58	33.35	281	Heneicosane (d)	Tr.	Tr.
59	35.05	295	Docosane (d)	Tr.	Tr.
60	36.33	309	Tricosane (d)	Tr.	Tr.
Glycerides					
61	39.25	369	Monopalmitvaccenin (a, d)	**F**	**F**
62	39.32	371	Monopalmitin (b, c, d)	1.62	1.46
63	42.02	395	Monolinolein (b, c, d)	0.99	0.88
64	42.05	397	Monoolein (b, c, d)	1.60	1.54
65	42.15	397	Monovaccenin (a, d)	**F**	**F**
66	42.16	393	Monolinolenin (d)	1.2	1.18
67	42.33	399	Monostearin (b, c, d)	0.71	0.79
68	47.71	385	1,2-Dipalmitin (c)	Tr.	Tr.
69	47.78	383	Palmitvaccenoylpalmitoylglyceride (a, d)	**F**	**F**
70	49.89	483	Monolignocerin (c, d)	1.35	0.92
Sterols					
71	47.00	329	Cholesterol (b, c)	0.84	0.87
72	48.53	341	24-Methylene cholesterol[f]	**F**	**F**
73	48.60	343	Campesterol (a,)	**F**	**F**
74	49.50	345	Stigmasterol (b, c)	1.07	1.01

[a] Characteristic fragments for fatty acids, fatty alcohols, and alkanes $[M-15]^+$, for sterols $[M-139]^+$, for monoglycerides $[M-103]^+$, for diglycerides $[M-Acyl]^+$.

[b] (a) MS of reference compounds and/or nonpolar reference extract from hyphae and spores of *Glomus intraradices*; (b) NIST Mass Spectral Library 2002; (c) The Golm Metabolome Database; (d) recursive procedure of metabolite assignment.

[c] F-Fungal origin.

[d] Significant differences ($p < 0.05$) of the mean values (M_{20P}, NM_{20P}, NM_{100P}) are shown in boldface.

[e] Tr., trace.

[f] Schmitz et al. (1991).

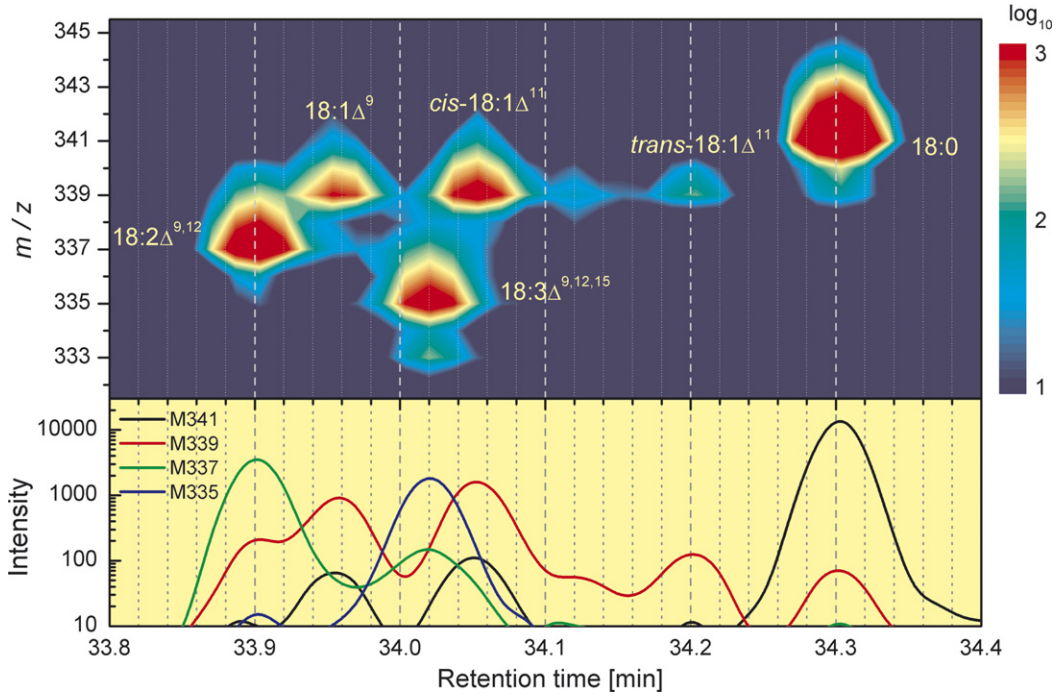

Fig. 7. R_t–*m/z*-plot of a retention time section around stearic acid of free fatty acids from hexane extracts (M_{20P}, 56 dai) analyzed by GC/TOF-MS (above) and ion current of characteristic fragments (below).

that the ratio of triacylglycerides and free fatty acids is 7:1 (Jabaji-Hare, 1988). To distinguish between different AM fungus species fatty acid methyl ester (FAME) profiling has been applied (Graham et al., 1995; Madan et al., 2002). All species showed the presence of palmitic acid (16:0). From all isolates, those of *G. intraradices*, showed

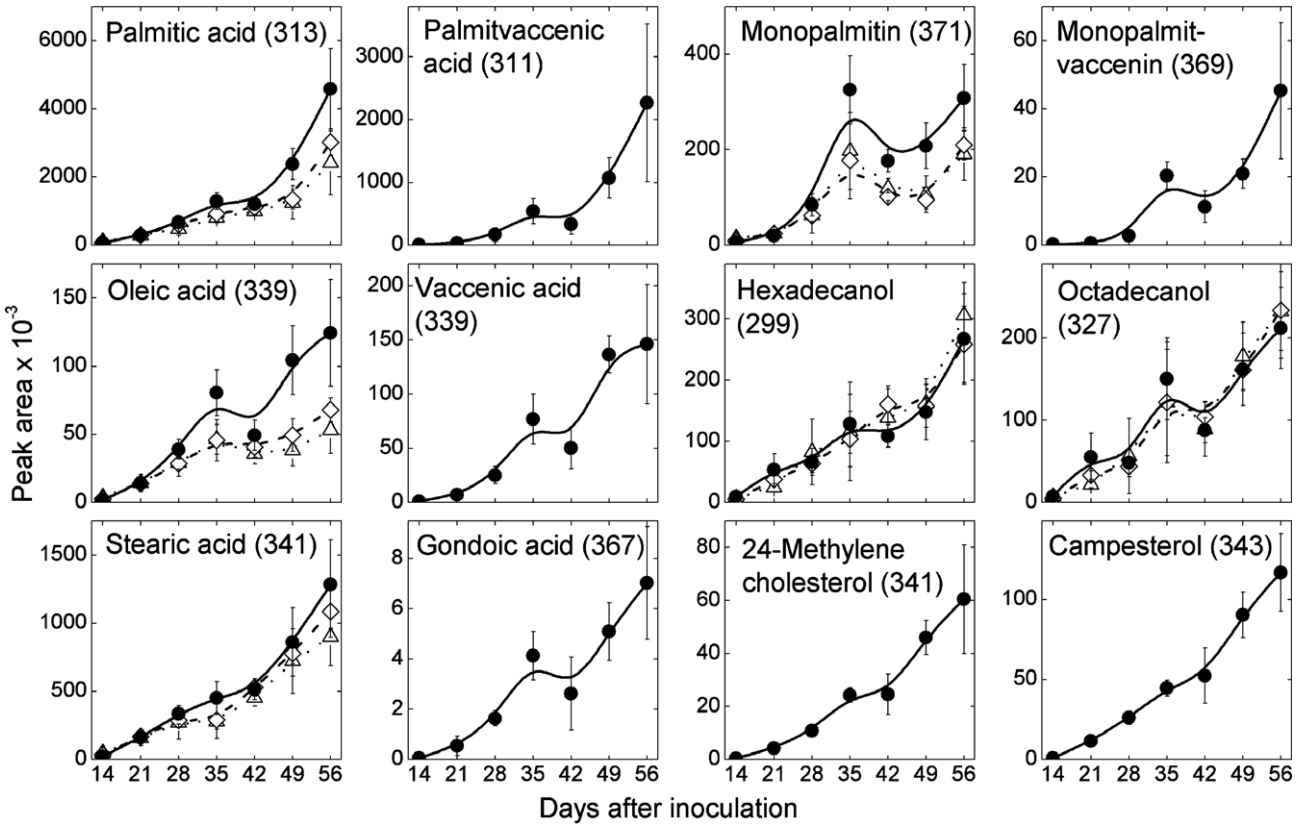

Fig. 8. Accumulation pattern (GC/TOF-MS) of primary nonpolar metabolite data. In brackets are the *m/z* values of characteristic fragment ions used for quantification. Left side: plant and fungal fatty acids, right side: selected monoglycerides, fatty alcohols and sterols (symbols as in Fig. 2). The amounts of two fatty acids from mycorrhizal roots at 42 dai were calculated as μmol (root system)$^{-1}$ and μmol (g dry wt)$^{-1}$: palmitic acid = 0.1 ± 0.02 and 3.3 ± 0.8; stearic acid = 0.04 ± 0.01 and 1.3 ± 0.3.

high levels of palmitvaccenic acid (>70% of total fatty acids), and low levels of vaccenic acid (18:1Δ^{11c}). Consequently, palmitvaccenic acid was called a signature fatty acid, and was used for AM fungal biomass estimation in roots and soil (Olsson, 1999; Olsson and Johansen, 2000; van Aarle and Olsson, 2003). Trépanier et al. (2005) published recently the most comprehensive analysis of fatty acids occurring in lipids of *G. intraradices* spores. They demonstrated the presence of more than 20 components and emphasized the specificity of palmitvaccenic acid for the fungus. Furthermore, they concluded from administration [^{14}C]labeled acetic acid and sucrose to carrot hairy root cultures colonized by *G. intraradices* that the fungus itself has no fatty acid synthase activity. Therefore, palmitic acid from the plant is required to be used for synthesis of palmitvaccenic and longer fatty acids. Moreover, it was suggested that genes of fatty acid synthesis in *G. intraradices* are expressed in intraradical hyphae, but not in extraradical ones. This regulation was claimed to be one of the reasons for the obligate symbiosis between AM fungi and their plant host (Trépanier et al., 2005). These data are in agreement with those published by Pfeffer et al. (1999). They showed that most of the fungal lipid synthesis occurs in the root compartment. Our fatty acid analysis of spores and hyphae of *G. intraradices* cultivated outside of plants revealed the dominance of both palmitic and palmitvaccenic acids (data not shown), which does not agree with the results of Trépanier et al. (2005).

Nordby et al. (1981) found campesterol (24-α-methyl-Δ^5-cholestenol) in *G. mosseae* as the predominant component. Its level, together with 24-methylene cholesterol, correlated with the degree of mycorrhization in maize and onions (Schmitz et al., 1991). Also in *G. intraradices*, campesterol was dominant with sitosterol, fucosterol and cholesterol as minor components, whereas ergosterol was not found (Fontaine et al., 2004). In the past, there was a debate on the occurrence and distribution of ergosterol in AM fungi due to frequent contamination with saprophytic fungi of high ergosterol contents. Whereas high ergosterol levels were found in ectomycorrhizal basidiomycetes, ascomycetes and saprophytic zygomycetes, neither HPLC nor GC–MSMS were able to detect ergosterol both in *G. intraradices* and in *Gigaspora margarita* (Olsson et al., 2003).

Stumpe et al. (2005) analyzed the alterations of esterified fatty acids in roots of *M. truncatula* colonized with *G. intraradices*. The fungal-specific fatty acids (16:1Δ^{11} and others) were only found in mycorrhizal roots, whereas the levels of palmitic (16:0) as well as oleic acid (18:1Δ^9) increased in comparison to nonmycorrhizal controls. These results agree with the free fatty acid levels reported here and previously published data (Lohse et al., 2005). In general, the increased levels of palmitic and oleic acids

(biosynthesized in plastids) in mycorrhizal roots in comparison to controls supports the statement of an activation of plastidial metabolism already deduced from the alterations of the amino acid levels discussed in Section 2.3. The increased phosphate concentrations in mycorrhizal roots (Fig. 2) may be one of the factors, which triggers this activation, but cannot be decisive as the levels of certain amino and fatty acids in M_{20P} are different from those of the NM_{100P} roots.

2.5. Root secondary metabolites

2.5.1. Isoflavonoids

In Fig. 9, a representative separation of the polar root extracts by HPLC is given. Identification of the well-known isoflavonoids and related compounds was mainly based on comparison with retention times and UV spectral data of reference compounds (daidzin, daidzein, formononetin, ononin, medicarpin) and to some extent on complete data from ESI-MS and ^{1}H NMR spectroscopy analyses (see Section 3). As malonylated isoflavone glucoside standards are not commercially available, the thermal transformation of e.g. malonylononin to ononin by heating-induced cleavage of the malonyl ester bond (Lin et al., 2000) was used to relate the prevailing malonylononin to the reference compound ononin. Isoflavone glucoside malonylation was also proven by MS fragmentation as described in Section 3.

During mycorrhization of *M. truncatula* roots, enhanced levels of isoflavonoids per root were confirmed, in particular for daidzein and ononin showing increased levels starting from 35 dai (Fig. 10). At 56 dai, the contents of daidzein, ononin, and malonylononin, were significantly higher in mycorrhizal roots than in the two nonmycorrhizal controls. By external standardization, the levels of ononin and the strongly dominating malonylononin were determined by HPLC analyses to be 0.5 and 5 μmol per g dry weight (M_{20P}, 56 dai), respectively. Both the isoflavonoid content and the root dry weight increased during the time course approximately tenfold. Medicarpin itself could not be detected, whereas the level of its conjugate, the 3-*O*-β-(6′-malonylglucoside), increased with time. However, no differences between mycorrhizal roots and the corresponding controls were observed. Besides tryptophan, detected in these chromatograms, several other components not identified so far showed significant quantitative differences (Table 3).

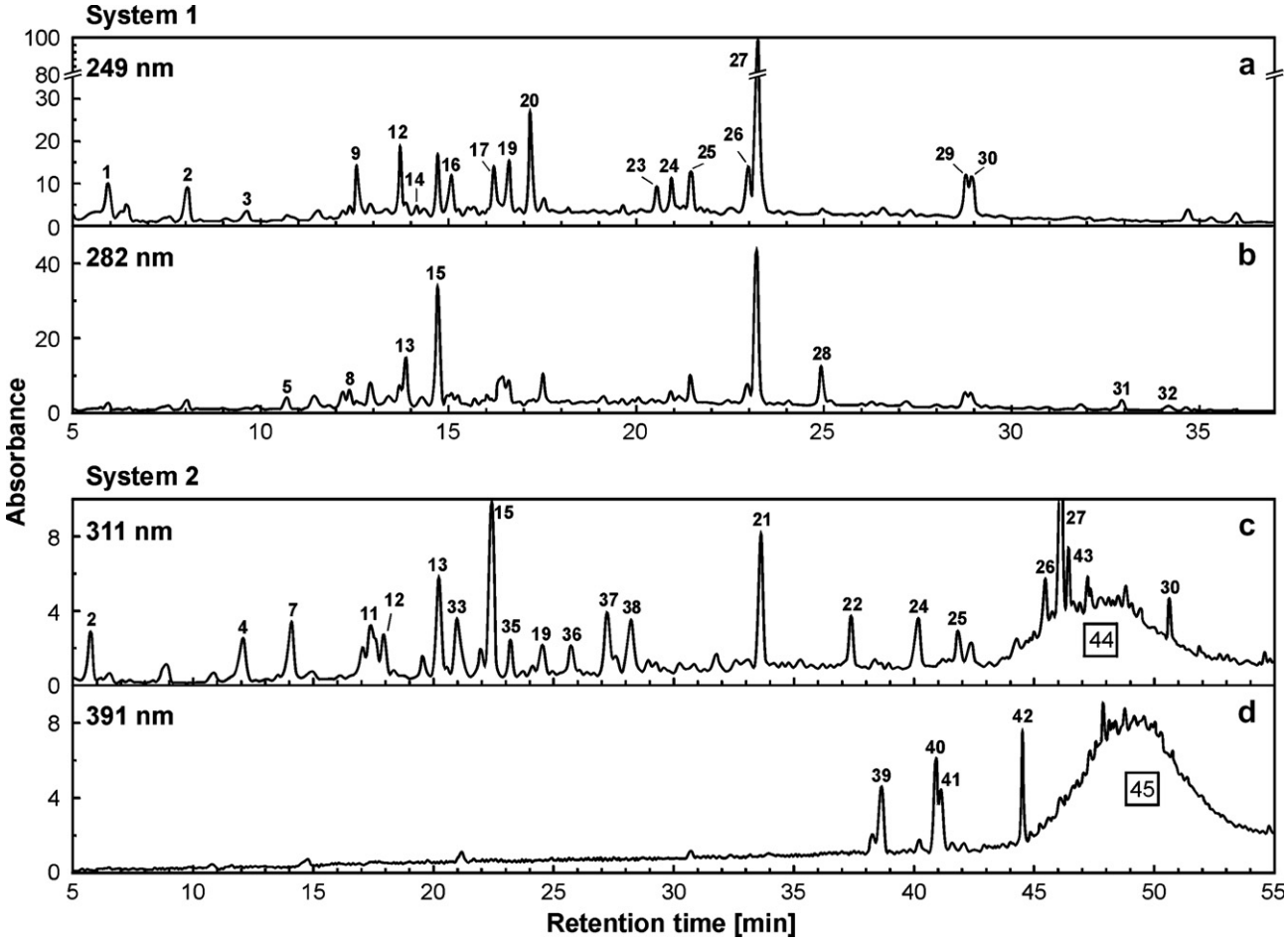

Fig. 9. HPLC chromatograms of soluble root metabolites, monitored at different wavelengths (M_{20P}, 56 dai). System 1: a, 249 nm; b, 282 nm; system 2: c, 311 nm; d, 391 nm. Peak numbering corresponds to metabolite numbering in Table 3.

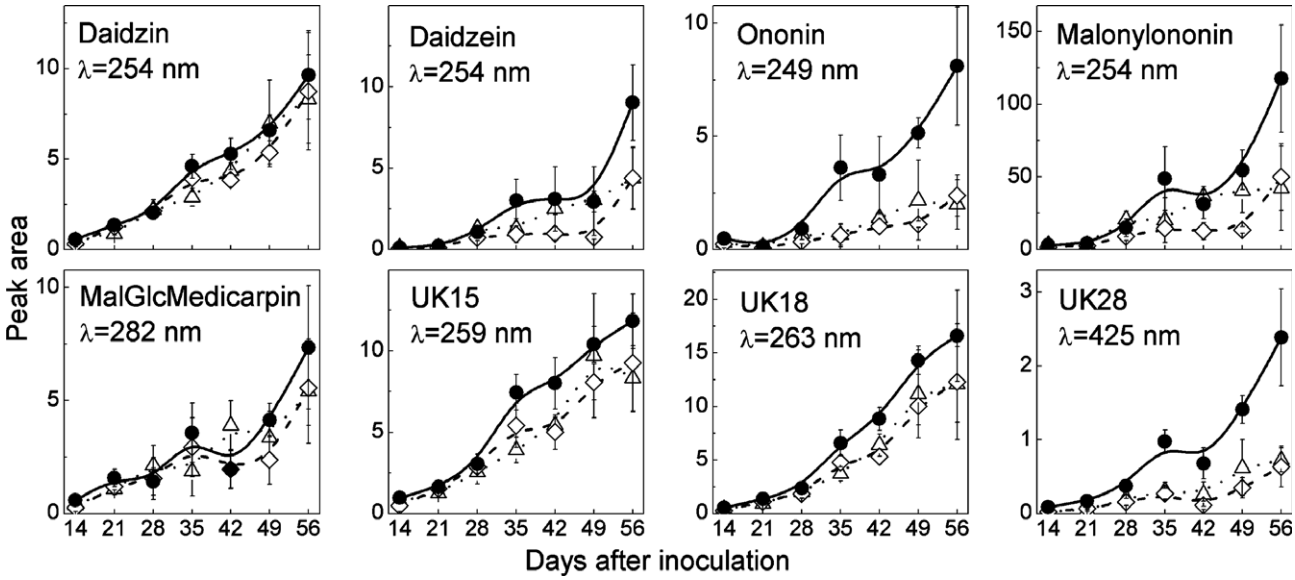

Fig. 10. Accumulation pattern (HPLC) of isoflavonoids and of some major unknowns. Compounds were quantified at the inserted λ-values (symbols as in Fig. 2). The amounts of two isoflavonoids from mycorrhizal roots at 56 dai were calculated as μmol (root system)$^{-1}$ and μmol (g dry wt)$^{-1}$: ononin = 0.02 ± 0.005 and 0.5 ± 0.2; malonylononin = 0.2 ± 0.05 and 5 ± 2.

Whereas the predominant classes of flavonoids, e.g. flavonols or flavones, accumulate in most families of the plant kingdom, the isoflavonoids are characteristic secondary metabolites of leguminous plants (Dixon, 1999). However, they also occur in at least 48 non-leguminous angiosperm families (Mackova et al., 2006). Different classes of isoflavonoids may be formed constitutively in various plant tissues, but may also be synthesized *de novo* in response to biotic or abiotic stress (Dixon, 1999).

In the forage legume alfalfa (*Medicago sativa*), glucosides and malonyl glucosides of the isoflavones daidzein and formononetin (Sumner et al., 1996) and of the pterocarpan medicarpin occur constitutively primarily in roots, whereas medicarpin itself and others (e.g. coumestrol, sativan, vestitol) are the prominent phytoalexins with antifungal activities (Dixon, 1999). Medicarpin is thought to be an important component of the defense response of these legumes to certain fungal pathogens, but direct proof is scarcely found (He and Dixon, 2000). These compounds also occur in *M. truncatula* (Baggett et al., 2002), but most of the results concerning the role of isoflavonoids in mycorrhizal interactions and in *Rhizobium*-legume symbiosis came from studies with alfalfa and other legumes. It was found that daidzein, the precursor of formononetin, stimulates germination of *G. mosseae* and *G. intraradices* spores (Kape et al., 1992). It was also shown that daidzein acts as one of the major *nod* gene inducers in the soybean-*Bradyrhizobium* symbiosis (Kosslak et al., 1987). A complex behavior of flavonoid formation was described for white clover (*Trifolium repens*) roots inoculated with *G. intraradices* (Ponce et al., 2004). Whereas two flavonoids occurring only in nonmycorrhizal roots stimulated most of the presymbiotic stages of *Gigaspora* in vitro, acacetin and rhamnetin, formed exclusively in mycorrhizal roots, exhibited inhibitory effects on both *Gigaspora* and *Glomus*, pointing towards a possible implication in the autoregulation of mycorrhization (Scervino et al., 2005).

One of the problems in studying root interactions with arbuscular fungi is the absence of synchronous colonization. Because roots usually contain all stages of developing and senescing arbuscules, measurements of transcriptional and enzymatic activities as well as metabolite levels produce mean values, which may obscure significant mycorrhiza-specific metabolic changes in arbuscule-harboring cells. It was found that the first contact of *M. truncatula* roots with *G. intraradices* led to induction of a chalcone synthase (*Mt-chs1*) (Bonanomi et al., 2001), a key enzyme in flavonoid biosynthesis. Colonization by *G. versiforme* resulted in down-regulation of the gene encoding isoflavone reductase, the penultimate enzyme of medicarpin biosynthesis, but medicarpin itself did not accumulate (Harrison and Dixon, 1993). This process was correlated with a reduction in the amounts of transcripts of enzymes specific for late stages of isoflavonoid biosynthesis, although the root cells harboring the arbuscules contained elevated transcript levels for enzymes of the general phenylpropanoid pathway. This may indicate a tight and differential control of different branches of secondary metabolism during establishment and maintenance of this symbiotic association (Harrison and Dixon, 1993, 1994). The isoflavonoid profiles of alfalfa and *M. truncatula* roots are similar and are dominated by the major compound formononetin 7-*O*-β-(6′-*O*-malonylglucoside) (malonylononin) (Sumner et al., 1996; Baggett et al., 2002), whereas formononetin 7-*O*-β-glucoside (ononin) and the aglycone formononetin (7-hydroxy-4′-methoxy-isoflavone) are minor components. Due to the sensitivity of the malonyl ester linkage to hydrolysis solvent extraction should be done

Table 3
HPLC separation and characteristics of metabolites of mycorrhizal roots of *M. truncatula* (56 dai) and M_{20P}/NM ratios

Peak	R_t (min)	λ_{max} (nm)	Assignment	Ratio	
				M_{20P}/NM_{20P}	M_{20P}/NM_{100P}
System 1					
1	5.92	258	UK1[a]	0.69	0.82
2	8.03	239, 261, 328	UK2	1.26	1.49
3	9.63	252	UK3	1.00	1.04
4	9.92	229, 312	UK4	1.21	1.14
5	10.70	276, 300sh	UK5	**1.54**[b]	**1.47**
6	11.42	235sh, 314	UK6	1.24	1.47
7	12.18	230, 316	UK7	1.14	1.11
8	12.37	218, 277	Tryptophan	1.72	**2.22**
9	12.55	258	UK8	1.42	1.58
10	12.93	296	UK9	1.23	1.67
11	13.40	230, 315	UK10	1.12	1.58
12	13.70	221, 249, 307	UK11	1.18	**1.81**
13	13.87	219, 282, 319	UK12	0.94	1.35
14	14.13	244	**1**	**M**[c]	**M**
15	14.70	230sh, 284, 325	UK13	**1.44**	**1.54**
16	15.07	230sh, 252, 297	Daidzin	1.10	1.17
17	16.20	246	**2**	**M**	**M**
18	16.32	230sh, 284, 326	UK14	1.24	1.14
19	16.58	223, 260, 295	UK 15	1.42	1.27
20	17.17	243	**3**	**M**	**M**
21	17.50	218, 314	UK16	0.88	1.43
22	19.12	220, 250sh, 313	UK17	1.48	0.91
23	20.52	245	**4**	**M**	**M**
24	20.90	251, 300sh	Ononin	**4.00**	**3.43**
25	21.42	222, 264, 294	UK18	1.22	1.30
26	22.95	252, 298	Daidzein	**2.07**	**2.07**
27	23.18	257, 300sh	Malonylononin	**2.78**	**2.38**
28	24.92	230sh, 283	Medicarpin 3-*O*-(6′-MalGlc)	1.35	1.33
29	28.73	258	UK19	1.13	0.97
30	28.92	249, 302	Formononetin	0.84	0.86
31	32.93	296	UK20	1.46	**6.90**
32	34.15	296	UK21	1.18	**17.25**
System 2					
33	21.02	240sh, 319, 340sh	UK22	**M**	**M**
34	22.02	280sh, 318	UK23	**M**	**M**
35	23.22	221, 316	UK24	**M**	**M**
36	25.77	220sh, 236, 295, 317	UK25	1.01	0.96
37	27.25	221, 265, 291, 335sh	UK26	**1.99**	**1.89**
38	28.23	220, 240sh, 285, 322	UK27	1.07	1.04
39	38.68	208, 247, 430	UK28	**3.29**	**3.83**
40	40.95	217, 370sh, 385, 406	Mycorradicin derivative 1	**M**	**M**
41	41.20	283, 380, 390, 405sh	Mycorradicin derivative 2	**M**	**M**
42	44.57	281, 360sh, 378, 397sh	Mycorradicin derivative 3	**M**	**M**
43	46.45	217, 285sh, 318	UK29	1.13	0.97
44	43.5–52.0	241, 314	315 nm-complex	**3.91**	**4.19**
45	44.0–54.0	315, 360sh, 382, 404	"Yellow pigment"	**M**	**M**
			Minor		
	38.37		Mycorradicin derivative 4	**M**	**M**
	40.28		Mycorradicin derivative 5	**M**	**M**
	41.63		Mycorradicin derivative 6	**M**	**M**
	42.10		Mycorradicin derivative 7	**M**	**M**

Peak numbers 1–32 are from HPLC system 1, 33–45 from system 2.
[a] UK – unknown metabolite.
[b] Significant differences ($p < 0.05$) of the mean values (M_{20P}, NM_{20P}, NM_{100P}) are shown in boldface.
[c] M-Mycorrhiza-induced.

with care. Harrison and Dixon (1993) found a 3.5-fold higher accumulation of malonylononin in 40-day-old *M. truncatula* roots colonized by *G. versiforme* in comparison to nonmycorrhizal controls. Interestingly, in alfalfa, the malonylononin level was considerably higher, but did not show a significant increase upon colonization. Volpin

et al. (1995) found a suppression of the isoflavonoid phytoalexin defense response in alfalfa roots colonized by *G. intraradices*. By HPLC analyses they assigned four peaks as formononetin 7-*O*-glycosides (malonylononin was not mentioned) and a consistent increase of the formononetin content was measured until 35 dai. By contrast, levels of medicarpin 3-*O*-glucoside in mycorrhizal roots were lower than in control roots at any time. Larose et al. (2002) reported on the modulation of isoflavonoid levels in roots of alfalfa dependent on the colonizing *Glomus* species. They found a fivefold higher level of formononetin than ononin (malonylononin was not mentioned again) that disagrees with other studies (Dakora et al., 1993; Harrison and Dixon, 1993; Tiller et al., 1994; Parry et al., 1994; Sumner et al., 1996; Baggett et al., 2002). The occurrence of daidzein, formononetin and medicarpin as major aglycones (after acid hydrolysis) already in one-week-old roots of *M. truncatula* cv Jemalong A17 has been recently reported (Wasson et al., 2006) supporting our results. Farag et al. (2007) reported on the identification of flavonoids and isoflavonoids in cell suspension cultures and roots of *M. truncatula*. Special attention was paid to the different occurrence and relative abundance of secondary metabolites based on umbelliferone as an internal standard. The flavonoid/isoflavonoid pattern of cell cultures was more complex than those of the roots. Major components of the latter remains unknown and the level of formononetin was higher than that of the corresponding glucoside (ononin) is an unexpected result.

In summary, it may be noted that different alterations of root isoflavonoid levels during mycorrhization have been observed depending on (i) the fungus used (Larose et al., 2002), (ii) the plant species involved (Harrison and Dixon, 1993) and (iii) the harvest time of the mycorrhizal roots and the extraction procedure applied. In general, an activation of certain parts of the isoflavonoid pathway resulting in increased levels of isoflavonoids in mycorrhizal roots can be ascertained by the present results. This corresponds to the expression analysis of genes in roots of *M. truncatula* colonized by *G. versiforme* showing the mycorrhiza-induced enhanced expression of an isoflavonoid glucosyltransferase gene (Liu et al., 2007).

2.5.2. Apocarotenoids

A clear-cut feature of mycorrhizal root extracts is the presence of cyclohexenone derivatives and the so-called "yellow pigment" (Gerdemann, 1964; Daft and Nicolson, 1972; Becker and Gerdemann, 1977). Besides their common occurrence, additional apocarotenoids containing the mycorradicin chromophore were found to accumulate steadily during the progress of mycorrhization (Fig. 11).

By aligning and averaging the HPLC data of five parallels of the different sample sets, a ratio plot was developed and used to easily detect at once all quantitative changes of the different plant sets. The ratio is given in a color code based on $\log_2$. In Fig. 12, the ratio plot for the M_{20P}/NM_{100P} pair at 56 dai is given. The occurrence of mycorrhiza-specific apocarotenoids can clearly be seen, i.e. cyclohexenone derivatives with absorption maxima at 245 nm and mycorradicin derivatives with absorption maxima at 390 nm. In addition to the increased levels of isoflavonoids discussed in Section 2.5.1, an enhanced level of a mixture of compounds with absorption maxima at 315 nm ("complex 315 nm") was observed. The compounds, which give rise to the red spots at R_t 32.9 and 34.1 min in Fig. 12, are due to a marked decrease in concentration upon full phosphate supply (NM_{100P}), which was not detected in NM_{20P}. Unfortunately, the identification

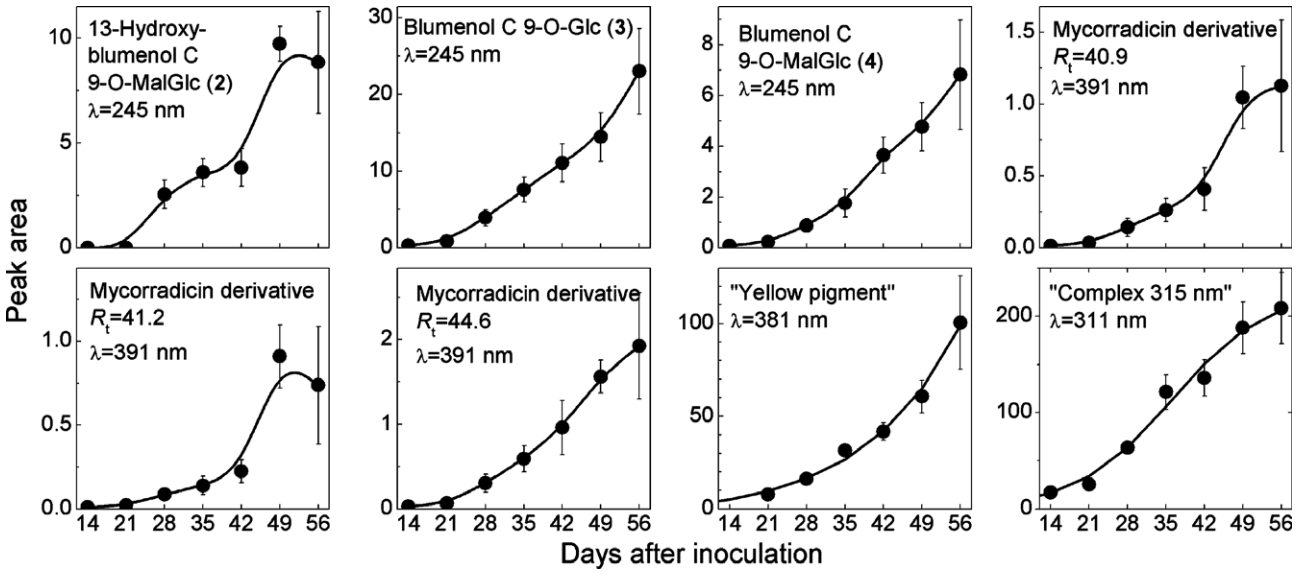

Fig. 11. Accumulation pattern (HPLC) of apocarotenoids and some major unknowns included in "complex 315". Compounds were quantified at the inserted λ-values (symbols as in Fig. 2). The amounts of cyclohexenone and mycorradicin derivatives in mycorrhizal roots (56 dai) were determined to be 0.73 ± 0.18 μmol and 0.69 ± 0.28 μmol (g dry wt)$^{-1}$, respectively.

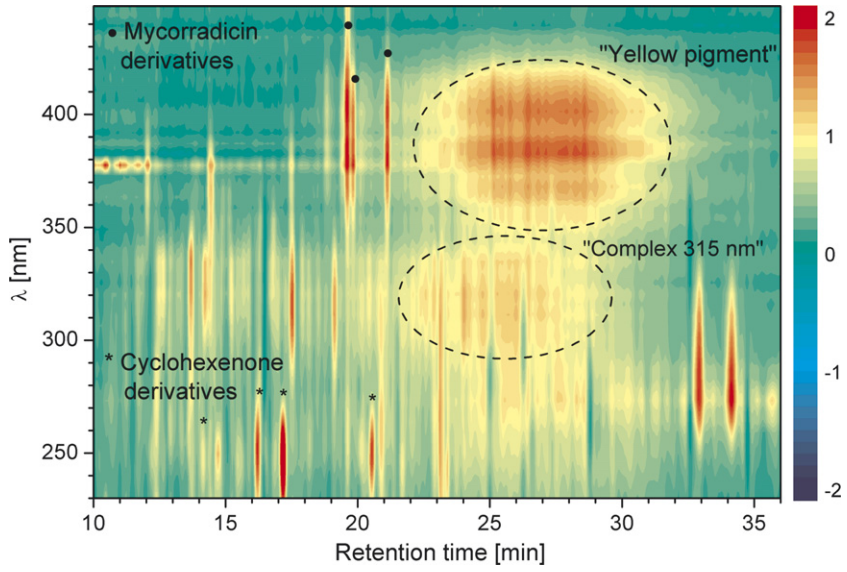

Fig. 12. Averaged R_t–λ-ratio plot (M_{20P}/NM_{100P}) (56 dai) of secondary metabolites analyzed by HPLC showing in lg_2 scale (second ordinate, right) AM-induced metabolite alterations.

of these compounds by MS and NMR spectroscopy failed due to strong contamination with major saponins (peak 19 and 20, see Section 2.5.3). Some yellow apocarotenoids eluting in front of the "yellow pigment" were also detected. Both the alkaline hydrolysis of these yellow apocarotenoids and the "yellow pigment" liberated mycorradicin isomers. Other hydrolysis products of this complex were not observed by UV detection. Until now no further structural information could be obtained for the mycorradicin-derived compounds and the "yellow pigment".

On the other hand, the cyclohexenone derivatives were isolated by preparative HPLC and identified by high resolution ESI-HRMS and ^{1}H NMR spectroscopy. Compound **1** was found to be identical by comparison of HPLC retention time and UV spectral data (R_t 14.13 min, λ_{max} 244 nm) as well as by ESI-HRMS and ^{1}H NMR spectroscopic analysis with 13-hydroxyblumenol C 9-*O*-β-glucoside, recently identified from mycorrhizal roots of *Ornithogalum umbellatum* (Schliemann et al., 2006a). Compound **2** was less polar (R_t 16.20 min, λ_{max} 246 nm) than **1** indicating possible acylation. This was indeed confirmed by ESI-HRMS resulting in a $[M+Na]^+$ ion of m/z 497.1990 ($C_{22}H_{34}O_{11}Na$) in comparison to 411.1990 for **1**. The mass difference of 86 and the elemental composition indicated the presence of a malonyl residue, an acyl moiety typical both for isoflavonoids (Dixon, 1999) and saponins (Huhman and Sumner, 2002) in legumes. Therefore, compound **2** was assigned as 13-hydroxyblumenol C 9-*O*-β-(6′-*O*-malonylglucoside). Compound **3** (R_t 17.17 min, λ_{max} 243 nm, $[M+Na]^+$ ion of m/z 395.2031, $C_{19}H_{32}O_7Na$) showed a mass difference of 16 in comparison to **1**, pointing to a lack of an oxygen. The ^{1}H NMR spectroscopic data of **3** concerning the aglycone were identical with those of blumenol C (Maier et al., 1995, 2000) and the characteristic chemical shifts proved the presence of glucose. The β-configuration of glucose was deduced from the large ^{1}H coupling constant for H-1′ ($J_{1',2'} = 7.7$ Hz), whereas long-range correlation showed an attachment of this glucose to C-9 of the aglycone. Hence, the structure of **3** is blumenol C 9-*O*-β-glucoside. Compound **4** (R_t 20.52 min, λ_{max} 245 nm, $[M+Na]^+$ ion of m/z 481.2042, $C_{22}H_{34}O_{10}Na$) differs from **3** by an additional malonyl moiety, determined by ESI-HRMS, leading to its structure as blumenol C 9-*O*-β-(6′-*O*-malonylglucoside) (Fig. 13). Whereas **1** was recently found as a component of the complex apocarotenoid pattern detected in mycorrhizal roots of *Ornithogalum umbellatum* (Schliemann et al., 2006a), compounds **2**, **3**, and **4** are new natural products. On the basis of CD spectra

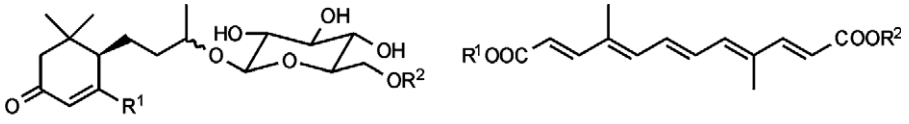

1 $R^1 = CH_2OH$, $R^2 = H$
2 $R^1 = CH_2OH$, $R^2 = -COCH_2CO_2H$
3 $R^1 = CH_3$, $R^2 = H$
4 $R^1 = CH_3$, $R^2 = -COCH_2CO_2H$

$R^1 = R^2 = H$, Mycorradicin
$R^1 = R^2 =$ unknown, "Yellow pigment"

Fig. 13. Structure scheme of identified apocarotenoids.

of blumenin isomers (Schliemann et al., 2006a) and comparison of the molar ellipticity data with literature (Miyase et al., 1988), a 6*R*-configuration has been assigned. This holds also true for the main cyclohexenone derivative isolated from mycorrhizal roots of *Ornithogalum umbellatum* (Schliemann et al., 2006a), suggesting this configuration for all mycorrhiza-induced cyclohexenone derivatives. With the progress of mycorrhization, the amounts of cyclohexenone derivatives, yellow apocarotenoids and the "yellow pigment" as mycorrhiza-induced secondary metabolites increase (Fig. 11). The amount of accumulating cyclohexenone and mycorradicin derivatives in mycorrhizal roots (56 dai) were determined to be 0.73 ± 0.18 μmol and 0.69 ± 0.28 μmol (g dry wt)$^{-1}$, respectively, by external standardization (see Section 3). This is a molar ratio of 1.05:1 for the two major apocarotenoid groups, deviating from the 2:1 ratio anticipated from degradation of a putative carotenoid precursor having α-ionyl rings at both ends. For the found ratio, it is tempting to propose a carotenoid with one α-ionyl end group (e.g. lutein, the most abundant hydroxylated carotenoid in plants) as putative precursor. But only *E*- and *Z*-ζ-carotene accumulated specifically in mycorrhizal roots of *M. truncatula* (Fester et al., 2002b) and β-ionone-type cyclohexenones have not been found as mycorrhiza-induced components so far. Searching for another possible precursor, the rare lactucaxanthin (Siefermann-Harms et al., 1981; Cunningham and Gantt, 2001) possessing two α-ionone end groups is structurally most closely related to the structures of the cyclohexenone derivatives (Strack and Fester, 2006). A mycorrhiza-specific carotenoid cleavage dioxygenase (CCD) has been identified from *Zea mays* as an AtCCD1 homolog (EMBL accession number AY773278; J. Hans, T. Fester and M.H. Walter, unpublished). Thus, we assume that cyclohexenone and mycorradicin derivatives should accumulate in a 2:1 ratio due to the symmetrical cleavage by CCD1 (Schwartz et al., 2001). It should be noted, however, in contrast to this assumed stoichiometric relation and to the present results a large part of the mycorradicin was not detectable in most of the other mycorrhizal plants studied so far (Fester et al., 2002a). In any case, a deviation from the expected stoichiometric relation is conceivable due to different metabolic fates of the C_{13}- and C_{14}-cleavage products of the putative carotenoid precursor (Strack and Fester, 2006).

It is long known (Jones, 1924) that many, but not all, plants form yellow colored roots when colonized by AM fungi. The chromophore of this "yellow pigment" was isolated from mycorrhizal maize roots and identified as a C_{14} polyenic acid (10,10′-diapocarotene-10,10′-dioic acid), named mycorradicin (Bothe et al., 1994; Klingner et al., 1995a). Because of structural similarities of mycorradicin with the C_{27}-apocarotenoid azafrin (Eschenmoser and Eugster, 1975), speculations of its formation suggested a C_{40}-carotenoid precursor from which two C_{13}-units have to be cleaved (Klingner et al., 1995a,b). Later on, carotenoid cleavage dioxygenases (AtCCD1, CsCCD) from *A. thaliana* and saffron (*Crocus sativus*) were functionally characterized (Schwartz et al., 2001; Bouvier et al., 2003) being responsible for the formation of a C_{14}-dialdehyde by splitting the 9,10(9′,10′) double bonds of certain carotenoids. Orthologs of the corresponding genes are present in a wide range of plants and the C_{14}-dialdehyde is the probable precursor of both rosafluen (C_{14}-diol) (Eugster and Märki-Fischer, 1991) and mycorradicin (C_{14}-dicarboxylic acid). At the same time at which mycorradicin was identified, the structure of a C_{13}-cyclohexenone glycoside (blumenin) occurring specifically in mycorrhizal cereal roots was elucidated. Its level was directly correlated with the degree of mycorrhization (Maier et al., 1995). That this C_{13} compound blumenin is also derived from carotenoids was shown by retrobiosynthetic studies (Maier et al., 1998). It was recognized that this type of compound may be the missing link (C_{13} apocarotenoid) between C_{40}-carotenoids and mycorradicin (C_{14} apocarotenoid). Consequently, the formation of both groups of apocarotenoids by oxidative cleavage of a carotenoid precursor was proposed (Walter et al., 2000). Mycorrhiza-induced cyclohexenone derivatives were found not only in roots of Poaceae (Maier et al., 1997), but also in Solanaceous plants (tobacco, tomato; Maier et al., 1999, 2000; see review, Strack et al., 2003; Strack and Fester, 2006). Recently, it was shown that mycorrhizal roots of *L. japonicus* (Leguminosae) contain also AM-specific cyclohexenone derivatives (Fester et al., 2005).

Fester et al. (2002a) demonstrated that the amounts of mycorradicin released by alkaline hydrolysis of extracts from different mycorrhizal roots are highly variable. Even the complete lack of mycorradicin in roots with a high degree of mycorrhization was observed. Until now, nothing is known about the possible function of the apocarotenoids in AM symbiosis despite extensive studies on these compounds. The main cyclohexenone glycoside isolated from mycorrhizal barley roots is blumenin (Maier et al., 1995). Repeated application of this compound to barley roots resulted in strong inhibition of fungal colonization accompanied by reduced arbuscule formation at early stages of mycorrhiza development. Furthermore, the accumulation of coumaroylputrescine and coumaroylagmatine, especially the latter at later stages, is reduced by the blumenin treatment, although blumenin and its aglycone blumenol C did not show any antifungal activity (Fester et al., 1999). While the role of apocarotenoids in mycorrhizal symbiosis is under debate (Strack and Fester, 2006; Walter et al., 2007), this group of compounds play essential roles in other systems. Recently, 5-deoxystrigol was isolated from *L. japonicus* root exudates as a hyphal branching factor in AM fungi (Akiyama et al., 2005). This compound also originates from cleavage of carotenoids (Matusova et al., 2005). Additionally, the related sorgolactone was identified in root exudates of *Sorghum bicolor*, which activates at very low concentrations fungal mitochondria leading to hyphal branching of *Gigaspora rosea* (Besserer et al., 2006). Also in Arabidopsis molecular cues

involved in the regulation of lateral root branching arise from carotenoid cleavage (Schwartz et al., 2004; Bouvier et al., 2005; Auldridge et al., 2006). Although the stimulation of carotenoid biosynthesis in AM roots as a prerequisite for the sometimes observed massive formation and accumulation of apocarotenoids seems to be a general phenomenon (Fester et al., 2002a, 2005), the rationale for the formation of both groups of apocarotenoids and their function in mycorrhiza development is under discussion (Strack and Fester, 2006; Akiyama, 2007; Walter et al., 2007).

2.5.3. Saponins

The LC–MS analysis of *M. truncatula* root extracts demonstrated the occurrence of 26 saponins, which were structurally assigned mainly on the basis of published fragmentation data under negative ionization (Huhman et al., 2005). The previously found malonyl conjugates of medicagenic acid 3-*O*-glucoside and medicagenic acid 3,28-*O*-diglucoside could be confirmed (Table 4). Additionally, on the basis of the characteristic $[M-86-H]^-$ and $[M-86+H]^+$ ions, indicating a malonyl moiety, the presence of new malonyl conjugates of 3-Rha-Gal-GlcU-soyasapogenol B and Rha-Gal-GlcU-soyasapogenol E is suggested. A representative saponin separation is shown in Fig. 14. The elution pattern of the saponins is illustrated (A, total ion current *m/z* 450–2000) including the intensities of characteristic deprotonated molecular ions of selected malonylated and the corresponding nonmalonylated saponins (Fig. 14b–g). Between the concentrations of saponins and the corresponding malonyl conjugate a strong linear correlation exists, exemplified for the pair Rha-Gal-GlcU-soyasapogenol E (saponin peak 19) (*m/z* 939) and Mal-Rha-Gal-GlcU-soyasapogenol E (saponin peak 20) (*m/z* 1025). The correlation coefficients between these two metabolites (in five parallels of seven harvest days) for the three different plant sets [M_{20P}, NM_{100P} and NM_{20P}] are 0.95, 0.92, and 0.98, respectively. The concentration of the malonyl conjugate (peak 20) is at all harvest times lower than that of the parent compound. The ratio between malonylated and the corresponding nonmalonylated saponin is identically reduced in both mycorrhizal roots (20% phosphate fertilization) and in NM_{100P} ones, but not in NM_{20P} roots. This demonstrates that both the mycorrhization and the full supply with phosphate show the same reducing effects on malonylation of saponins (data not shown).

The second important group of constitutive secondary metabolites in roots of *Medicago* besides isoflavonoids

Table 4
Saponins from roots of *M. truncatula* (NM_{100P}, 56 dai) and LC/ESI-MS characteristics (fragment mass, R_t)

Peak	R_t (min)	$[M-H]^-$ *m/z*	Fragments in negative ion ESI-MS *m/z*	Positive ion ESI-MS *m/z*	Structural assignment and peak numbers according to Huhman et al. (2005)
1	55.5	987	722		Unknown saponin
2	57.5	973	811 $[M-Hex]^-$	997 $[M+Na]^+$	Hex-Hex-Hex-**Bayogenin** (3)
3	59.6	1103	941 $[M-Hex]^-$	1127 $[M+Na]^+$	Rha-Hex-Hex-Hex-**Hederagenin** (5)
4	60.8	825			3-Glc-28-Glc-**Medicagenic acid** (7)
5	63.1	911	867 $[M-CO_2]^-$	935 $[M+Na]^+$	Mal-3-Glc-28-Glc-**Medicagenic acid** (8)
6	66.4	1087	925 $[M-Hex]^-$, 911, 765 $[911-Rha]^-$		Rha-Hex-Hex-Hex-**Soyasapogenol E** (11)
7	71.3	957	851		Hex-Hex-Rha-**Bayogenin** (13)
8	73.1	897	837, 735 $[M-Hex]^-$		Unknown saponin
9	74.6	941			Rha-Hex-Hex-**Hederagenin** (15)
10	75.4	811			Hex-Hex-**Bayogenin** (16)
11	76.2	825	663 $[M-Hex]^-$		3-Glc-Glc-**Medicagenic acid** (17)
12	77.8	649			Hex-**Bayogenin** (20)
13	79.2	663			3-Glc-**Medicagenic acid** (21)
14	79.8	941		943 $[M+H]^+$, 797 $[M-Rha+H]^+$	3-Rha-Gal-GlcU-**Soyasapogenol B** (18)
15	80.6	809			Hex-Hex-(unknown Aglycone) (19)
16	81.3	749	705 $[M-CO_2]^-$		Mal-3-Glc-**Medicagenic acid** (22)
17	81.7	1027	983 $[M-CO_2]^-$, 939 $[M-Mal]^-$	1029 $[M+H]^+$	Mal-3-Rha-Gal-GlcU-**Soyasapogenol B**
18	82.7	765			Ara-Hex-**Hederagenin** (25)
19	83.7	939	647	963 $[M+Na]^+$, 941 $[M+H]^+$, 795 $[M-Rha+H]^+$	Rha-Gal-GlcU-**Soyasapogenol E** (23)
20	85.3	1025	981 $[M-CO_2]^-$, 939 $[M-Mal+H]^-$, 793 $[M-Mal-Rha+H]^-$	1027 $[M+H]^+$, 941 $[M-Mal+H]^+$, 795 $[M-Mal-Rha+H]^+$, 439 $[Agly-H_2O+H]^+$	Mal-Rha-Gal-GlcU-**Soyasapogenol E**
21	87.6	689	629		Unknown saponin
22	89.2	603			Pen-**Hederagenin** (29)
23	91.0	647			GlcU-**Hederagenin** (27)
24	92.6	633			Hex-**Hederagenin**1 (26)
25	96.8	633			Hex-**Hederagenin**2 (30)
26	98.5	617			Hex-**Soayasapogenol E** (31)

Abbreviations: Agly – Aglycone; Hex – Hexose; Pen – Pentose; Mal – Malonyl.

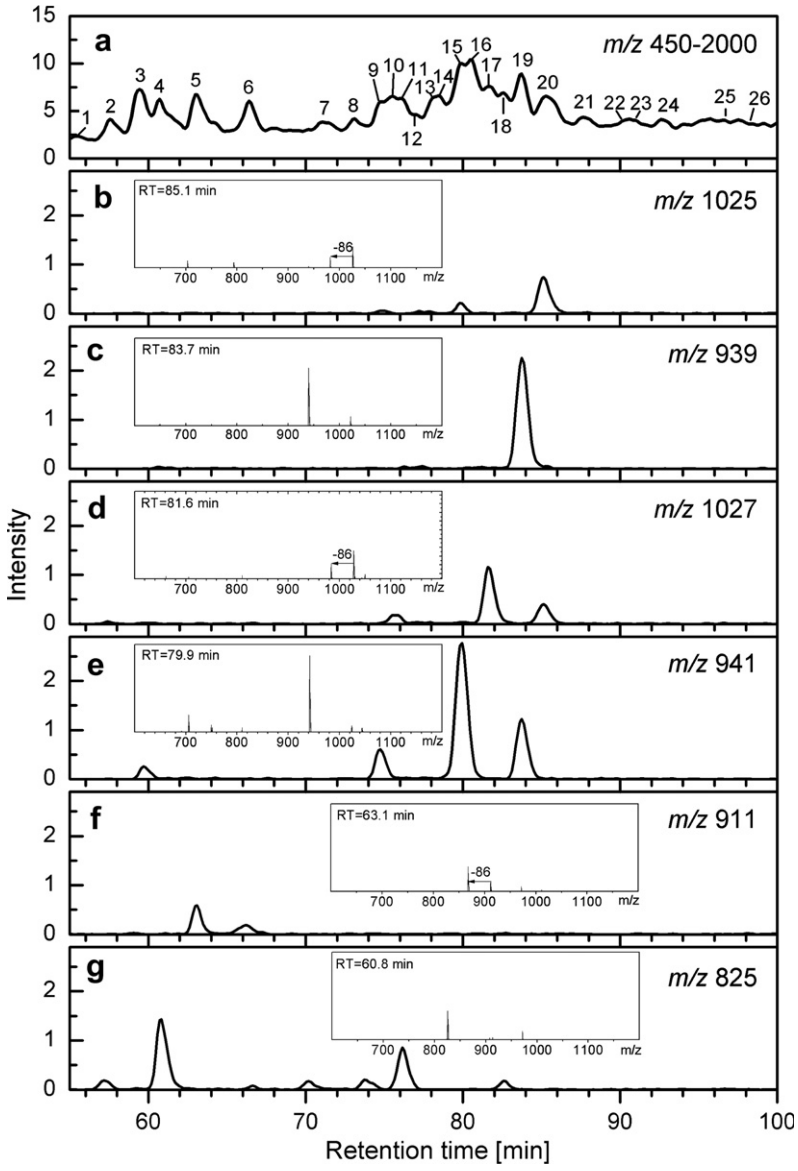

Fig. 14. Representative total ion and selected ion chromatograms of saponins (LC–MS, negative ionization, NM_{100P}, 56 dai). a – TIC (*m/z* 450–2000; numbering corresponds to Table 4). b – Selected ion chromatogram (*m/z* 1025, $[M-H]^-$, inset: MS of Mal-Rha-Gal-GlcU-soyasapogenol E); c – Selected ion chromatogram (*m/z* 939, $[M-H]^-$, inset: MS of Rha-Gal-GlcU-soyasapogenol E); d – Selected ion chromatogram (*m/z* 1027, $[M-H]^-$, inset: MS of Mal-3-Rha-Gal-GlcU-soyasapogenol B); e – Selected ion chromatogram (*m/z* 941, $[M-H]^-$, inset: MS of 3-Rha-Gal-GlcU-soyasapogenol B); f – selected ion chromatogram (*m/z* 911, $[M-H]^-$, inset: MS of Mal-3-Glc-28-Glc-medicagenic acid); g – selected ion chromatogram (*m/z* 825, $[M-H]^-$, inset: MS of 3-Glc-28-Glc-medicagenic acid); the inset in b, d, f show the preferential cleaving off $[M-86]^-$ of the malonyl moieties from the malonyl conjugates.

are triterpene glycosides (saponins). In alfalfa, the saponins are glycosylated derivatives of medicagenic acid, zanhic acid, bayogenin, hederagenin and soyasapogenols B and E (Oleszek et al., 1990, 1992; Oleszek, 1996; Bialy et al., 1999). Identification of the structures of aglycones and sugar linkages are mainly based on MS and NMR spectroscopic analyses (Massiot et al., 1988, 1991; Kapusta et al., 2005). In a comparative analysis of root saponins of two alfalfa cultivars and barrel medic (*Medicago truncatula* cv Jemalong A17) (Huhman and Sumner, 2002), the presence of 15 saponins in roots of alfalfa was shown. In contrast, in *M. truncatula* roots 27 saponins were assigned. Recently Huhman et al. (2005) quantified 31 saponins in root and shoot tissues of this variety assuming that the same set of compounds are occurring in both tissues, but this disagrees with the studies of Kapusta et al. (2005) with the identical variety Jemalong A17.

In general, the saponin levels show large biological variability strongly depending on the age of root material analyzed (Duran et al., 2002, 2003). With plant growth the amount of root saponins increases, but no significant differences between mycorrhizal and the control plants were observed. With regard to the biological activities of saponins their antifungal properties may be relevant in plant/AM fungus interactions (Nagata et al., 1985; Oleszek et al., 1990) however, this remains to be proven.

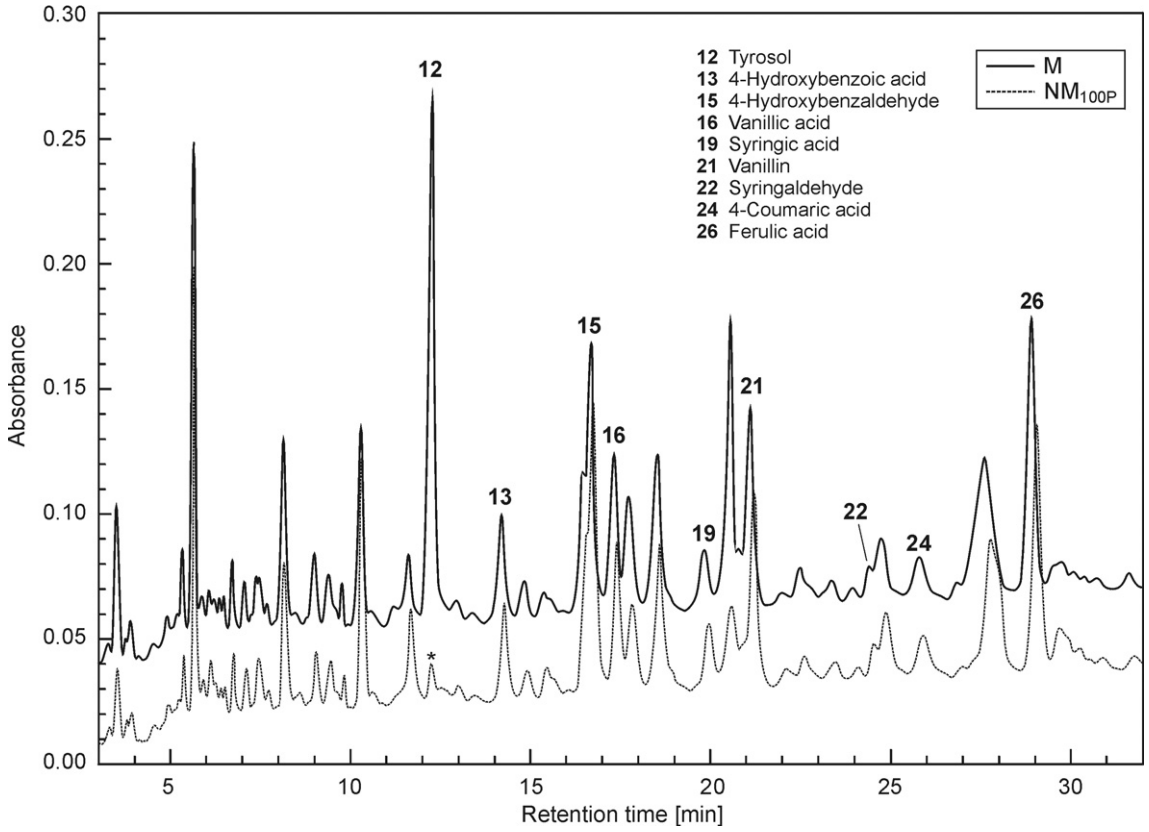

Fig. 15. HPLC chromatogram of cell wall-bound phenolics (maxplot detection; 56 dai). Numbering corresponds to Table 5. Quantification was based on reference compounds and the amounts of major cell wall-bound phenolics in mycorrhizal roots are presented as μmol (root system)$^{-1}$ and μmol (g dry wt)$^{-1}$: tyrosol = 0.05 ± 0.01 and 1.4 ± 0.4; 4-hydroxybenzaldehyde = 0.02 ±0.007 and 0.7 ± 0.2; vanillin = 0.01 ± 0.05 and 0.4 ± 0.2; ferulic acid = 0.02 ± 0.007 and 0.7 ± 0.2. The peak marked with an asterisk occurring at the R_t of tyrosol in the nonmycorrhizal control show UV spectral properties different from those of tyrosol.

2.6. Root cell wall-bound phenolics

Following purification of the insoluble residues of *M. truncatula* root extraction according to Tan et al. (2004), cell wall-bound phenolics were liberated by alkaline hydrolysis. The compound mixtures released were analyzed by HPLC (Fig. 15) and the components were assigned as 4-hydroxybenzaldehyde, vanillin, syringaldehyde, 4-hydroxybenzoic, vanillic and syringic acids, 4-coumaric acid and ferulic acids by comparison with reference compounds (Table 5) and GC–MS analyses. Whereas these phenolics occur in the cell walls of all investigated sample sets and do not show significant changes between the different sample sets at different harvest days, an additional major component was detected in HPLC and identified by its typical fragmentation pattern (*m*/*z* 282 $[M]^+$, 267 $[M-15]^+$, 193, 179) as tyrosol [2-(4-hydroxyphenyl)ethanol], only detected in the root cell walls of mycorrhizal plants.

It is well known that changes in cell wall-bound phenolics occur in plant/pathogen interactions and are proposed to be involved in an increase of cell wall resistance against enzymes of the invader as well as in strengthening of a physical barrier against pathogens (Stewart and Mansfield, 1985; Dixon, 2001; Hahlbrock et al., 2003). The cell wall-bound phenolics from roots of *A. thaliana* were identified as a set of three complete series of 4-hydroxy-, 4-hydroxy-3-methoxy, and 4-hydroxy-3,5-dimethoxy-substituted benzaldehydes, hydroxybenzoic and hydroxycinnamic acids their concentrations changed upon infection of roots with *Pythium sylvaticum* (Tan et al., 2004). The cell wall-bound phenolics from stems and leaves of the alfalfa were assigned as vanillin, 4-hydroxybenzoic acid, vanillic, 4-coumaric, and ferulic acids (Chen et al., 2003). Parsley suspension cultures (*Petroselinum crispum* L.), challenged with an elicitor from *Phytophthora megasperma* f. sp. *glycinea*, react with an increased incorporation of phenylpropanoid derivatives into cell walls, a minor component therefrom was identified as tyrosol (Kauss et al., 1993). In cell wall-bound phenolics of nonmycorrhizal leek roots (*Allium porrum* L.), tyrosol was found as a main compound besides vanillic, syringic and ferulic acids, but tyrosol did not show quantitative alteration upon mycorrhization (Codignola et al., 1989).

Tyrosol is a well known compound from yeast (*Saccharomyces cerevisiae*) (Sentheshanmuganathan and Elsden, 1958) and plays a quorum-sensing role in *Candida albicans* (Chen et al., 2004). Formed by fungi and phytopathogenic bacteria (Schneider et al., 1996; Gamboa-Angulo et al., 2001), it exhibits antifungal activity (Tarus et al., 2003;

Table 5
HPLC of cell wall-bound metabolites of mycorrhizal roots of *M. truncatula* (56 dai)

Peak	R_t (min)	λ_{max} (nm)	Assignment	Ratio	
				M_{20P}/NM_{20P}	M_{20P}/NM_{100P}
1	3.53	<210	CW1[a]	1.37	0.91
2	5.37	222/250sh/285	CW2	1.27	1.33
3	5.65	<210	CW3	1.06	1.05
4	6.75	286	CW4	1.09	1.10
5	7.08	225/260sh	CW5	1.10	1.34
6	8.15	230sh/282/320sh	CW6	1.19	1.10
7	9.02	250sh/318	CW7	1.64	1.35
8	9.40	230/284/311	CW8	0.88	1.03
9	9.78	243	CW9	**2.88**[b]	0.93
10	10.30	230sh/266	CW10	1.02	0.92
11	11.63	267/316	CW11	0.99	0.80
12	12.23	220/275	Tyrosol	**M**[c]	**M**
13	14.20	255	4-Hydroxybenzoic acid	1.00	1.24
14	14.82	224/283/321	CW12	1.08	0.98
15	16.67	221/283	4-Hydroxybenzaldehyde	1.20	0.92
16	17.28	218/260/293	Vanillic acid	0.93	0.85
17	17.70	230/282/317	CW13	1.43	1.31
18	18.48	256/294	CW14	1.19	0.93
19	19.82	218/270sh/305sh	Syringic acid	1.13	0.86
20	20.52	241/280	CW15	1.31	1.20
21	21.08	230/279/309	Vanillin	0.73	0.71
22	24.37	220sh/231/303	Syringaldehyde	0.78	0.78
23	24.72	226/274/302sh	CW16	0.86	0.71
24	25.75	228/290sh/309	4-*E*-coumaric acid	1.14	0.91
25	27.58	230sh/274/310	CW17	1.22	1.04
26	28.87	216/235/323	*E*-ferulic acid	1.17	1.09
27	34.72	226/242/300	CW18	1.27	1.45
28	39.45	257/295	CW19	1.48	1.43

[a] CW – unknown cell wall-bound metabolite.
[b] Significant differences ($p < 0.05$) of the mean values (M_{20P}, NM_{20P}, NM_{100P}) are shown in boldface.
[c] M-Mycorrhiza-induced.

Slininger et al., 2004). Furthermore, tyrosol occurs in flowers of *Osmanthus fragrans* (Ishiguro et al., 1955), in the underground part of roseroot (*Rhodiola rosea* L., Crassulaceae) (Linh et al., 2000; Yousef et al., 2006) and in olive fruits (*Olea europaea* L., Oleaceae) (Giovannini et al., 1999).

Analyses of cell wall-bound phenolics of hyphae and spores of *G. intraradices* by HPLC and GC–MS established the presence of 4-hydroxybenzaldehyde, 4-hydroxybenzoic, and vanillic acids as well as a trace of tyrosol (data not shown). As fungal cell walls are part of the cell wall fraction obtained from mycorrhizal roots, it may be argued that the detected tyrosol originated from the fungal partner. This is unlikely because tyrosol is already a major component of the cell wall-bound phenolics at early time points of mycorrhization at which the amounts of fungal material determined by staining are negligibly low. Furthermore, as the tyrosol level shows a growth-related increase like the other typical cell wall-bound phenolics of plant origin, this behavior could be an argument in favor of its formation by the plant. It may be suggested that the plant/fungus interaction leads to an induced synthesis and integration of tyrosol into cell wall material of mycorrhizal roots in order to strengthen the cell walls and to restrict fungal colonization. This appealing assumption, however, awaits further studies.

2.7. Multivariate analysis

Multivariate analyses of root metabolite data have been carried out to characterize the holistic metabolic behavior in the time period of interest. Both hierarchical cluster analysis (HCA) (Fig. 16) as well as principal component analysis (PCA) (Figs. 17 and 18) gave similar results establishing the dominant influence of growth, whereas the detection of effects due to mycorrhization depend on the number of mycorrhiza-specific compounds (e.g. apocarotenoids, fungal fatty acids) of the corresponding metabolite class. Fig. 16a and b show dendrograms of samples for nonpolar primary metabolites and secondary metabolites, respectively, obtained by HCA. In both figures clear discrimination is apparent between early and late harvest days. At late harvest days, a clear clustering is observed between nonmycorrhizal and mycorrrhizal plants corresponding to the higher values of the mycorrhization degree as determined by *Glomus* rRNA and *MtPT4* expression (Fig. 1). As expected, this effect is stronger pronounced for secondary metabolites due to mycorrhiza-induced isoflavonoid increase and mycorrhiza-specific apocarotenoid

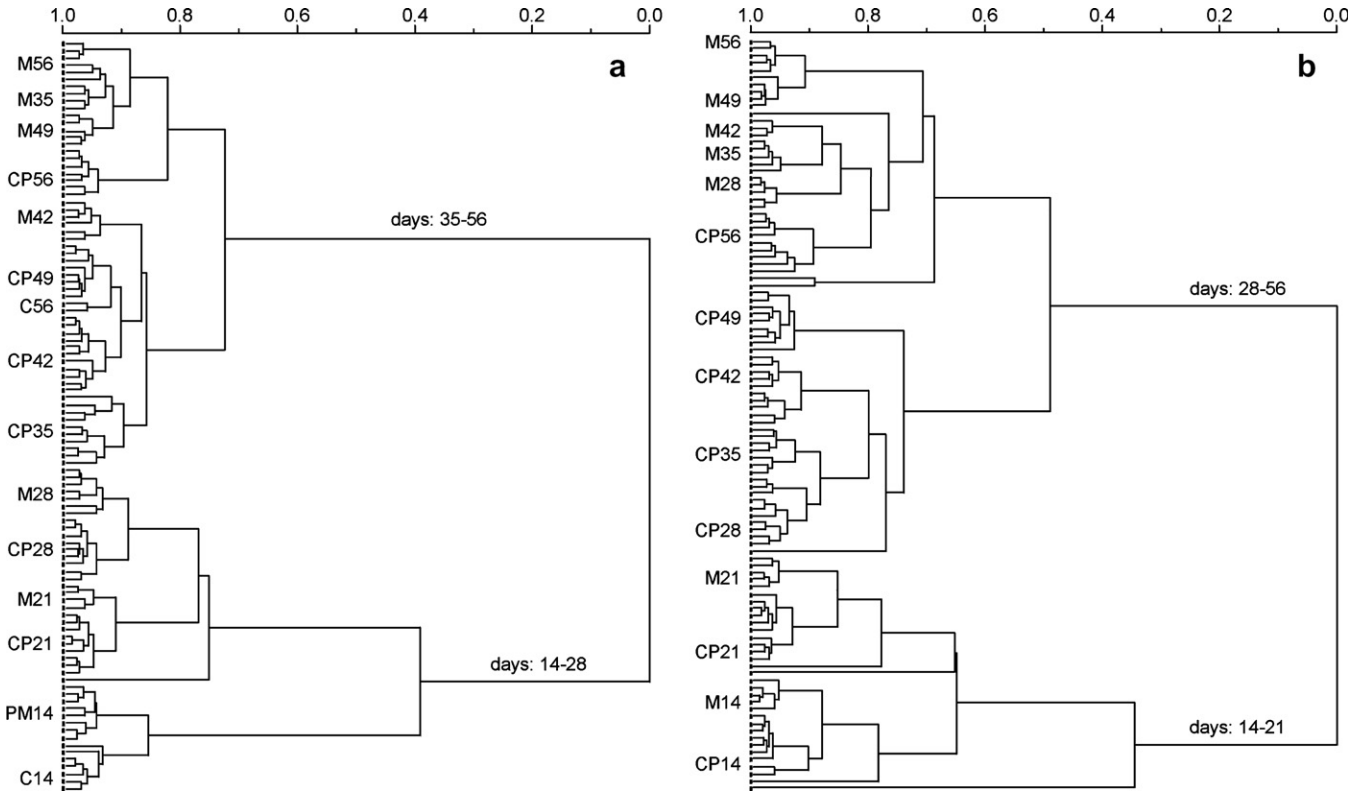

Fig. 16. Hierarchical cluster analysis of (a) primary nonpolar metabolites (GC/TOF-MS) and (b) secondary metabolites (HPLC); M = M_{20P}; C = NM_{20P}; P = NM_{100P}.

formation (Fig. 16b). Here, a distinct subclustering according to harvest days was observed. In all cases, nonmycorrhizal control plants supplied with high and low amounts of phosphate were not separated in different clusters.

The results of a PCA analysis are shown in Fig. 17. In the factor 1 versus factor 2 score-plot describing 83% (nonpolar metabolites) and 85% (secondary metabolites) of the total variance a distinct separation is observed with increasing tendency at later harvest days between nonmycorrhizal and mycorrhizal plants. Additionally, a harvest day-depending subclustering is visible for secondary metabolites in nonmycorrhizal as well as mycorrhizal plants. Hence, the separation in nonmycorrhizal and mycorrhizal plants is controlled by the factor 2 (7.5% variance) and those of harvest days by the factor 1 (77.5% of variance) assuming an assignment to mycorrhization and growth, respectively. Furthermore, Fig. 18a–c demonstrates PCA loading plots of primary and secondary metabolites using both main factors 1 and 2. The fungus-derived and mycorrhiza-induced metabolites are clearly separated from the others. In case of polar primary metabolites (Fig. 18a), trehalose (metabolite 78) is placed separately, supporting the suggestion that it is a fungus-derived metabolite and does not correlate with the other polar metabolites assumed to be of plant root origin. The majority of amino acids are grouping together (right dashed ellipse) with some exceptions, but note that all measurements in the time course are snapshots from dynamic metabolic pathways with changing metabolite fluxes and concentrations. The sugars ribose (metabolite 36), galactose (metabolite 49), and galactosylglycerol (metabolite 72) form a loose separate cluster (left dashed ellipse) with trehalose (metabolite 78) and especially sucrose (metabolite 77) located outside. In addition, the significantly increased phosphate (metabolite 10) and the significantly decreased fumaric acid (metabolite 17) are included in this cluster.

In case of the nonpolar primary metabolites (Fig. 18b) all the fungal-derived fatty acids, glycerides and sterols show a separate cluster. An extraordinary behavior can be observed for octacosanol (metabolite 46) and triacontanol (metabolite 47), both occur in trace amounts. In the pattern of secondary metabolites (Fig. 18c), the mycorrhiza-induced apocarotenoids (both cyclohexenone and mycorradicin derivatives), ononin (metabolite 24) and some unknown components form a cluster with adjacent daidzein and malonylononin (metabolite 26 and 27). Here, the unknown metabolites 31 and 32, which are strongly reduced in high phosphate control roots (NM_{100P}, see Table 3), are clearly separated from the other metabolites.

2.8. Correlation and network analysis

Linear correlations between metabolites were determined by Pearson coefficients for normalization to constant dry weight and to one root system. Normalization to individual root system emphasizes the effect of plant growth on metabolic levels. The effect is much stronger for nonpolar primary metabolites than for polar primary

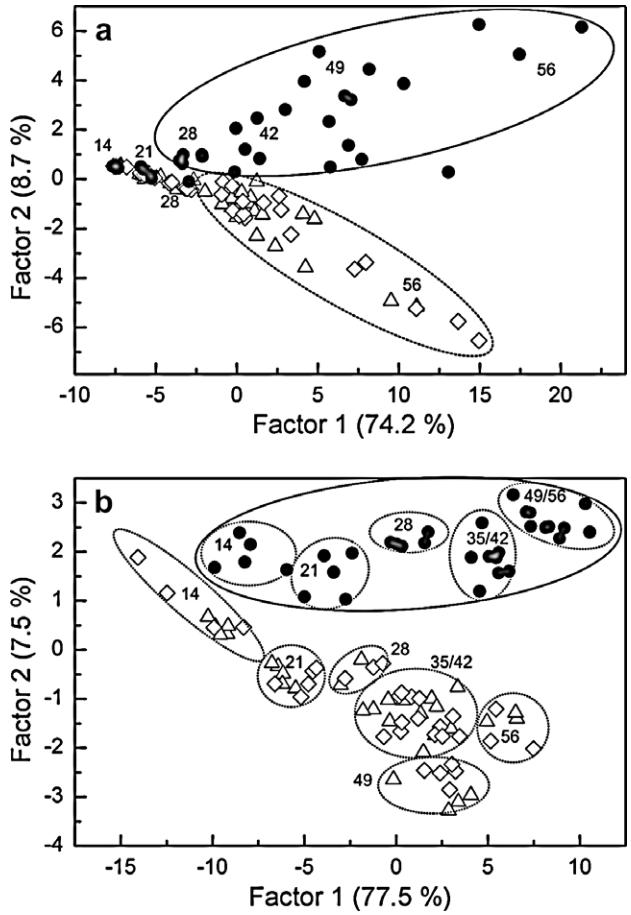

Fig. 17. Principal component analysis (scores) of (a) primary nonpolar metabolites (GC/TOF-MS) and (b) secondary metabolites (HPLC); the numbers refer to the harvest days; symbols as in Fig. 2.

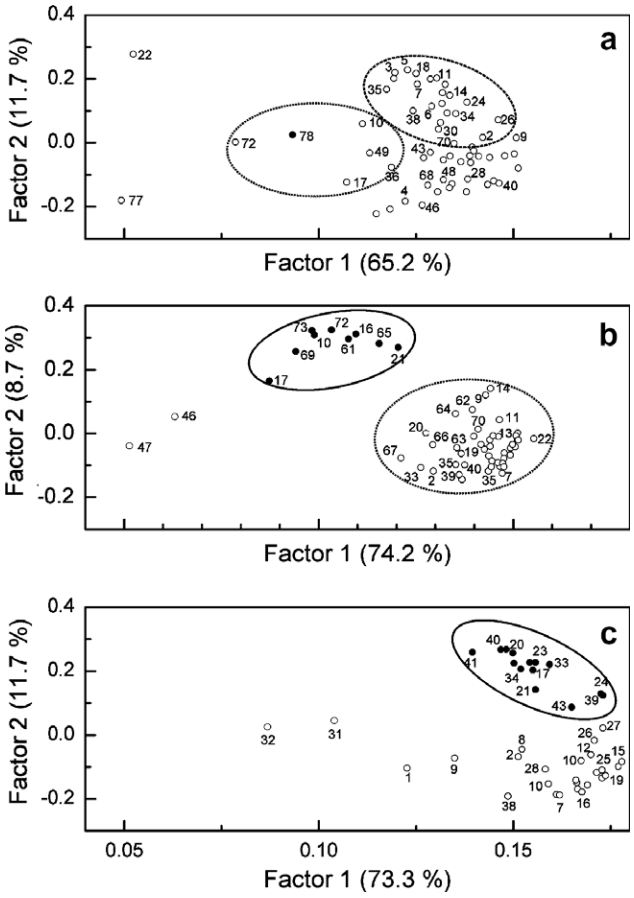

Fig. 18. Principal component analysis (loadings) of (a) primary polar metabolites, (b) primary nonpolar metabolites (GC/TOF-MS) and (c) secondary metabolites (HPLC). Fungal-derived and mycorrhiza-induced compounds are indicated as black dots. Numbers correspond to metabolite assignment in Tables 1 (a), 2 (b) and 3 (c).

metabolites as shown in Figs. 19 and 20. As a consequence, the nonpolar metabolites behave more conformable and the corresponding Pearson coefficients reflect a high correlation. The Pearson coefficients of polar metabolites are generally smaller than those of the nonpolar ones and the normalization to one root system does not lead to such an increase of the correlation coefficients as in case of nonpolar metabolites.

The Pearson correlation coefficients configure metabolic correlation networks (Fiehn, 2003), shown in Figs. 19 and 20. The density of lines in the circular networks represents the strength of correlations between the metabolites. In Fig. 19, only correlations higher than 0.8 are shown. As shown already in the matrix plots, fatty acids and monoglycerides correlate strongly among themselves. Certain metabolites are centers of multiple high correlations between fatty acids and fatty alcohols with similar numbers of carbon atoms (e.g. decanoic acid, tetradecanoic acid and especially the fatty alcohols tetradecanol and tetracosanol). Note the high correlations between the unsaturated fatty acids ($18{:}1\Delta^{9}$, $18{:}2\Delta^{9,12}$, $18{:}3\Delta^{9,12,15}$) to the corresponding monoglycerides. These results emerge most clearly in the NM_{100P} and M_{20P} samples.

In Fig. 20 (middle), an alternative network representation using the 2D Fruchterman-Reingold algorithm in the program Pajek (Batagelj and Mrvar, 2006) was chosen. This reveals distinct clusters of metabolite groups. In all three plant sets, the majority of amino acids are arranged in clusters. Sugars/polyols and aliphatic acids form a correlation cluster only in nonmycorrhizal samples, whereas in the mycorrhizal roots the cluster seems to expand the relations between the single metabolites. While GABA (4-aminobutyric acid, metabolite 26) is included in the amino acid clusters of the NM_{20P} and NM_{100P} controls, this component is in the network presentation of AM roots clearly outside and correlates with several members of the enlarged sugar/polyol/aliphatic acid area. Due to the closer connection and more frequent relations of this cluster with the amino acid cluster, a tighter and more intensive metabolic interaction between these metabolic areas may be assumed in mycorrhizal root metabolism.

The amino acid clusters shown in the middle of Fig. 20 can be resolved in maximal cliques (Kose et al., 2001) that combine metabolites, which are highly correlated among one another. Overlapping areas of maximal cliques are

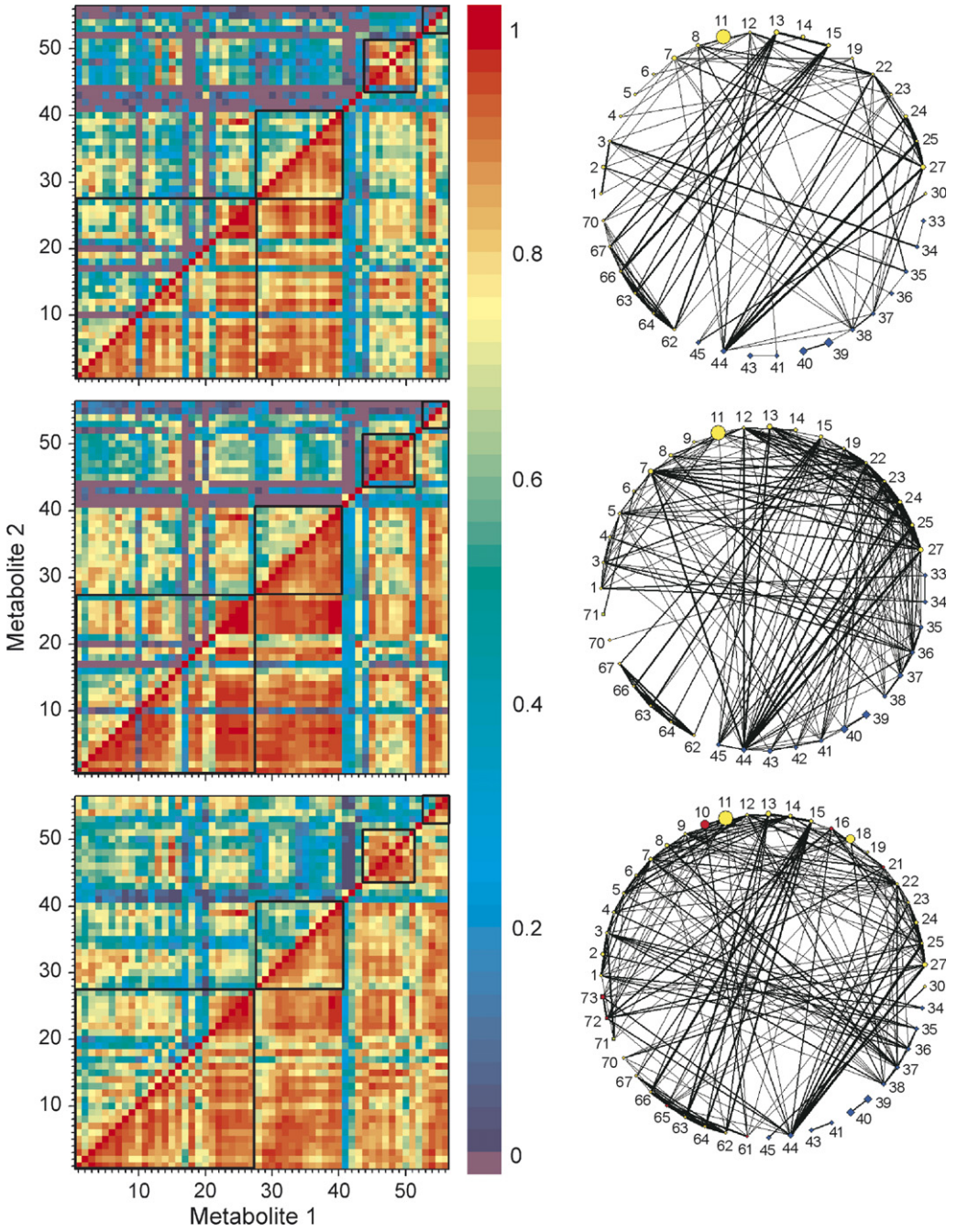

Fig. 19. Matrix plots of Pearson correlation coefficients of nonpolar metabolites (left) and circular network representations (right) for the plant sets NM_{20P} (top), NM_{100P} (middle) and M_{20P} (bottom). The left triangle in the matrix plots are based on peak areas normalized to constant dry weight; the right triangle of peaks are normalized to individual root system. The boxes in the matrix plots group fatty acids, fatty alcohols, monoglycerides, and sterols (left to right). In the network representation, fatty acids (yellow circles), fatty alcohols (blue diamonds), monoglycerides (orange circles) and sterols (green boxes) are grouped in a circular arrangement. Fungus-related metabolites are shown in red color. The size of the symbols represent the relative amounts of the compounds deduced from characteristic fragment ions. The lines between the metabolites represent correlations higher than 0.8 with increasing thickness at increasing correlation. Numbers correspond to Table 2. (For interpretation of the references to colour in figure, the reader is referred to the web version of this article.)

characterized by submaximal cliques. For clarity, a correlation threshold higher than 0.9 has been chosen. It can clearly be ascertained that the amino acid composition of the cliques varies in the different plant sets, which stands for different correlations between individual amino acids in mycorrhizal and the corresponding control roots.

2.9. Conclusions

Our approach was directed to the detection of general trends in root metabolite levels to differentiate between plant development-, nutritional- and mycorrhiza-specific effects in AM roots of *M. truncatula*. To cope with the large

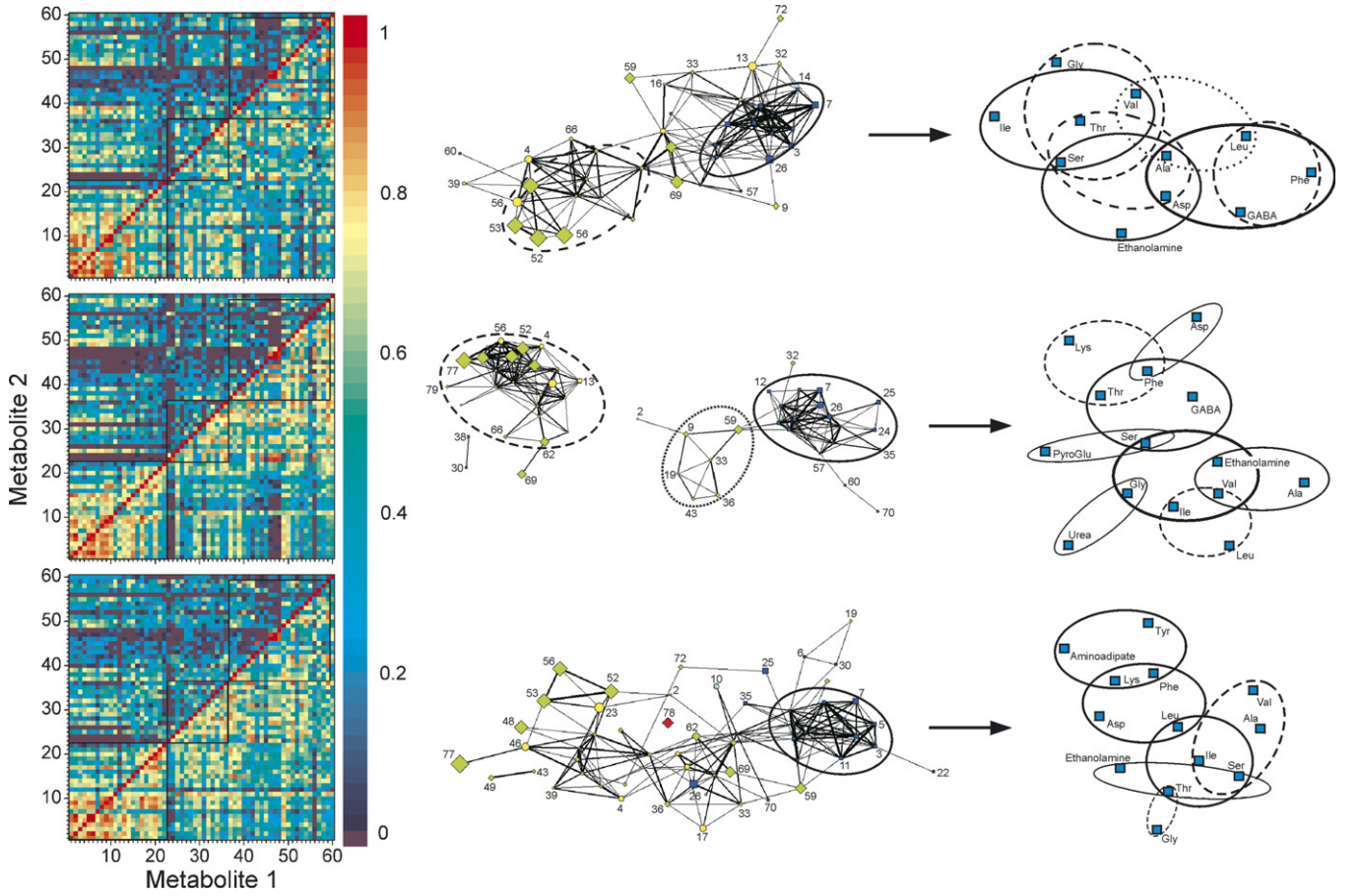

Fig. 20. Matrix plots of Pearson correlation coefficients of polar metabolites (left), network representation (middle), and selected cliques of amino acids (right) for the plant sets NM_{20P} (top), NM_{100P} (middle) and M_{20P} (bottom). The left triangle in the matrix plots bases on peak areas normalized to constant dry weight, the right triangle bases on peak areas normalized to individual root systems. The boxes in the matrix plots group amino acids, aliphatic acids, and sugars/polyols (left to right). The metabolic networks with correlations higher than 0.8 are generated by the program Pajek. Amino acids, sugars/polyols and aliphatic acids are marked in blue, green and yellow colors, respectively; red for the fungus-specific trehalose. Size of the symbols represent the relative amounts of the compounds deduced from characteristic MS fragment ions. The numbers at the network refer to peak numbers in Table 1. On the right side are maximal cliques derived from amino acid clusters (shown in the middle) with correlations higher than 0.9.

biological variability of the experimental plant, five roots of five parallel samples at seven harvest days (2–8 weeks after inoculation) were pooled and subsequently analyzed in this time course experiment. The most pronounced metabolic alterations could be found at the most dynamic phase of root colonization (35–42 dai), characterized by both high expression of the phosphate transporter MtPT4 and *Glomus* rRNA. The successful establishment of the AM symbiosis led to a gain of 30–35% of fresh shoot biomass similar to the NM_{100P} control shoots indicating that the selected phosphate concentration was suitable to differentiate between phosphate effects and AM fungus-induced metabolic changes.

The levels of nonpolar primary metabolites normalized per individual root system show that the increases are mainly growth-related throughout the entire plant development, whereas for polar metabolites often accumulation maxima at 35–42 dai were found. Besides the accumulation of fungus-specific metabolites (trehalose, Δ^{11}-unsaturated fatty acids, sterols), the levels of certain amino acids (Glu, Asp, Asn) and fatty acids (16:0; 18:1Δ^{9}) were higher in mycorrhizal roots in comparison to both controls indicating a mycorrhiza-specific activation of the plastidial metabolism. This is supported by the previous proven proliferation of plastids and the corresponding changes in transcript levels (Lohse et al., 2005).

From the constitutively formed secondary root metabolites, only the isoflavonoids (daidzein, ononin, malonylononin) showed mycorrhiza-induced higher levels at 56 dai that corresponds to the increased expression of an isoflavonoid glucosyltransferase gene (Liu et al., 2007). The levels of complex saponins showed only a development-dependent increase. Unlike the constitutive isoflavonoids and saponins, the AM-specific apocarotenoid (cyclohexenone and mycorradicin derivatives) accumulation strongly correlated with the course of mycorrhization. Their functional involvement in the mycorrhizal symbiosis is not understood and awaits further studies.

While the main emphasis in the metabolite profiling approach was directed to the soluble (polar and nonpolar)

root metabolites, our attention was turned also to the cell wall-bound phenolics. Analyses of these phenolics revealed mycorrhiza-specific occurrence of tyrosol, besides the presence of a typical set of phenolics (Tan et al., 2004). Tyrosol is known to possess antifungal activity (Gil-Turnes and Fenical, 1992; Armstrong et al., 2000; Tarus et al., 2003; Slininger et al., 2004), but whether its deposition in cell walls is involved in the regulation and restriction of mycorrhizal colonization or other processes is an open question.

Clustering of metabolite data by HCA and PCA reveals clearly a different influence of growth and mycorrhization and separates mycorrhizal samples from controls according to harvest days. Network analyses show for nonpolar metabolites of mycorrhizal roots a stronger correlation between each other. This is accompanied by a closer connection and more frequent relations of the metabolites of the sugar/aliphatic acid area with those of the amino acid cluster indicating a tighter and a more intensive interaction in activated mycorrhizal root metabolism.

The present work shows for the first time that there are clear differences in development-, nutritional- and mycorrhiza-dependent primary and secondary metabolism of *M. truncatula* roots. However, we have to admit that our experimental approach has only touched the "tip of the iceberg" of the almost hidden multitude of metabolites, especially signaling molecules involved in the molecular dialog between the plant and the fungus cannot be detected by our approach. Considering the lack of knowledge of fluxes through metabolic networks (Shachar-Hill, 2007) and cellular metabolic events (metabolism of arbuscule-harboring root cells and adjacent tissue), we are unable yet to give a comprehensive interpretation of the mycorrhiza-specific metabolic changes to provide integrative information to functional genomics approaches in research on arbuscular mycorrhizas.

3. Experimental

3.1. Plant and fungal material, inoculation, and plant cultivation

Barrel medic (*M. truncatula* Gaertn., cv. Jemalong A17) seeds (obtained from Department of Genetics, University Bielefeld, Germany) were scarified with a 4-min treatment with concentrated H_2SO_4, rinsed with distilled H_2O and germinated on wet filter paper in Petri dishes for 4 d at 8 °C in the dark, 2 d at room temperature in the dark and 1 d in the light. The 7-d-old seedlings (5 plants per 500-ml pot) were inoculated with the AM fungus *G. intraradices* Schenk and Smith (isolate 49, provided by H. von Alten, University Hannover, Germany), enriched by previous co-cultivation with leek (*Allium porrum* L.) as the host plant in expanded clay (Lecaton, 2–5 mm particle size; Fibo Exclay, Pinneberg, Germany), and grown in a green-house with a 16-h daily light period.

To modulate the mycorrhization velocity different ratios of inoculum to sterile expanded clay were applied [kinetics 3, 3:7, 5 plants per pot, 5 parallels, harvest time: 14, 21, 28, 35, 42, 49, and 56 dai (v/v)]. The inoculated plants, as well as the control plants (without fungal inoculate, designated as NM_{20P}), were watered 3 times per week and fertilized once per week with a modified Long Ashton nutrient solution (tenfold strength, except double strength phosphate) containing 40 mM KNO_3, 40 mM $Ca(NO_3)_2 \cdot 4H_2O$, 15 mM $MgSO_4 \cdot 7H_2O$, 2.7 mM $NaH_2PO_4 \cdot H_2O$ and common micro- and trace elements (Hewitt, 1966) (5 ml per pot). An additional control experiment with plants receiving 13.3 mM phosphate supply (designated as NM_{100P}) was included to discriminate between effects induced by a five times increased phosphate supply from those of mycorrhization (M_{20P}).

Fungal material (spores and hyphae) of *G. intraradices* SY 167 grown in the presence and absence of *Paenibacillus validus* (Hildebrandt et al., 2002, 2006) were provided by U. Hildebrandt (University Würzburg) and used as reference material to assign fungal metabolites after extraction.

3.2. Harvesting, determination of mycorrhization parameters and extraction

At the harvest times specified above, the roots were separated, cleaned from Lecaton, pooled, and after weighing immediately shock frozen with liquid N_2 prior to lyophilization. At the same time, roots of the same age were used after alkaline root treatment and trypan blue (Philips and Hayman, 1970) as well as ink staining (Vierheilig et al., 1998) for estimation of the approximate colonization percentage. Furthermore, shock frozen roots were used for determination of the *MtPT4* and *G. intraradices* rRNA transcript level according to Isayenkov et al. (2004).

Lyophilized roots (30 mg) were homogenized in a mortar with addition of solid CO_2 and extracted with *n*-hexane (3×0.5 ml) after addition of methyl nonadecanoate (15 µl, 2 mg ml^{-1} $CHCl_3$, internal standard) to obtain the nonpolar fraction. Subsequently, the residue was extracted with MeOH:H_2O (3×0.5 ml, 4:1, v/v) after addition of 75 µl ribitol (2 mg ml^{-1} H_2O, internal standard) to yield the polar fraction. The extraction residue was treated according to Tan et al. (2004) to purify the cell walls from which cell wall-bound phenolics were released by alkaline treatment (0.5 ml 1 N NaOH at 80 °C for 16 h in the dark). After acidification of the hydrolysis mixture to pH 1–2 by conc. HCl, the released phenolics were partitioned with EtOAc (2×0.5 ml). The combined extracts were evaporated to dryness at 30 °C with a Speed Vac and the residues dissolved in 50 µl of MeOH:H_2O (50 µL, 4:1, v/v) prior to HPLC analysis.

3.3. Metabolite extraction and sample preparation

Metabolite extraction of lyophilized *M. truncatula* roots as well as of mycelia and spores of *G. intraradices*, was

carried out using *n*-hexane yielding the fraction of nonpolar metabolites, whereas the subsequent extraction of the residue with MeOH:H_2O (4:1, v/v) resulted in the fraction of polar metabolites. Internal standards were added in both procedures in order to correct alterations occurring during sample preparation and analysis. Aliquots of the fractions of nonpolar compounds containing mainly fatty acids, fatty alcohols, sterols and glycerides were trimethylsilylated prior to the GC–MS analyses, whereas aliquots of fractions of polar compounds were methoximated and trimethylsilylated for analyses of the hydroxy carboxylic and amino acids, sugars, polyols and others by GC–MS. The polar fraction was further used without derivatization for analysis of isoflavonoids and apocarotenoids by HPLC, and for saponins by LC–MS. Compound identification was performed by comparison of mass spectra and retention times with those of authentic reference compounds. Furthermore compound assignment was done with the help of the NIST MS database (http://chemdata.nist.gov/mass-spc/Srch_v1.7/index.html, National Institute of Standards and Technology, Gaithersburg, USA; Stein et al., 1998) and especially on the basis of the online available plant-specific MS database (The Golm Metabolome Database; http://csbdb.mpimp-golm.mpg.de/csbdb/gmd/gmd.html). Identification of isoflavonoids were done by comparison of UV spectra and retention times with those of reference compounds in HPLC, saponin assignment was performed on the basis of published MS fragmentation patterns (Huhman et al., 2005).

3.4. Analytical and preparative high performance liquid chromatography

Analytical and semi-prep. HPLC was performed with a system from Waters (Milford, USA), including the separation module 2690. The liquid chromatograph was equipped with a 5 μm Nucleosil C_{18} column (250 × 4 mm i.d.; Macherey-Nagel, Düren, Germany). The following analytical solvent and gradient systems were used. System 1 (for separation of isoflavonoids): A, 1.5% aq. H_3PO_4; B, MeCN; constant gradient from 0% B to 100% B in (A + B) within 60 min; system 2 (for the separation of the apocarotenoids): A, 1.5% aq. H_3PO_4; B, MeCN; constant gradient from 5% B to 25% B within 40 min and then 25% B to 80% B in additional 20 min; system 3 (for the separation of the cell wall-bound phenolics): A, 0.1% aq. TFA; B, MeCN:H_2O:TFA, (98:1.9:0.1,v/v); constant gradient from 0% B to 6% B within 3 min and then 6% B to 24% B in additional 37 min; the flow rate was 1 ml min^{-1}. The compounds were photometrically detected (at 250 and 380 nm; maxplot between 210 and 500 nm) by a Waters 2996 photodiode array detector (injection volume: 20 μl). In semi-prep. HPLC, the 1.5% aq. H_3PO_4 was replaced by 1.0% HOAc.

Whereas the cyclohexenone derivatives were quantified by external standardization based on abscisic acid (ABA) having the identical 1,1,5-trimethyl-cyclohex-4-en-3-one moiety, the levels of mycorradicin liberated from its derivatives by alkaline hydrolysis were calculated using mycorradicin dimethyl ester as standard (provided by H. Bothe, University Cologne, Germany). The results were expressed as μmol ABA or mycorradicin dimethyl ester equivalents per g dry wt, respectively.

For preparative HPLC, the Waters Delta 600 liquid chromatograph was equipped with a VP 250/40 Nucleosil 100–10 C_{18} column (Macherey-Nagel, Düren, Germany) using different gradients depending on the separation problem with 1% HOAc (solvent A) and MeCN or MeOH (solvent B) with flow rates of 20 ml min^{-1}. The compounds were photometrically detected as in the analytical HPLC at a flow rate of 20 ml min^{-1} (5 ml injection volume). Data acquisition and evaluation run with Empower 5.0.

3.5. Liquid chromatography/electrospray ionization mass spectrometry, NMR and CD

For the profiling of the saponins, an Agilent LC system equipped with an autosampler (CTC-PAL) and coupled with an API 150EX™ mass spectrometer (Applied Biosystems/MDS SCIEX, San Francisco, USA) was used under following conditions: column (150 × 2 mm i.d., 5 μm, Sepserv); Solvents: A, 0.2% HOAc; B, MeCN/0.2% HOAc; constant gradient: 86/14 to 78/22 in 36 min; 78/22 to 48/52 in 64 min according Lin et al. (2000); flow: 0.2 ml min^{-1}; injection volume: 3 μl; detection: 250 nm; mass range: m/z 50–2000.

Positive ion electrospray ionisation mass spectra were recorded on a Finnigan MAT TSQ 7000 instrument and high resolution ESI mass spectra were obtained on a Bruker Apex III Fourier transform ion cyclotron resonance (FT-ICR) mass spectrometer (Bruker Daltonics, Billerica, USA).

1D and 2D (COSY and ROESY) ^1H and ^{13}C (1D) NMR spectra were recorded at 300 K on Bruker AVANCE DMX 600 spectrometer locked to the major deuterium signal of the solvent, CD_3OD. Chemical shifts are reported in ppm relative to TMS and coupling constants in Hz. Circular dichroism measurement were performed in cooperation under conditions recently described (Schliemann et al., 2006b).

3.6. Gas chromatography/mass spectrometry

Hexane extracts (100 μl aliquots) were derivatized after reducing to dryness in glass injection vials with 10 μl *N*-methyl-*N*-(trimethylsilyl)-trifluoroacetamide (MSTFA) for 30 min at 70 °C and diluted with hexane (90 μl) prior to injection. For the derivatization of MeOH-soluble compounds, 10 μl aliquots were first derivatized with 10 μl methoxyamine hydrochloride (MOA, 20 mg ml^{-1} pyridine) for 90 min at 30 °C, reduced to dryness and then treated as described for the hexane extracts.

GC/TOF-MS measurements were performed with an Agilent 6890 series gas chromatograph equipped with an autosampler 7683 series and a MicroMass (Manchester,

UK, now Waters Corporation, Milford, USA) GCT with a time-of-flight (TOF) detector. Following conditions were used: EI-voltage 70 eV; source temp. 240 °C; column Rtx-5MS w/IntegraGuard (Restek GmbH, Bad Homburg, Germany), 30 m × 0.25 mm i.d., 0.25 μm film thickness; carrier gas helium at constant flow of 1 ml min^{-1}; temp. program: 50 °C (2 min), 50–260 °C (6° min^{-1}), 260 °C (3 min), 260–300 °C(10° min^{-1}), 300 °C (6 min); injection temp.: 240 °C, splitless injection, mass range of m/z 40 to m/z 800. Data acquisition and evaluation run with MassLynx 3.5 software.

GC–MS measurements were performed with an Trace 2000 GC equipped with an Autosampler 3000 and a single quadrupole Trace DSQ™ (ThermoElectron GmbH, Dreieich, Germany) under the same conditions as GC/TOF-MS using a J&W DB-5 MS (30 m × 0.25 mm, i.d.; 0.25 μm film thickness) column (Agilent, Folsom, USA). Data acquisition and evaluation run with Xcalibur 1.4.1. Quantification of a selected set of metabolites was based on measurements of reference compounds (separate and in mixtures) using characteristic fragment ions.

3.7. Hydrolysis and thermal transformation of malonyl conjugates

The yellow apocarotenoid and the "yellow pigment" fractions were isolated by HPLC (system 2, containing 1% HOAc), reduced to dryness, dissolved in MeOH:H_2O (27 μl, 4:1, v/v) and treated with 10 N KOH (3 μl) for 3 h at 30 °C. Subsequently, aliquots (20 μl) were analyzed by HPLC (system 2) to detect hydrolysis products. For thermal treatment, root extracts were reduced to dryness, dissolved in H_2O–MeOH (55:55, v/v) and heated at 80 °C for 16 h. This treatment transforms malonyl conjugates to their glucosides (Lin et al., 2000) that were confirmed by HPLC (system 1).

3.8. Metabolite assignment

Metabolite assignment was performed in four different ways indicated in the metabolite tables. Additionally, compounds were isolated and structurally elucidated by MS and NMR spectroscopic analyses. The direct comparison of R_t and UV spectra (in HPLC) or R_t and mass fragmentation pattern (in GC/TOF-MS and GC–MS) of reference compounds is the identification procedure (a) with the highest reliability. Peaks in GC–MS runs were assigned with the help of the NIST MS database (b) (http://chemdata.nist.gov/mass-spc/Srch_v1.7/index.html, USA; Stein et al., 1998) and especially on the basis of the online available plant-specific MS database (c) (The Golm Metabolome Database; http://csbdb.mpimp-golm.mpg.de/csbdb/gmd/gmd.html, Schauer et al., 2005). The recursive procedure (d) requires a certain number of known metabolites of a specific substance class and related metabolites of the same substance class can be assigned by a best-fitting curve. The measured mass spectra are deconvoluted by the Automated Mass Spectral Deconvolution and Identification System (AMDIS) before comparison with the databases (b) and (c). The spectra of individual components are transferred to the NIST Mass Spectral Search Program MS Search 2.0 where they matched against reference compounds of the NIST Mass Spectral Library 2002 and the Golm Metabolome Database. The number of compounds resolved by AMDIS depends strongly on the settings, a reasonable number of components are detected by using the default settings. Even if the result reflects a high matching factor and probability the result must be critically proven.

3.9. Data analysis

The complete set of GC/TOF-MS data of each run (five parallels of hexane and MeOH extracts at seven harvest days) were transformed to ASCII-data, separately for non-polar and polar metabolites. To reduce the huge amount of data, the intensities of high resolution masses of each run are summarized to those of nominal masses for each R_t by an self-written FORTRAN program. These intensities arranged in (R_t, m/z)-data matrices are transferred to the Scientific Graphing and Analysis Software package Origin 7.5 (http://www.originlab.com/) which permits automated handling of the data analysis and visualization by proper programming. The integration of the detected peaks is carried out after background subtraction and searching the maximum in a small R_t-window allowing a slight R_t–displacement of the peak. The integrated values are normalized to the mean value of the internal standard calculated for the whole set of experiments per extract. The specific mass fragment m/z 319 is chosen for ribitol, the internal standard for MeOH extracts, yielding a rational compromise between sufficient peak intensity and specificity for the whole derivatized molecule (M_r 512). Concomitant calculations using other mass fragments or the TIC intensity did not affect the results significantly. For methyl nonadecanoate, the internal standard for hexane extracts, the m/z 312 is selected representing the whole molecule.

The experimental data were obtained from aliquots of extracts prepared from 30 mg lyophilized roots. In the kinetic analyses, the results are related to one root system, whereby the integrated values are multiplied by normalization factors determined by the biomass of plants in individual pots. Before averaging of the data originating from the five parallel samples an outlier analysis is performed using the chemometrics software package Pirouette v3.11 of Infometrix (http://www.infometrix.com/software/pirouette.html) combined with a visual check of the integrated data of each metabolite for all harvest days. The peak areas of compounds (assigned or unknown) in the different sample sets (M_{20P}, NM_{20P}, NM_{100P}) were tested for Gaussian distribution with similar variances. Subsequently, t-tests were performed to determine significant differences between the mean values of the different sample sets at $p < 0.05$.

The handling of the HPLC data is similar to that of GC/TOF-MS. The data are exported as (R_t, λ)-matrices.

The displacements of HPLC peaks in the different runs were often relatively strong and could not completely adjusted by the freely available COWTOOL software (Nielsen et al., 1998). The selected wavelength-dependent peaks were additionally proven and aligned simultaneously in all 105 chromatograms of an experimental set (15 pots × 7 harvest days). Further steps of analysis are analogous to the handling of GC/TOF-MS data. LC–MS data were only analyzed for several selected metabolites using the instrument software for integration.

3.10. Statistics of the time course analyses

Specifications of number of harvest days and plants as well as number of extracts and data sets from different methods applied in the metabolite profiling approach are given in a tabulated overview.

Plants		Analytical specification	
Time points of harvest	7	Samples per harvest day	15
Plants per pot	5	Extracts/HPLC Gradients	2
Pots per harvest day	17	Range of *m/z* values in GC/TOF-MS	40–800
Plants per harvest day	85	Range of *m/z* values in LC–MS	450–2000
Sum of plants	595	Range of λ in HPLC ($\Delta\lambda = 4.8$ nm)	212–449 nm
Used data sets per harvest day		Total data sets of analysis	
GC/TOF-MS (*m/z* = 100–500)	12,030	GC/TOF-MS (*m/z* = 100–500)	84,210
LC–MS (*m/z* = 450–1200)	11,265	LC–MS (*m/z* = 450–1200)	78,855
HPLC (polar metabolites)	1530	HPLC (polar metabolites)	10,710
HPLC (cell wall-bound)	765	HPLC (cell wall-bound)	5355

3.11. Mass spectral and NMR spectroscopic data of root metabolites

*13-Hydroxyblumenol C 9-O-β-glucoside (**1**)*: ESI-HRMS and ^{1}H NMR spectroscopic data were identical with those published recently (Schliemann et al., 2006a).

*13-Hydroxyblumenol C 9-O-β-(6′-malonylglucoside) (**2**)*: ESI-HRMS, *m/z* 497.19897 ([M+Na]$^+$, $C_{22}H_{34}O_{11}Na$, calc. 497.1993), *m/z* 411.1983 ([M−malonyl+Na]$^+$, $C_{19}H_{32}O_8Na$, calc. 411.1989). ESI-MS, *m/z* (rel. int.): 497 [M+Na]$^+$ (10), 411 [M−malonyl+Na]$^+$ (100), 209 [(13-Hydroxyblumenol C+H)−H_2O]$^+$ (7). Negative ion ESI-MS, *m/z* (rel. int.): 473 [M−H]$^-$ (18), 387 [(M−H)-malonyl]$^-$ (100). ESI–MSMS of *m/z*475 [M+H]$^+$: 457 [(M+H)−H_2O]$^+$ (22), 227 [13-Hydroxyblumenol C+H]$^+$ (41), 209 [(13-Hydroxyblumenol C+H)−H_2O]$^+$ (90). ^{1}H NMR spectroscopic data indicate that the major component is the glucoside of 13-hydroxyblumenol C; no evidence of a malonyl moiety at the glucose probably due to decomposition of the labile conjugate as MS showed that it was initially present.

*Blumenol C 9-O-β-glucoside (**3**)*: ESI-HRMS, *m/z* 395.2031 ([M+Na]$^+$, $C_{19}H_{32}O_7Na$, calc. 395.2040). ESI-MS, *m/z* (rel. int.): 395 [M+Na]$^+$ (100), 211 [Blumenol C+H]$^+$ (8); Negative ion ESI-MS, *m/z* (rel. int.): 371 [M−H]$^-$ (74); ESI–MSMS of *m/z* 373 [M+H]$^+$: 211 [Blumenol C+H]$^+$ (100); ^{1}H NMR (400 MHz, CD_3OD): δ 5.84 [1H, *bs*, H-4], 4.36 [1H, *d*, H-1′, $J_{1',2'} = 7.7$ Hz], 3.88 [1H, *dd*, H-6α, $J_{6'\alpha,5'} = 2.1$ Hz, $J_{6'\alpha,6'\beta} = 11.8$ Hz], 3.85 [1H, *m*, H-9], 3.70 [1H, *dd*, H-6′β, $J_{6'\beta,5'} = 5.3$ Hz], 3.4–3.15 [4H, *m*, H-2′, H-3′, H-4′, H-5′], 2.52 [1H, *d*, H-2α, $J_{2\alpha,2\beta} = 17.9$ Hz], 2.09 [3H, *d*, H-13, $J_{13,4} = 1.3$ Hz], 2.02 [1H, *d*, H-2β], 2.02 [1H, *m*, H-6], 1.86 [1H, *m*, H-7α], 1.75–1.58 [3H, *m*, H-7β, H-8α, β], 1.29 [3H, *d*, H-10, $J_{10,9} = 6.2$ Hz], 1.14 [3H, *s*, H-11], 1.06 [3H, *s*, H-12].

*Blumenol C 9-O-β-(6′-malonylglucoside) (**4**)*: ESI-HRMS, *m/z* 481.2042 ([M+Na]$^+$, $C_{22}H_{34}O_{10}Na$, calc. 481.2044), *m/z* 395.2034 ([M−malonyl+Na]$^+$, $C_{19}H_{32}O_7Na$, calc. 395.2040), *m/z* 211.1692 ([Blumenol C+H]$^+$, $C_{13}H_{23}O_2$, calc. 211.1693). ESI-MS, *m/z* (rel. int.): 481 [M+Na]$^+$ (26), 395 [M−malonyl+Na]$^+$ (100), 211 [Blumenol C+H]$^+$ (8); Negative ion ESI-MS, *m/z* (rel. int.): 457 [M−H]$^-$ (11), 371 [(M−H)–malonyl]$^-$ (61); Positive ion ESI–MSMS of *m/z* 459 [M+H]$^+$: 211 [Blumenol C+H]$^+$ (100). ^{1}H NMR spectroscopic data indicate that the major component is the glucoside of blumenol C; no evidence of a malonyl moiety at the glucose probably due to decomposition of the labile conjugate as MS showed that it was initially present.

7-Hydroxy-4′-methoxy-isoflavone 7-O-β-glucopyranoside (Ononin): ESI-MS, *m/z* (rel. int.): 453 [M+Na]$^+$ (100), 431 [M+H]$^+$ (16), 269 [A+H]$^+$ (18); ESI-MS, *m/z* (rel. int.): 429 [M−H]$^-$ (12), 267 [A−H]$^-$ (100); ESI-HRMS, *m/z* 453.1148 ([M+Na]$^+$, $C_{22}H_{22}O_9Na$, calc. 453.1156). ^{1}H NMR (400 MHz, CD_3OD): δ 8.26 [1H, *s*, H-2], 8.20 [1H, *d*, H-5, $J_{5,6} = 8.9$ Hz], 7.53 [2H, AA′, H-2′/6′, $J_{2',3'} + J_{2',5'} = 8.6$ Hz], 7.30 [1H, *d*, H-8, $J_{8,6} = 2.2$ Hz], 7.27 [1H, *dd*, H-6], 7.03 [2H, BB′, H-3′/5′], 5.15 [1H, "*d*", H-1″, $J_{1'',2''} = 7.5$ Hz], 3.97 [1H, *dd*, H-6″α, $J_{6''\alpha,5''} = 2.3$ Hz, $J_{6''\alpha,6''\beta} = 12.1$ Hz], 3.87 [3H, *s*, H-4′OMe], 3.76 [1H, *dd*, H-6″β, $J_{6''\beta,5''} = 5.8$ Hz], 3.61–3.55 [3H, *m*, H-2″, H-3″, H-5″], 3.46 [1H, *dd*, H-4″, $J_{4'',3''} = 9.3$ Hz, $J_{4'',5''} = 9.3$ Hz]. The ^{1}H NMR spectroscopic data clearly assign ononin, although they were only partly comparable to those recently published (Coronado et al., 1995; Xiao et al., 2005), together with those of malonylononin, due to different experimental conditions.

7-Hydroxy-4′-methoxy-isoflavone 7-O-β-[(6′-O-malonyl)-glucopyranoside (Malonylononin): ESI-MS, *m/z* (rel.

int.): 539 $[M+Na]^+$ (61), 453 $[M-malonyl+Na]^+$ (51), 269 $[A+H]^+$ (18); ESI-MS, *m/z* (rel. int.): 429 $[(M-H)-malonyl]^-$ (4), 267 $[formononetin-H]^-$ (100); HR-ESI-MS, *m/z* 539.1168 ($[M+Na]^+$, $C_{25}H_{24}O_{12}Na$, calc. 539.1160). ^1H NMR spectroscopic data indicate that the major component is ononin and the second minor is ononin acylated at *O*-6 of glucose. Fragmentation in MS showed that it is the malonyl derivative.

7-Hydroxy-4′-methoxy-isoflavone (Formononetin): ESI-MS, *m/z* (rel. int.): 291 $[M+Na]^+$ (100), 269 $[M+H]^+$ (49); ESI-MS, *m/z* (rel. int.): 267 $[M-H]^-$ (100); HR-ESI-MS, *m/z* 291.0632 ($[M+Na]^+$, $C_{16}H_{12}O_4Na$, calc. 291.0628), *m/z* 267.0661 ($[M-H]$, $C_{16}H_{12}O_4$, calc. 267.0663). ^1H NMR (600 MHz, CD_3OD): δ 8.20 [1H, *s*, H-2], 8.11 [1H, *d*, H-5, $J_{5,6} = 8.9$ Hz], 7.51 [2H, AA′, H-2′/6′, $J_{2',3'} + J_{2',5'} = 8.7$ Hz], 7.03 [2H, BB′, H-3′/5′], 6.99 [1H, *dd*, H-6, $J_{6,8} = 2.2$ Hz], 6.90 [1H, *d*, H-8], 3.88 [3H, *s*, H-4′OMe].

Acknowledgements

We thank B. Kolbe and M. Lerbs (Leibniz Institute of Plant Biochemistry, IPB) for experimental assistance, J. Schmidt (IPB) for LC/ESI-MS and HR-ESI-MS analyses, V. Wray (Helmholtz Centre for Infection Research, Braunschweig) for NMR analysis, U. Hildebrandt (University Würzburg) and H. Bothe (University Cologne) for providing mycorradicin dimethyl ester and *Glomus* material, C. Tretner (IPB) for determination of *MtPT4* and *Glomus* rRNA expression level and P.A. Olsson (University Lund, Sweden) for help in the identification of fatty acids.

This work was financially supported by the Deutsche Forschungsgemeinschaft, Bonn, Germany (Priority Program SPP 1084 "Molecular Basics of Mycorrhizal Symbioses").

References

Akiyama, K., 2007. Chemical identification and functional analysis of apocarotenoids involved in the development of arbuscular mycorrhizal symbiosis. Biosci. Biotechnol. Biochem. 71, 1405–1414.

Akiyama, K., Matsuzaki, K.-I., Hayashi, H., 2005. Plant sesquiterpenes induce hyphal branching in arbuscular mycorrhizal fungi. Nature 435, 824–827.

Armstrong, E., Boyd, K.G., Burgess, J.G., 2000. Prevention of marine biofouling using natural compounds from marine organisms. In: EI-Gewely, M.R. (Ed.), In: Biotechnology Annual Review, vol. 6. Elsevier Science B.V., London, pp. 221–241.

Asirvatham, V.S., Watson, B.S., Sumner, L.W., 2002. Analytical and biological variances associated with proteomic studies of *Medicago truncatula* by two-dimensional polyacrylamide gel electrophoresis. Proteomics 2, 960–968.

Auldridge, M.E., Block, A., Vogel, J.T., Dabney-Smith, C., Mila, I., Bouzayen, M., Magallanes-Lundback, M., DellaPenna, D., McCarty, D.R., Klee, H.J., 2006. Characterization of three members of the Arabidopsis carotenoid cleavage dioxygenase family demonstrates the divergent roles of this multifunctional enzyme family. Plant J. 45, 982–993.

Baggett, B.R., Cooper, J.D., Hogan, E.T., Carper, J., Paiva, N., Smith, J.T., 2002. Profiling isoflavonoids found in legume root extracts using capillary electrophoresis. Electrophoresis 23, 1642–1651.

Bago, B., Pfeffer, P.E., Shachar-Hill, Y., 2000. Carbon metabolism and transport in arbuscular mycorrhizas. Plant Physiol. 124, 949–957.

Batagelj, V., Mrvar, A., 2006. Pajek – Program for large network analysis. http://vlado.fmf.uni-lj-si/pub/networks/pajek/.

Becker, W.N., Gerdemann, J.W., 1977. Colorimetric quantification of vesicular–arbuscular mycorrhizal infection in onion. New Phytol. 78, 289–295.

Bell, C.A., Dixon, R.A., Farmer, A.D., Flores, R., Inman, J., Gonzales, R.A., Harrison, M.J., Paiva, N.L., Scott, A.D., Weller, J.W., May, G.D., 2000. The Medicago genome initiative: a model legume database. Nucleic Acids Res. 29, 1–4.

Besserer, A., Puech-Pagès, V., Kiefer, P., Gomez-Roldan, V., Jauneau, A., Roy, S., Portais, J.-C., Roux, C., Bécard, G., Séjalon-Delmas, N., 2006. Strigolactones stimulate arbuscular mycorrhizal fungi by activating mitochondria. PLoS Biol. 4, 1239–1247.

Bestel-Corre, G., Dumas-Gaudot, E., Poinsot, V., Dieu, M., Dierick, J.F., van Tuinen, D., Remacle, J., Gianinazzi-Pearson, V., Gianinazzi, S., 2002. Proteome analysis and identification of symbiosis-related proteins from*Medicago truncatula* Gaertn. by two-dimensional electrophoresis and mass spectrometry. Electrophoresis 23, 122–137.

Bestel-Corre, G., Gianinazzi, S., Dumas-Gaudot, E., 2004. Impact of sewage sludges on *Medicago truncatula* symbiotic proteome. Phytochemistry 65, 1651–1659.

Bialy, Z., Jurzysta, M., Oleszek, W., Piacente, S., Pizza, C., 1999. Saponins in alfalfa (*Medicago sativa* L.) root and their structural elucidation. J. Agric. Food Chem. 47, 3185–3192.

Bino, R.J., Hall, R.D., Fiehn, O., Kopka, J., Saito, K., Draper, J., Nikolau, B.J., Mendes, P., Roessner-Tunali, U., Beale, M.H., Trethewey, R.N., Lange, B.M., Wurtele, E.S., Sumner, L.W., 2004. Potential of metabolomics as a functional genomics tool. Trends Plant Sci. 9, 418–425.

Bonanomi, A., Oetiker, J.H., Guggenheim, R., Boller, T., Wiemken, A., Vögeli-Lange, R., 2001. Arbuscular mycorrhizal symbiosis in minimycorrhizotrons: first contact of *Medicago truncatula* roots with *Glomus intraradices* induces chalcone synthase. New Phytol. 150, 573–582.

Bothe, H., Klingner, A., Kaldorf, M., Schmitz, O., Esch, H., Hundeshagen, B., Kernebeck, H., 1994. Biochemical approaches to the study of plant-fungal interactions in arbuscular mycorrhiza. Experientia 50, 919–925.

Bouvier, F., Isner, J.-C., Dogbo, O., Camara, B., 2005. Oxidative tailoring of carotenoids: a prospect towards novel functions in plants. Trends Plant Sci. 10, 187–194.

Bouvier, F., Suire, C., Mutterer, J., Camara, B., 2003. Oxidative remodeling of chromoplast carotenoids: identification of the carotenoid dioxygenase *CsCCD* and *CsZCD* genes involved in crocus secondary metabolite biogenesis. Plant Cell 15, 47–62.

Brechenmacher, L., Weidmann, S., van Tuinen, D., Chatagnier, O., Gianinazzi, S., Franken, P., Gianinazzi-Pearson, V., 2004. Expression profiling of up-regulated plant and fungal genes in early and late stages of *Medicago truncatula–Glomus mosseae* interactions. Mycorrhiza 14, 253–262.

Broeckling, C.D., Huhman, D.V., Farag, M.A., Smith, J.T., May, G.D., Mendes, P., Dixon, R.A., Sumner, L.W., 2005. Metabolic profiling of *Medicago truncatula* cell cultures reveals the effects of biotic and abiotic elicitors on metabolism. J. Exp. Bot. 56, 323–336.

Burleigh, S.H., Cavagnaro, T., Jakobsen, I., 2002. Functional diversity of arbuscular mycorrhizas extends to the expression of plant genes involved in P nutrition. J. Exp. Bot. 53, 1593–1601.

Chen, F., Duran, A.L., Blount, J.W., Sumner, L.W., Dixon, R.A., 2003. Profiling phenolic metabolites in transgenic alfalfa modified in lignin biosynthesis. Phytochemistry 64, 1013–1021.

Chen, H., Fujita, M., Feng, Q., Clardy, J., Fink, G.R., 2004. Tyrosol is a quorum-sensing molecule in *Candida albicans*. Proc. Natl. Acad. Sci. USA 101, 5048–5052.

Codignola, A., Verotta, L., Spanu, P., Maffei, M., Scannerini, S., Bonfante-Fasolo, P., 1989. Cell wall bound-phenols on roots of vesicular–arbuscular mycorrhizal plants. New Phytol. 112, 221–228.

Cook, D.R., 1999. *Medicago truncatula* – a model in the making. Curr. Opin. Plant Biol. 2, 301–304.

Cordier, C., Pozo, M., Barea, J., Gianinazzi, S., Gianinazzi-Pearson, V., 1998. Cell defense responses associated with localized and systemic resistance to *Phytophthora parasitica* induced in tomato by an arbuscular mycorrhizal fungus. Mol. Plant Microbe Interact. 11, 1017–1028.

Coronado, C., Zuanazzi, J.A.S., Sallaud, C., Quirion, J.-C., Esnault, R., Husson, H.-P., Kondorosi, A., Ratet, P., 1995. Alfalfa root flavonoid production is nitrogen regulated. Plant Physiol. 108, 533–542.

Cress, W.A., Throneberry, G.O., Lindsey, D.L., 1979. Kinetics of phosphorus absorption by mycorrhizal and nonmycorrhizal tomato roots. Plant Physiol. 64, 484–487.

Cunningham Jr., F.X., Gantt, E., 2001. One ring or two? Determination of ring number in carotenoids by lycopene ε-cyclases. Proc. Natl. Acad. Sci. USA 98, 2905–2910.

Daft, M.J., Nicolson, T.H., 1972. Effect of *Endogone* mycorrhiza on plant growth. IV. Quantitative relationships between the growth of the host and the development of the endophyte in tomato and maize. New Phytol. 71, 287–295.

Dakora, F.D., Joseph, C.M., Phillips, D.A., 1993. Alfalfa (*Medicago sativa* L.) root exudates contain isoflavonoids in the presence of *Rhizobium meliloti*. Plant Physiol. 101, 819–824.

Desbrosses, G.G., Kopka, J., Udvardi, M.K., 2005. *Lotus japonicus* metabolic profiling. Development of gas chromatography–mass spectrometry resources for the study of plant–microbe interactions. Plant Physiol. 137, 1302–1318.

Diop, T.A., Krasova-Wade, T., Diallo, A., Douf, M., Gueyer, M., 2003. *Solanum* cultivar responses to arbuscular mycorrhizal fungi: growth and mineral status. Afr. J. Biotechnol. 2, 429–433.

Dixon, R.A., 1999. Isoflavonoids: biochemistry, molecular biology, and biological functions. In: Barton, D., Nakanishi, K., Meth-Cohn, O. (Eds.), Comprehensive Natural Products Chemistry. In: Sankawa, U. (Ed.), Polyketides and Other Secondary Metabolites Including Fatty Acids and their Derivatives, vol. 1. Elsevier, Oxford, pp. 773–823.

Dixon, R.A., 2001. Natural products and plant disease resistance. Nature 411, 843–847.

Doll, J., Hause, B., Demchenko, K., Pawlowski, K., Krajinski, F., 2003. A member of the germin-like protein family is a highly conserved mycorrhiza-specific induced gene. Plant Cell Physiol. 44, 1208–1214.

Douds Jr., D.D., Pfeffer, P.E., Shachar-Hill, Y., 2000. Carbon partitioning, cost and metabolism of arbuscular mycorrhizas. In: Kapulnik, Y., Douds, D.D., Jr. (Eds.), Arbuscular Mycorrhizas: Physiology and Function. Kluwer Academic Press, Dordrecht, pp. 107–130.

Duponnois, R., Colombet, A., Hien, V., Thioulouse, J., 2005. The mycorrhizal fungus *Glomus intraradices* and rock phosphate amendment influence plant growth and microbial activity in the rhizosphere of *Acacia holosericea*. Soil Biol. Biochem. 37, 1460–1468.

Duran, A.L., Broeckling, C.D., Huhman, D.V., Sumner, L.W., 2002. Metabolome profiling of *Medicago truncatula* yields insight into biological variance and development. In: Proceedings of the 50th ASMS Conference on Mass Spectrometry and Allied Topics, Orlando, USA.

Duran, A.L., Broeckling, C., Huhman, D.V., Suzuki, H., Dixon, R.A., Sumner, L.W., 2003. Metabolomics: temporal and spatial snapshots of *Medicago truncatula* biochemistry. In: Proceedings of the 51st ASMS Conference on Mass Spectrometry and Allied Topics, Montreal, Canada.

Eschenmoser, W., Eugster, C.H., 1975. Absolute Konfiguration von Azafrin. Helv. Chim. Acta 58, 1722–1727.

Eugster, C.H., Märki-Fischer, E., 1991. The chemistry of rose pigments. Angew. Chem. Int. Ed. Engl. 30, 654–672.

Farag, M.A., Huhman, D.V., Lei, Z., Sumner, L.W., 2007. Metabolic profiling and systematic identification of flavonoids and isoflavonoids in roots and cell suspension cultures of *Medicago truncatula* using HPLC–UV–ESI–MS and GC–MS. Phytochemistry 68, 342–354.

Fernie, A.R., 2003. Metabolome characterisation in plant system analysis. Funct. Plant Biol. 30, 111–120.

Fester, T., Maier, W., Strack, D., 1999. Accumulation of secondary compounds in barley and wheat roots in response to inoculation with an arbuscular fungus and co-inoculation with rhizosphere bacteria. Mycorrhiza 8, 241–246.

Fester, T., Hause, B., Schmidt, D., Halfmann, K., Schmidt, J., Wray, V., Hause, G., Strack, D., 2002a. Occurrence and localization of apocarotenoids in arbuscular mycorrhizal plant roots. Plant Cell Physiol. 43, 256–265.

Fester, T., Schmidt, D., Lohse, S., Walter, M.H., Giuliano, G., Bramley, P.M., Fraser, P.D., Hause, B., Strack, D., 2002b. Stimulation of carotenoid metabolism in arbuscular mycorrhizal roots. Planta 216, 148–154.

Fester, T., Wray, V., Nimtz, M., Strack, D., 2005. Is stimulation of carotenoid biosynthesis in arbuscular mycorrhizal roots a general phenomenon? Phytochemistry 66, 1781–1786.

Fiehn, O., 2001. Combining genomics, metabolome analysis, and biochemical modelling to understand metabolic networks. Comp. Funct. Genomics 2, 155–168.

Fiehn, O., 2002. Metabolomics – the link between genotypes and phenotypes. Plant Mol. Biol. 48, 155–171.

Fiehn, O., 2003. Metabolic networks of *Cucurbita maxima* phloem. Phytochemistry 62, 875–886.

Fiehn, O., Weckwerth, W., 2003. Deciphering metabolic networks. Eur. J. Biochem. 270, 579–588.

Fiehn, O., Kopka, J., Dörmann, P., Altmann, T., Trethewey, R.T., Willmitzer, L., 2000a. Metabolite profiling for plant functional genomics. Nat. Biotechnol. 18, 1157–1161.

Fiehn, O., Kopka, J., Trethewey, R.N., Willmitzer, L., 2000b. Identification of uncommon plant metabolites based on calculation of elemental compositions using gas chromatography and quadrupole mass spectrometry. Anal. Chem. 72, 3573–3580.

Fontaine, J., Grandmougin-Ferjani, A., Glorian, V., Durand, R., 2004. 24-Methyl/methylene sterols increase in monoxenic roots after colonization by arbuscular mycorrhizal fungi. New Phytol. 163, 159–167.

Franken, P., Requena, N., 2001. Analysis of gene expression in arbuscular mycorrhiza: new approaches and challenges. New Phytol. 150, 431–439.

Frenzel, A., Manthey, K., Perlick, A.M., Meyer, F., Pühler, A., Küster, H., Krajinski, F., 2005. Combined transcriptome profiling reveals a novel family of arbuscular mycorrhizal-specific *Medicago truncatula* lectin genes. Mol. Plant Microbe Interact. 18, 771–782.

Gamboa-Angulo, M.M., Garcia-Sosa, K., Alejos-Gonzales, F., Escalante-Erosa, F., Delgado-Lamas, G., Pena-Rodriguez, L.M., 2001. Tagetolone and tagetenolone: two phytotoxic polyketides from *Alternaria tagetica*. J. Agric. Food Chem. 49, 1228–1232.

Gaspar, L., Pollero, R., Cabello, M., 1997. Variations in the lipid composition of alfalfa roots during colonization with the arbuscular mycorrhizal fungus *Glomus versiforme*. Mycologia 89, 37–42.

Gavito, M.E., Curtis, P.S., Mikkelsen, T.N., Jakobsen, I., 2000. Atmospheric CO_2 and mycorrhiza effects on biomass allocation and nutrient uptake of nodulated pea (*Pisum sativum* L.) plants. J. Exp. Bot. 51, 1931–1938.

Gerdemann, J.W., 1964. The effect of mycorrhiza on the growth of maize. Mycologia 56, 342–349.

Gianinazzi-Pearson, V., Dumas-Gaudot, E., Gollotte, A., Tahiri-Alaoui, A., Gianinazzi, S., 1996. Cellular and molecular defence-related root responses to invasion by arbuscular mycorrhizal fungi. New Phytol. 133, 45–57.

Gianinazzi-Pearson, V., Maldonado-Mendoza, I., Lopez-Meyer, M., Weidmann, S., Harrison, M.J., 2006. Arbuscular mycorrhiza. In: The *Medicago truncatula* handbook. http://www.noble.org.Medicago-Handbook/.

Gil-Turnes, M.S., Fenical, W., 1992. Embryos of *Homarus americanus* are protected by epibiotic bacteria. Biol. Bull. 182, 105–108.

Giovannini, C., Straface, E., Modesti, D., Coni, E., Cantafora, A., De Vincenzi, M., Malorni, W., Masella, R., 1999. Tyrosol, the major olive oil biophenol, protects against oxidized-LDL-induced injury in Caco-2 cells. J. Nutr. 129, 1269–1277.

Govindarajulu, M., Pfeffer, P.E., Jin, H., Abudaker, J., Douds, D.D., Allen, J.W., Bücking, H., Lammers, P.J., Shachar-Hill, Y., 2005. Nitrogen transfer in the arbuscular mycorrhizal symbiosis. Nature 435, 819–823.

Graham, J.H., Hodge, N.C., Morton, J.B., 1995. Fatty acid methyl ester profiles and characterization of Glomalean fungi and their endomycorrhizae. Appl. Environ. Microbiol. 61, 58–64.

Grandmougin-Ferjani, A., Dalpé, Y., Veignie, E., Hartmann, M.A., Rafin, C., Sancholle, M., 1995. Infection by arbuscular mycorrhizal fungus *Glomus mosseae* of leek plants (*Allium porrum* L.): effect on lipids. In: Kader, J.-C., Mazliak, P. (Eds.), Plant Lipid Metabolism. Kluwer Academic Publishers, Dordrecht, pp. 444–446.

Grunwald, U., 2004. Analyse der Genregulation in *Medicago truncatula* und *Pisum sativum* während der Entwicklung arbuskulärer Mykorrhiza. Thesis, University Marburg.

Grunwald, U., Nyamsuren, O., Tamasloukht, M., Lapopin, L., Becker, A., Mann, P., Gianinazzi-Pearson, V., Krajinski, F., Franken, P., 2004. Identification of mycorrhiza-regulated genes with arbuscule development-related expression profile. Plant Mol. Biol. 55, 553–566.

Hahlbrock, K., Bednarek, P., Ciolkowski, I., Hamberger, B., Heise, A., Liedgens, H., Logemann, E., Nürnberger, T., Schmelzer, E., Somssich, I.E., Tan, J.W., 2003. Non-self recognition, transcriptional reprogramming, and secondary metabolite accumulation during plant/pathogen interactions. Proc. Natl. Acad. Sci. USA 100, 14569–14576.

Hall, R., Beale, M., Fiehn, O., Hardy, N., Sumner, L., Bino, R., 2002. Plant metabolomics. The missing link in functional genomics strategies. Plant Cell 14, 1437–1440.

Hamberg, M., Ponce de Leon, I., Sanz, A., Castresana, G., 2002. Fatty acid alpha-dioxygenases. Prostag. Other Lipid Mediat. 68–69, 363–374.

Harrison, M., 1998. Development of the arbuscular mycorrhizal symbiosis. Curr. Opin. Plant Biol. 1, 360–365.

Harrison, M., 1999. Molecular and cellular aspects of the arbuscular mycorrhizal symbiosis. Annu. Rev. Plant Physiol. Plant Mol. Biol. 50, 361–389.

Harrison, M.J., 2005. Signaling in the arbuscular mycorrhizal symbiosis. Annu. Rev. Microbiol. 59, 19–42.

Harrison, M., Dixon, R., 1993. Isoflavonoid accumulation and expression of defense gene transcripts during establishment of vesicular–arbuscular mycorrhizal associations in roots of *Medicago truncatula*. Mol. Plant Microbe Interact. 6, 643–654.

Harrison, M., Dixon, R., 1994. Spatial patterns of expression of flavonoid/isoflavonoid pathway genes during interactions between roots of *Medicago truncatula* and the mycorrhizal fungus *Glomus versiforme*. Plant J. 6, 9–20.

Harrison, M.J., Dewbre, G.R., Liu, J., 2002. A phosphate transporter from *Medicago truncatula* involved in the acquisition of phosphate released by arbuscular mycorrhizal fungi. Plant Cell 14, 2413–2429.

Harwood, J.L., 1996. Recent advances in the biosynthesis of plant fatty acids. Biochim. Biophys. Acta 1301, 7–56.

Hause, B., Fester, T., 2005. Molecular and cell biology of arbuscular mycorrhizal symbiosis. Planta 221, 184–196.

Hause, B., Mrosk, C., Isayenkov, S., Strack, D., 2007. Jasmonates in arbuscular mycorrhizal interactions. Phytochemistry 68, 101–110.

He, X.-Z., Dixon, R.A., 2000. Genetic manipulation of isoflavone 7-*O*-methyltransferase enhances biosynthesis of 4′-*O*-methylated isoflavonoid phytoalexins and disease resistance in alfalfa. Plant Cell 12, 1689–1702.

Hewitt, E.J., 1966. Sand and Water Culture Methods Used in the Study of Plant Nutrition. Commonwealth Agricultural Bureaux, Farnhan Royal, Bucks, UK, pp. 187–237.

Hildebrandt, U., Janetta, K., Bothe, H., 2002. Towards growth of arbuscular mycorrhizal fungi independent of a plant host. Appl. Environ. Microbiol. 68, 1919–1924.

Hildebrandt, U., Ouziad, F., Marner, F.-J., Bothe, H., 2006. The bacterium *Paenibacillus validus* stimulates growth of the arbuscular mycorrhizal fungus *Glomus intraradices* up to the formation of fertile spores. FEMS Microbiol. Lett. 254, 258–267.

Hohnjec, N., Perlick, A.M., Pühler, A., Küster, H., 2003. The *Medicago truncatula* sucrose synthase gene *MtSucS1* is activated both in the infected region of root nodules and in the cortex of roots colonised by arbuscular mycorrhizal fungi. Mol. Plant Microbe Interact. 16, 903–915.

Hohnjec, N., Vieweg, M.F., Pühler, A., Becker, A., Küster, H., 2005. Overlaps in the transcriptional profiles of *Medicago truncatula* roots inoculated with two different *Glomus* fungi provide insights into the genetic program activated during arbuscular mycorrhiza. Plant Physiol. 137, 1283–1301.

Huhman, D.V., Sumner, L.W., 2002. Metabolic profiling of saponins in *Medicago sativa* and *Medicago truncatula* using HPLC coupled to an electrospray ion-trap mass spectrometer. Phytochemistry 59, 347–360.

Huhman, D.V., Berhow, M.A., Sumner, L.W., 2005. Quantification of saponins in aerial and subterranean tissues of *Medicago truncatula*. J. Agric. Food Chem. 53, 1914–1920.

Isayenkov, S., Fester, T., Hause, B., 2004. Rapid determination of fungal colonisation and arbuscule formation in roots of *Medicago truncatula* using Real-time (RT) PCR. J. Plant Physiol. 161, 1379–1383.

Ishiguro, T., Koga, N., Takamura, K., Maruyama, T., 1955. Components of the flowers of *Osmanthus fragrans*. J. Pharm. Sci. Jpn. 75, 781–785.

Jabaji-Hare, S., 1988. Lipid and fatty acid profiles of some vesicular–arbuscular mycorrhizal fungi: contribution to taxonomy. Mycologia 80, 622–629.

Jin, H., Pfeffer, P.E., Douds, D.D., Piotrowski, E., Lammers, P.J., Shachar-Hill, Y., 2005. The uptake, metabolism, transport and transfer of nitrogen in an arbuscular mycorrhizal symbiosis. New Phytol. 168, 687–696.

Jones, F.R., 1924. A mycorrhizal fungus in the roots of legumes and some other plants. J. Agric. Res. 29, 459–470.

Journet, E.P., van Tuinen, D., Gouzy, J., Crespeau, H., Carreau, V., Farmer, M.J., Niebel, A., Schiex, T., Jaillon, O., Chatagnier, O., Godiard, L., Micheli, F., Kahn, D., Gianinazzi-Pearson, V., Gamas, P., 2002. Exploring root symbiotic programs in the model legume *Medicago truncatula* using EST analysis. Nucleic Acids Res. 30, 5579–5592.

Kape, R., Wex, K., Parniske, M., Görge, E., Wetzel, A., Werner, D., 1992. Legume root metabolites and VA-mycorrhiza development. J. Plant Physiol. 141, 54–60.

Kapusta, I., Stochmal, A., Perrone, A., Piacente, S., Pizza, C., Oleszek, W., 2005. Triterpene saponins from barrel medic (*Medicago truncatula*) aerial parts. J. Agric. Food Chem. 53, 2164–2170.

Kauss, H., Franke, R., Krause, K., Conrath, U., Jeblick, W., Grimmig, B., Matern, U., 1993. Conditioning of parsley (*Petroselinum crispum* L.) suspension cells increases elicitor-induced incorporation of cell wall phenolics. Plant Physiol. 102, 459–466.

Klingner, A., Bothe, H., Wray, V., Marber, F.-J., 1995a. Identification of a yellow pigment formed in maize roots upon mycorrhizal colonization. Phytochemistry 38, 53–55.

Klingner, A., Hundeshagen, B., Kernebeck, H., Bothe, M., 1995b. Localization of the yellow pigment formed in roots of gramineous plants colonized by arbuscular fungi. Protoplasma 185, 50–57.

Kopka, J., Fernie, A., Weckwerth, W., Gibon, Y., Stitt, M., 2004. Metabolite profiling in plant biology: platforms and destinations. Genome Biol. 5, 109.

Kose, F., Weckwerth, W., Linke, T., Fiehn, O., 2001. Visualizing plant metabolomic correlation networks using clique-metabolite matrices. Bioinformatics 17, 1198–1208.

Kosslak, R.M., Bookland, R., Barkei, J., Paaren, H.E., Appelbaum, E.R., 1987. Induction of *Bradyrhizobium japonicum* common nod genes by isoflavones isolated from *Glycine max*. Proc. Natl. Acad. Sci. USA 84, 7428–7432.

Krajinski, F., Biela, A., Schubert, D., Gianinazzi-Pearson, V., Kaldenhoff, R., Franken, P., 2000. Arbuscular mycorrhiza development regulates

the mRNA abundance of *Mtaqp1* encoding a mercury-insensitive aquaporin of *Medicago truncatula*. Planta 211, 85–90.

Krajinski, F., Hause, B., Gianinazzi-Pearson, V., Franken, P., 2002. *Mtha1*, a plasma membrane H^+-ATPase gene from *Medicago truncatula*, shows arbuscule-specific induced expression. Plant Biol. 4, 754–761.

Küster, H., Hohnjec, N., Krajinski, F., El Yahyaoui, F., Manthey, K., Gouzy, J., Dondrup, M., Meyer, F., Kalinowski, J., Brechenmacher, L., van Tuinen, D., Gianinazzi-Pearson, V., Pühler, A., Gamas, P., Becker, A., 2004. Construction and validation of cDNA-based Mt6k-RIT macro- and microarrays to explore root endosymbioses in the model legume *Medicago truncatula*. J. Biotechnol. 108, 95–113.

Larose, G., Chênevert, R., Moutoglis, P., Gagné, S., Piché, Y., Vierheilig, H., 2002. Flavonoid levels in roots of *Medicago sativa* are modulated by the developmental stage of the symbiosis and the root colonizing arbuscular mycorrhizal fungus. J. Plant Physiol. 159, 1329–1339.

Lerat, S., Lapointe, L., Gutjahr, S., Piché, Y., Vierheilig, H., 2003. Carbon partitioning in a split-root system of arbuscular mycorrhizal plants is fungal and plant species dependent. New Phytol. 157, 589–595.

Lin, L.-Z., He, X.-G., Lindenmaier, M., Nolan, G., Yang, J., Cleary, M., Qiu, S.-X., Cordell, G.A., 2000. LC-ESIMS study of the flavonoid glycoside malonates of red clover *Trifolium pratense*. J. Agric. Food Chem. 48, 354–365.

Linh, P.T., Kim, Y.H., Hong, S.P., Jian, J.J., Kang, J.S., 2000. Quantitative determination of salidroside and tyrosol from the underground part of *Rhodiola rosea* by high performance liquid chromatography. Arch. Pharm. Res. 23, 349–352.

Liu, J., Blaylock, L.A., Endre, G., Cho, J., Town, C.D., VandenBosch, K.A., Harrison, M.J., 2003. Transcript profiling coupled with spatial expression analyses reveals genes involved in distinct developmental stages of an arbuscular mycorrhizal symbiosis. Plant Cell 15, 2106–2123.

Liu, J., Maldonado-Mendoza, I., Lopez-Meyer, M., Cheung, F., Town, C.D., Harrison, M.J., 2007. Arbuscular mycorrhizal symbiosis is accompanied by local and systemic alterations in gene expression and an increase in disease resistance in the shoots. Plant J. 50, 529–544.

Lohse, S., Schliemann, W., Ammer, C., Kopka, J., Strack, D., Fester, T., 2005. Organization and metabolism of plastids and mitochondria in arbuscular mycorrhizal roots of *Medicago truncatula*. Plant Physiol. 139, 329–340.

Mackova, Z., Koblovska, R., Lapcik, O., 2006. Distribution of isoflavonoids in non-leguminous taxa – an update. Phytochemistry 67, 849–855.

Madan, R., Pankhurst, C., Hawke, B., Smith, S., 2002. Use of fatty acids for identification of AM fungi and estimation of the biomass of AM spores in soil. Soil Biol. Biochem. 34, 125–128.

Maeda, D., Ashida, K., Iguchi, K., Chechetka, S.A., Hijikata, A., Okusako, Y., Deguchi, Y., Izui, K., Hata, D., 2006. Knockdown of an arbuscular mycorrhiza-inducible phosphate transporter gene of *Lotus japonicus* suppresses mutualistic symbiosis. Plant Cell Physiol. 47, 807–817.

Maier, W., Peipp, H., Schmidt, J., Wray, V., Strack, D., 1995. Levels of a terpenoid glycoside (blumenin) and cell wall-bound phenolics in cereal mycorrhizas. Plant Physiol. 109, 465–470.

Maier, W., Hammer, K., Dammann, U., Schulz, B., Strack, D., 1997. Accumulation of sesquiterpenoid cyclohexenone derivatives induced by an arbuscular mycorrhizal fungus in members of the Poaceae. Planta 202, 36–42.

Maier, W., Schneider, B., Strack, D., 1998. Biosynthesis of sesquiterpenoid cyclohexenone derivatives in mycorrhizal barley roots proceeds via the glyceraldehyde 3-phosphate/pyruvate pathway. Tetrahedron Lett. 39, 521–524.

Maier, W., Schmidt, J., Wray, V., Walter, M.H., Strack, D., 1999. The mycorrhizal fungus, *Glomus intraradices*, induces the accumulation of cyclohexenone derivatives in tobacco roots. Planta 207, 620–623.

Maier, W., Schmidt, J., Nimtz, M., Wray, V., Strack, D., 2000. Secondary products in mycorrhizal roots of tobacco and tomato. Phytochemistry 54, 473–479.

Manthey, K., Krajinski, F., Hohnjec, N., Firnhaber, C., Pühler, A., Perlick, A., Küster, H., 2004. Transcriptome profiling in root nodules and arbuscular mycorrhiza identifies a collection of novel genes induced during *Medicago truncatula* root endosymbioses. Mol. Plant Microbe Interact. 17, 1063–1077.

Massiot, G., Lavaud, C., Le Men-Olivier, L., van Binst, G., Miller, S.F., Fales, H.M., 1988. Structural elucidation of alfalfa root saponins by mass spectrometry and nuclear magnetic resonance analysis. J. Chem. Soc., Perkin Trans., 3071–3079.

Massiot, G., Lavaud, C., Bresson, V., Le Men-Olivier, L., van Binst, G., 1991. Saponins from aerial parts of alfalfa (*Medicago sativa*). J. Agric. Food Chem. 39, 78–82.

Massoumou, M., van Tuinen, D., Chatagnier, O., Arnould, C., Brechenmacher, L., Sanchez, L., Selim, S., Gianinazzi, S., Gianinazzi-Pearson, V., 2007. *Medicago truncatula* gene responses specific to arbuscular mycorrhiza interactions with different species and genera of Glomeromycota. Mycorrhiza 17, 223–234.

Mathesius, U., Keijzers, G., Natcra, S.H.A., Winman, J.J., Djordjevic, M.A., Rolfe, B.G., 2001. Establishment of a root proteome reference map for the model legume *Medicago truncatula* using the expressed sequence tag database for peptide mass fingerprinting. Proteomics 1, 1424–1440.

Matusova, R., Rani, K., Verstappen, F.W.A., Franssen, M.C.R., Beale, M.H., Bouwmeester, H.J., 2005. The strigolactone germination stimulants of the plant-parasitic Striga and Orobanche spp. are derived from the carotenoid pathway. Plant Physiol. 139, 920–934.

Miyase, T., Ueno, A., Takizawa, N., Kobayashi, H., Oguchi, H., 1988. Studies on the glycosides of *Epimedium grandiflorum* Morr. var. *thunbergianum* (Miq.) Nakai. III. Chem. Pharm. Bull. 36, 2475–2484.

Nagata, T., Tsushida, T., Hamaya, E., Enoki, N., Manabe, S., Nishino, C., 1985. Camellidins: antifungal saponins isolated from *Camellia japonica*. Agric. Biol. Chem., Tokyo 49, 1181–1186.

Nielsen, N.-P.V., Carstensen, J.M., Smedsgaard, J., 1998. Aligning of single and multiple wavelength chromatographic profiles for chemometric data analysis using correlation optimized warping. J. Chromatogr. A 805, 17–35.

Ning, J., Cumming, J.R., 2001. Arbuscular mycorrhizal fungi alter phosphorus relations of broomsedge (*Andropogon virginicus* L.) plants. J. Exp. Bot. 52, 1883–1891.

Nordby, H.E., Nemec, S., Nagy, S., 1981. Fatty acids and sterols associated with citrus root mycorrhizae. J. Agric. Food Chem. 29, 396–401.

Oleszek, W., 1996. Alfalfa saponins: structure, biological activity and chemotaxonomy. In: Waller, G.R., Yamasaki, K. (Eds.), Saponins used in Food and Agriculture. Plenum Publishing, New York, pp. 155–170.

Oleszek, W., Price, K.R., Colquohoun, I.J., Jurzysta, M., Płoszynski, M., Fenwick, G.R., 1990. Isolation and identification of alfalfa (*Medicago sativa* L.) root saponins: their activity in relation to a fungal bioassay. J. Agric. Food Chem. 38, 1810–1817.

Oleszek, W., Jurzysta, M., Płoszynski, M., Colquohoun, I., Price, K.R., Fenwick, G.R., 1992. Zahnic acid tridesmoside and other dominant saponins from alfalfa (*Medicago sativa* L.). J. Agric. Food Chem. 40, 191–196.

Olsson, P.A., 1999. Signature fatty acids provide tools for determination of the distribution and interaction of mycorrhizal fungi in soil. FEMS Microbiol. Ecol. 29, 303–310.

Olsson, P.A., Johansen, A., 2000. Lipid and fatty acid composition of hyphae and spores of arbuscular mycorrhizal fungi at different growth stages. Mycol. Res. 104, 429–434.

Olsson, P.A., Larsson, L., Bago, B., Wallander, H., van Aarle, I.M., 2003. Ergosterol and fatty acids for biomass estimation of mycorrhizal fungi. New Phytol. 159, 7–10.

Parry, A.D., Tiller, S.A., Edwards, R., 1994. The effects of heavy metals and root immersion on isoflavonoid metabolism in alfalfa (*Medicago sativa* L.). Plant Physiol. 106, 195–202.

Peipp, H., Maier, W., Schmidt, J., Wray, V., Strack, D., 1997. Arbuscular mycorrhizal fungus-induced changes in the accumulation of secondary compounds in barley roots. Phytochemistry 44, 581–587.

Peters, N.K., Frost, J.W., Long, S.R., 1986. A plant flavone, luteolin, induces expression of *Rhizobium meliloti* nodulation genes. Science 233, 977–980.

Pfeffer, P.E., Douds, D.D., Bécard, G., Shachar-Hill, Y., 1999. Carbon uptake and the metabolism and transport of lipids in an arbuscular mycorrhiza. Plant Physiol. 120, 587–598.

Philips, J.M., Hayman, D.S., 1970. Improved procedures for cleaning roots and staining parasitic and vesicular–arbuscular mycorrhizal fungi for rapid assessment of infection. Trans. Br. Mycol. Soc. 55, 158–162.

Ponce, M.A., Scervino, J.M., Erra-Balsells, R., Ocampo, J.A., Godeas, A.M., 2004. Flavonoids from shoots and roots of *Trifolium repens* (white clover) grown in presence or absence of the arbuscular mycorrhizal fungus *Glomus intraradices*. Phytochemistry 65, 1925–1930.

Rabie, G.H., 2005. Contribution of arbuscular mycorrhizal fungus to red kidney and wheat plants tolerance grown in heavy metal-polluted soil. Afr. J. Biotechnol. 4, 332–345.

Reinhardt, D., 2007. Programming good relations – development of the arbuscular mycorrhizal symbiosis. Curr. Opin. Plant Biol. 10, 98–105.

Roessner, U., Luedemann, A., Brust, D., Fiehn, O., Linke, T., Willmitzer, L., Fernie, A.R., 2001. Metabolic profiling allows comprehensive phenotyping of genetically or environmentally modified plant systems. Plant Cell 13, 11–29.

Roessner-Tunali, U., Urbanczyk-Wochniak, E., Czechowski, T., Kolbe, A., Willmitzer, L., Fernie, A.R., 2003. De novo amino acid biosynthesis in potato tubers is regulated by sucrose levels. Plant Physiol. 133, 683–692.

Ruotsalainen, A.L., Kytoviita, M.M., 2004. Mycorrhiza does not alter low temperature impact on *Gnaphalium norvegicum*. Oecologia 140, 226–233.

Scervino, J.M., Ponce, M.A., Erra-Balsells, R., Vierheilig, H., Ocampo, J.A., Godeas, A.M., 2005. Flavonoids exclusively present in mycorrhizal roots of white clover exhibit a different effect on arbuscular mycorrhizal fungi than flavonoids exclusively present in non-mycorrhizal roots of white clover. J. Plant Interact. 1, 15–22.

Schauer, N., Steinhauser, D., Strelkov, S., Schomburg, D., Allison, G., Moritz, T., Lundgren, K., Roessner-Tunali, U., Forbes, M.G., Wilmitzer, L., Fernie, A.R., Kopka, J., 2005. GC–MS libraries for the rapid identification of metabolites in complex biological samples. FEBS Lett. 579, 1332–1337.

Schliemann, W., Schmidt, J., Nimtz, M., Wray, V., Fester, T., Strack, D., 2006a. Accumulation of apocarotenoids in mycorrhizal roots of *Ornithogalum umbellatum*. Phytochemistry 67, 1196–1205.

Schliemann, W., Schneider, B., Wray, V., Schmidt, J., Nimtz, M., Porzel, A., Böhm, H., 2006b. Flavonols and a novel indole alkaloid skeleton bearing identical acylated glycosidic groups from yellow petals of *Papaver nudicaule*. Phytochemistry 67, 191–201.

Schmitz, O., Danneberg, G., Hundeshagen, B., Klingner, A., Bothe, H., 1991. Quantification of vesicular–arbuscular mycorrhiza by biochemical parameters. J. Plant Physiol. 139, 106–114.

Schneider, G., Anke, H., Sterner, O., 1996. Xylaramide, a new antifungal compound, and other secondary metabolites from *Xylaria longipes*. Z. Naturforsch. C 51, 802–806.

Schüßler, A., 2001. Molecular phylogeny, taxonomy, and evolution of *Geosiphon pyriformis* and arbuscular mycorrhizal fungi. Plant Soil 244, 75–83.

Schüßler, A., Schwarzott, D., Walker, C., 2001. A new fungal phylum, the *Glomeromycota*: phylogeny and evolution. Mycol. Res. 105, 1413–1421.

Schwartz, S.H., Qin, X., Zeevaart, J.A.D., 2001. Characterization of a novel carotenoid cleavage dioxygenase from plants. J. Biol. Chem. 276, 25208–25211.

Schwartz, S.H., Qin, X., Loewen, M.C., 2004. The biochemical characterization of two carotenoid cleavage enzymes from *Arabidopsis* indicates that a carotenoid-derived compound inhibits lateral branching. J. Biol. Chem. 279, 46940–46945.

Sentheshanmuganathan, S., Elsden, S.R., 1958. The mechanism of the formation of tyrosol by *Saccharomyces cerevisiae*. Biochem. J. 69, 210–218.

Shachar-Hill, Y., 2007. Quantifying flows through metabolic networks and the prospects for fluxomic studies of mycorrhizas. New Phytol. 174, 235–240.

Siefermann-Harms, D., Hertzberg, S., Borch, G., Liaaen-Jensen, S., 1981. Carotenoids of higher plants. 13. Lactucaxanthin, an ε,ε-caroten-3,3′-diol from *Lactuca sativa*. Phytochemistry 20, 85–88.

Slininger, P.J., Burkhead, K.D., Schisler, D.A., 2004. Antifungal and sprout regulatory bioactivities of phenylacetic acid, indole-3-acetic acid, and tyrosol isolated from the potato dry rot suppressive bacterium *Enterobacter cloacae* S11:t:07. J. Ind. Microbiol. Biotechnol. 31, 517–524.

Smith, S.E., Gianinazzi-Pearson, V., 1990. Phosphate uptake and arbuscular activity in mycorrhizal *Allium cepa* L.: effects of photon irradiance and phosphate nutrition. Aust. J. Plant Physiol. 17, 177–188.

Smith, S.E., Read, D.J., 1997. Mycorrhizal Symbiosis. second ed. Academic Press, San Diego.

Stein, S.E., Fateev, O.V., Tchekhovskoi, D., Zaikin, V., Zhu, D., Mikaya, A., Sparkman, O.D., Ausloos, P., Clifton, C., Lias, S.G., Levitsky, A., Mallard, W.G., 1998. NIST/ EPA NIH Mass Spectral Database-NIST 98, Standard Reference Database No. 1, Software Release Version 1.

Stewart, A., Mansfield, J.W., 1985. The composition of wall alterations and appositions (reaction material) and their role in the resistance of onion bulb scale epidermis to colonization by *Botrytis allii*. Plant Pathol. 34, 25–37.

Strack, D., Fester, T., 2006. Isoprenoid metabolism and plastid reorganization in arbuscular mycorrhizal roots. New Phytol. 172, 22–34.

Strack, D., Fester, T., Hause, B., Schliemann, W., Walter, M.H., 2003. Arbuscular mycorrhiza: biological, chemical and molecular aspects. J. Chem. Ecol. 29, 1955–1979.

Stumpe, M., Carsjens, J.-G., Stenzel, I., Göbel, C., Lang, I., Pawlowski, K., Hause, B., Feussner, I., 2005. Lipid metabolism in arbuscular mycorrhizal roots of *Medicago truncatula*. Phytochemistry 66, 781–791.

Sumner, L.W., Paiva, N.L., Dixon, R.A., Geno, P.W., 1996. High-performance liquid chromatography/continuous-flow liquid secondary ion mass spectrometry of flavonoid glycosides in leguminous plant extracts. J. Mass Spectrom. 31, 472–485.

Sumner, L.W., Mendes, P., Dixon, R.A., 2003. Plant metabolomics: large-scale phytochemistry in the functional genomics era. Phytochemistry 62, 817–836.

Tan, J., Bednarek, P., Liu, J., Schneider, B., Svatoš, A., Hahlbrock, K., 2004. Universally occurring phenylpropanoid and species-specific indolic metabolites in infected and uninfected *Arabidopsis thaliana* roots and leaves. Phytochemistry 65, 691–699.

Tarus, P.K., Lang'at-Thoruwa, C.C., Wanyonyi, A.W., Chhabra, S.C., 2003. Bioactive metabolites from *Trichoderma harzianum* and *Trichoderma longibrachiatum.*. Bull. Chem. Soc. Ethiop. 17, 185–190.

Tiller, S.A., Parry, A.D., Edwards, R., 1994. Changes in the accumulation of flavonoid and isoflavonoid conjugates associated with plant-age and nodulation in alfalfa (*Medicago sativa*). Physiol. Plant. 91, 27–36.

Toussaint, J.-P., St-Arnaud, M., Charest, C., 2004. Nitrogen transfer and assimilation between the arbuscular mycorrhizal fungus *Glomus intraradices* Schenck & Smith and Ri T-DNA roots of *Daucus carota* L. in an in vitro compartmented system. Can. J. Microbiol. 50, 251–260.

Trépanier, M., Bécard, G., Moutoglis, P., Willemot, C., Gagné, S., Avis, T.J., Rioux, J.-A., 2005. Dependence of arbuscular–mycorrhizal fungi on their plant host for palmitic acid synthesis. Appl. Environ. Microbiol. 71, 5341–5347.

Urbanczyk-Wochniak, E., Lüdemann, A., Kopka, J., Selbig, J., Rössner-Tunali, U., Willmitzer, L., Fernie, A.R., 2003. Parallel analysis of transcript and metabolic profiles: a new approach in systems biology. EMBO Reports 4, 989–993.

Valentine, A.J., Osborne, B.A., Mitchell, D.T., 2001. Interactions between phosphorus supply and total nutrient availability on mycorrhizal

colonization, growth and photosynthesis of cucumber. Sci. Hortic. 88, 177–189.

Valot, B., Dieu, M., Recorbet, G., Raes, M., Gianinazzi, S., Dumas-Gaudot, E., 2005. Identification of membrane-associated proteins regulated by the arbuscular symbiosis. Plant. Mol. Biol. 59, 565–580.

Valot, B., Negroni, L., Michel Zivy, M., Gianinazzi, S., Dumas-Gaudot, E., 2006. A mass spectrometric approach to identify arbuscular mycorrhiza-related proteins in root plasma membrane fractions. Proteomics 6, S145–S155.

van Aarle, I.M., Olsson, P.A., 2003. Fungal lipid accumulation and development of mycelial structures by two arbuscular mycorrhizal fungi. Appl. Environ. Microbiol. 69, 6762–6767.

van Buuren, M.L., Maldonado-Mendoza, I.E., Trieu, A.T., Blaylock, L.A., Harrison, M.J., 1999. Novel genes induced during an arbuscular mycorrhizal (AM) symbiosis formed between *Medicago truncatula* and *Glomus versiforme*. Mol. Plant Microbe Interact. 12, 171–181.

Vierheilig, H., Coughlan, A.P., Wyss, U., Piché, Y., 1998. Ink and vinegar, a simple staining technique for arbuscular–mycorrhizal fungi. Appl. Environ. Microbiol. 64, 5004–5007.

Vieweg, M.F., Frühling, M., Quandt, H.-J., Heim, U., Bäumlein, H., Pühler, A., Küster, H., Perlick, A., 2004. The promoter of the *Vicia faba* L. leghemoglobin gene *VfLb29* is specifically activated in the infected cells of root nodules and in the arbuscule-containing cells of mycorrhizal roots from different legume and nonlegume plants. Mol. Plant Microbe Interact. 17, 62–69.

Vieweg, M.F., Hohnjec, N., Küster, H., 2005. Two genes encoding different truncated hemoglobins are regulated during root nodule and arbuscular mycorrhiza symbioses of *Medicago truncatula*. Planta 220, 757–766.

Volpin, H., Phillips, D.A., Okon, Y., Kapulnik, Y., 1995. Suppression of an isoflavonoid phytoalexin defense response in mycorrhizal alfalfa roots. Plant Physiol. 108, 1449–1454.

Walter, M.H., Fester, T., Strack, D., 2000. Arbuscular mycorrhizal fungi induce the non-mevalonate methylerythritol phosphate pathway of isoprenoid biosynthesis correlated with accumulation of the "yellow pigment" and other apocarotenoids. Plant J. 21, 571–578.

Walter, M.H., Hans, J., Strack, D., 2002. Two distantly related genes encoding 1-deoxy-D-xylulose 5-phosphate synthases: differential regulation in shoots and apocarotenoid-accumulating mycorrhizal roots. Plant J. 31, 243–254.

Walter, M.H., Floß, D.S., Hans, J., Fester, T., Strack, D., 2007. Apocarotenoid biosynthesis in arbuscular mycorrhizal roots: contributions from methylerythritol phosphate pathway isogenes and tools for its manupulation. Phytochemistry 68, 130–138.

Wasson, A.P., Pellerone, F.I., Mathesius, U., 2006. Silencing the flavonoid pathway in *Medicago truncatula* inhibits root nodule formation and prevents auxin transport regulation by rhizobia. Plant Cell 18, 1617–1629.

Watson, B.S., Asirvatham, V.S., Wang, L., Sumner, L.W., 2003. Mapping of the proteome of barrel medic (*Medicago truncatula*). Plant Physiol. 131, 1104–1123.

Weckwerth, W., 2003. Metabolomics in systems biology. Annu. Rev. Plant Biol. 54, 669–689.

Weckwerth, W., Fiehn, O., 2002. Can we discover novel pathways using metabolomic analysis? Curr. Opin. Biotechnol. 13, 156–160.

Wu, Q.-S., Xia, R.-X., 2006. Arbuscular mycorrhizal fungi influence growth, osmotic adjustment and photosynthesis of citrus under well-watered and water stress conditions. J. Plant Physiol. 163, 417–425.

Wulf, A., Manthey, K., Doll, J., Perlick, A.M., Linke, B., Bekel, T., Meyer, F., Franken, P., Küster, H., Krajinski, F., 2003. Transcriptional changes in response to arbuscular mycorrhiza development in the model plant *Medicago truncatula*. Mol. Plant Microbe Interact. 16, 306–314.

Xiao, H.B., Krucker, M., Putzbach, K., Albert, K., 2005. Capillary liquid chromatography-microcoil ^{1}H nuclear magnetic resonance spectroscopy and liquid chromatography–ion trap mass spectrometry for on-line structure elucidation of isoflavones in Radix astragali. J. Chromatogr. A 1067, 135–143.

Yang, W.-L., Bernards, M.A., 2006. Wound induced metabolism in potato (*Solanum tuberosum*) tubers: biosynthesis of aliphatic domain monomers. Plant Signaling and Behavior 1, 59–66.

Yousef, G.G., Grace, M.H., Cheng, D.M., Belolipov, I.V., Raskin, I., Lila, M.A., 2006. Comparative phytochemical characterization of three *Rhodiola* species. Phytochemistry 67, 2380–2391.

Zhang, F., Smith, D.L., 1996. Genistein accumulation in soybean [*Glycine max* (L.) Merr] root systems under sub-optimal root zone temperatures. J. Exp. Bot. 47, 785–792.

Zhang, F., Smith, D.L., 2002. Interorganismal signaling in suboptimal environments: the legume-rhizobia symbiosis. Adv. Agron. 76, 125–161.